frontiers | Frontiers in Marine Science

TYPE Review
PUBLISHED 08 December 2023
DOI 10.3389/fmars.2023.1221701

OPEN ACCESS

EDITED BY
Yang-Ki Cho,
Seoul National University, Republic of Korea

REVIEWED BY
Joellen Russell,
University of Arizona, United States
Dmitry Frey,
P.P. Shirshov Institute of Oceanology (RAS), Russia

*CORRESPONDENCE
Alessandro Silvano
A.Silvano@soton.ac.uk

RECEIVED 12 May 2023
ACCEPTED 01 November 2023
PUBLISHED 08 December 2023

CITATION
Silvano A, Purkey S, Gordon AL, Castagno P, Stewart AL, Rintoul SR, Foppert A, Gunn KL, Herraiz-Borreguero L, Aoki S, Nakayama Y, Naveira Garabato AC, Spingys C, Akhoudas CH, Sallée J-B, de Lavergne C, Abrahamsen EP, Meijers AJS, Meredith MP, Zhou S, Tamura T, Yamazaki K, Ohshima KI, Falco P, Budillon G, Hattermann T, Janout MA, Llanillo P, Bowen MM, Darelius E, Østerhus S, Nicholls KW, Stevens C, Fernandez D, Cimoli L, Jacobs SS, Morrison AK, Hogg AM, Haumann FA, Mashayek A, Wang Z, Kerr R, Williams GD and Lee WS (2023) Observing Antarctic Bottom Water in the Southern Ocean.
Front. Mar. Sci. 10:1221701.
doi: 10.3389/fmars.2023.1221701

Observing Antarctic Bottom Water in the Southern Ocean

Alessandro Silvano[1*], Sarah Purkey[2], Arnold L. Gordon[3], Pasquale Castagno[4], Andrew L. Stewart[5], Stephen R. Rintoul[6,7,8], Annie Foppert[8,9], Kathryn L. Gunn[1], Laura Herraiz-Borreguero[6,7], Shigeru Aoki[10], Yoshihiro Nakayama[10], Alberto C. Naveira Garabato[1], Carl Spingys[11], Camille Hayatte Akhoudas[12,13], Jean-Baptiste Sallée[13], Casimir de Lavergne[13], E. Povl Abrahamsen[14], Andrew J. S. Meijers[14], Michael P. Meredith[14], Shenjie Zhou[14], Takeshi Tamura[15,16], Kaihe Yamazaki[15,17], Kay I. Ohshima[10], Pierpaolo Falco[18], Giorgio Budillon[19], Tore Hattermann[20,21,22], Markus A. Janout[20], Pedro Llanillo[20], Melissa M. Bowen[23], Elin Darelius[24], Svein Østerhus[25], Keith W. Nicholls[14], Craig Stevens[26,27], Denise Fernandez[26], Laura Cimoli[2,28], Stanley S. Jacobs[3], Adele K. Morrison[29], Andrew McC. Hogg[30], F. Alexander Haumann[20,31,32], Ali Mashayek[33], Zhaomin Wang[34], Rodrigo Kerr[35], Guy D. Williams[36] and Won Sang Lee[37]

[1]Ocean and Earth Science, National Oceanography Centre, University of Southampton, Southampton, United Kingdom, [2]Scripps Institution of Oceanography, University of California, San Diego, La Jolla, CA, United States, [3]Lamont-Doherty Earth Observatory, Columbia University, Palisades, NY, United States, [4]Department of Mathematics, Computer Sciences, Physics and Earth Sciences, University of Messina, Messina, Italy, [5]Department of Atmospheric and Oceanic Sciences, University of California, Los Angeles, Los Angeles, CA, United States, [6]Department of Environment, The Commonwealth Scientific and Industrial Research Organisation (CSIRO), Hobart, TAS, Australia, [7]Centre for Southern Hemisphere Oceans Research, Hobart, TAS, Australia, [8]Australian Antarctic Program Partnership, University of Tasmania, Hobart, TAS, Australia, [9]Institute for Marine and Antarctic Studies, University of Tasmania, Hobart, TAS, Australia, [10]Institute of Low Temperature Science, Hokkaido University, Sapporo, Japan, [11]National Oceanography Centre, Southampton, United Kingdom, [12]Department of Geological Sciences, Stockholm University, Stockholm, Sweden, [13]LOCEAN Laboratory, Sorbonne Université/CNRS/IRD/MNHN, Paris, France, [14]British Antarctic Survey, Cambridge, United Kingdom, [15]National Institute of Polar Research, Tachikawa, Japan, [16]SOKENDAI, Graduate University for Advanced Studies, Tachikawa, Japan, [17]Australian Centre for Excellence in Antarctic Science (ACEAS), Institute for Marine and Antarctic Studies, University of Tasmania, Hobart, TAS, Australia, [18]Department of Life and Environmental Sciences, Marche Polytechnic University of Ancona, Ancona, Italy, [19]Department of Sciences and Technologies, Parthenope University, Naples, Italy, [20]Alfred Wegener Institute Helmholtz Centre for Polar and Marine Research, Bremerhaven, Germany, [21]Akvaplan-niva AS, Tromsø, Norway, [22]Norwegian Polar Institute, Tromsø, Norway, [23]School of Environment, University of Auckland, Auckland, New Zealand, [24]Geophysical Institute, University of Bergen and the Bjerknes Centre for Climate Research, Bergen, Norway, [25]Norwegian Research Center, and the Bjerknes Centre for Climate Research, Bergen, Norway, [26]Ocean Dynamics Group, New Zealand National Institute of Water and Atmospheric Research, Wellington, New Zealand, [27]Department of Physics, University of Auckland, Auckland, New Zealand, [28]Department of Applied Mathematics and Theoretical Physics, University of Cambridge, Cambridge, United Kingdom, [29]Research School of Earth Sciences and Australian Centre for Excellence in Antarctic Science, Australian National University, Canberra, ACT, Australia, [30]Research School of Earth Sciences and Australian Research Council (ARC) Centre of Excellence for Climate Extremes, Australian National University, Canberra, ACT, Australia, [31]Ludwig Maximilian University Munich, Munich, Germany, [32]Atmospheric and Oceanic Sciences, Princeton University, Princeton, NJ, United States, [33]Department of Earth Sciences, University of Cambridge, Cambridge, United Kingdom, [34]Southern Marine Science and Engineering Guangdong Laboratory (Zhuhai), Zhuhai, China, [35]Laboratório de Estudos dos Oceanos e Clima, Instituto de Oceanografia,

Universidade Federal do Rio Grande – FURG, Rio Grande, RS, Brazil, [36]First Institute of Oceanography, Qingdao, China, [37]Division of Glacial Environment Research, Korea Polar Research Institute, Incheon, Republic of Korea

Dense, cold waters formed on Antarctic continental shelves descend along the Antarctic continental margin, where they mix with other Southern Ocean waters to form Antarctic Bottom Water (AABW). AABW then spreads into the deepest parts of all major ocean basins, isolating heat and carbon from the atmosphere for centuries. Despite AABW's key role in regulating Earth's climate on long time scales and in recording Southern Ocean conditions, AABW remains poorly observed. This lack of observational data is mostly due to two factors. First, AABW originates on the Antarctic continental shelf and slope where *in situ* measurements are limited and ocean observations by satellites are hampered by persistent sea ice cover and long periods of darkness in winter. Second, north of the Antarctic continental slope, AABW is found below approximately 2 km depth, where *in situ* observations are also scarce and satellites cannot provide direct measurements. Here, we review progress made during the past decades in observing AABW. We describe 1) long-term monitoring obtained by moorings, by ship-based surveys, and beneath ice shelves through bore holes; 2) the recent development of autonomous observing tools in coastal Antarctic and deep ocean systems; and 3) alternative approaches including data assimilation models and satellite-derived proxies. The variety of approaches is beginning to transform our understanding of AABW, including its formation processes, temporal variability, and contribution to the lower limb of the global ocean meridional overturning circulation. In particular, these observations highlight the key role played by winds, sea ice, and the Antarctic Ice Sheet in AABW-related processes. We conclude by discussing future avenues for observing and understanding AABW, impressing the need for a sustained and coordinated observing system.

KEYWORDS

Antarctic Bottom Water (AABW), Southern Ocean, ice shelves, ocean warming, ocean freshening, Antarctic sea ice, observations

1 Introduction

Antarctic Bottom Water (AABW) plays a primary role in the climate system, as it supplies the lower branch of the global Meridional (i.e., north–south) Overturning Circulation (MOC; Lumpkin and Speer, 2007; Talley, 2013). The process of AABW formation near the Antarctic coast and its northward spreading allows ventilation of most of the abyssal (>2 km depth) ocean (Johnson, 2008), supplying oxygen (Gordon, 2013) and storing heat and carbon at depth for centuries (de Lavergne et al., 2017; Holzer et al., 2021). Sinking AABW also carries nutrients that have not been utilized by marine organisms due to local light and iron limitation and thereby affects global primary production and the efficiency of the biological carbon pump (Marinov et al., 2006). Changes in AABW formation and circulation are thus thought to influence atmospheric carbon dioxide, and consequently Earth's climate, on centennial to millennial time scales (Sigman and Boyle, 2000; Ferrari et al., 2014; Marzocchi and Jansen, 2019).

AABW originates on the Antarctic continental shelf (Figure 1), where extremely cold and salty waters are produced. Seawater that is near the surface freezing point and has absolute salinities higher than 34.6 g/kg is known as high-salinity shelf water (HSSW) and is produced on the shelf as a result of surface heat loss and salt input through brine rejection when sea ice forms. Sea ice formation is enhanced near the Antarctic coast, especially in ice-free coastal polynyas where sea ice is continuously formed and advected away by katabatic winds (see Figure 2B for locations of the main Antarctic coastal polynyas). In some locations (e.g., Ross and Weddell Seas, Prydz Bay), HSSW is further cooled by ice–ocean interaction at the base of ice shelves, producing supercooled water colder than the surface freezing point, known as Ice Shelf Water (ISW) that is typically below −2°C. Once formed, a fraction of

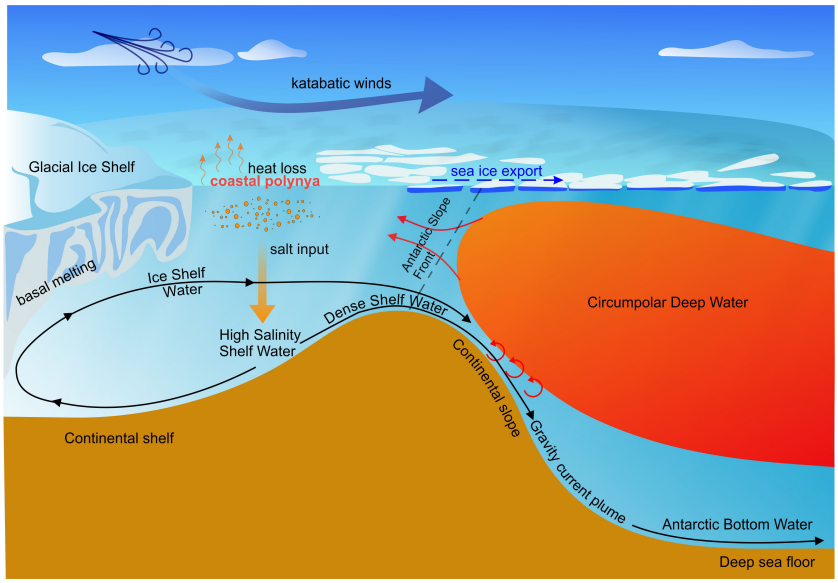

FIGURE 1
Schematic diagram summarizing Antarctic Bottom Water (AABW) formation. AABW originates on the Antarctic continental shelf where intense surface cooling and salt input occur during sea ice formation. Enhanced sea ice formation in coastal polynyas allows high-salinity shelf water (HSSW) formation. In some regions, HSSW interacts with the ice shelf base to produce supercooled (below the surface freezing point) Ice Shelf Water (ISW). These cold shelf waters are often referred to as Dense Shelf Water (DSW), as they are dense enough to descend down the continental slope as a gravity plume. Entrainment with Southern Ocean waters during their descent produces AABW.

HSSW/ISW escapes the continental shelf and cascades into the abyssal Southern Ocean. Dense waters produced on the continental shelf (HSSW and ISW) are usually referred altogether to as Dense Shelf Water (DSW). While sinking as a gravity plume down the continental slope, DSW mixes with other Southern Ocean waters, mostly with warmer (approximately 1°C to 2°C) Circumpolar Deep Water (CDW) and fresher (absolute salinity<34.6 g/kg) Antarctic Surface Water (Orsi et al., 1999; Akhoudas et al., 2021). This mixing process produces AABW, which is water that is colder than 0°C with neutral densities (Jackett and McDougall, 1997) greater than 28.27 kg/m^3 (Figure 1). AABW properties and formation rates can also be influenced by offshore polynyas, as the one observed in the 1970s in the Weddell Sea causing convection up to 3,000 m depth (Gordon, 1978). However, such offshore vigorous deep convective events have not been observed since the 1970s, indicating that the present-day main source region of AABW is the Antarctic continental shelf (see Figures 2B, 3).

AABW forms in localized areas around the Antarctic continent (see Figures 2B, 3). After sinking into the deep ocean, AABW flows along isobaths on the lower continental slope until its flow is diverted northward along deep western boundary currents (Stommel, 1958; see Figure 3). AABW's unique cold and fresh signature is steered topographically through the Southern Ocean and can be found over much of the global ocean abyss. Within the Antarctic Circumpolar Current (ACC), distinct varieties of AABW are homogenized before moving north, with more recent modeling work suggesting the Weddell and Cape Darnley regions primarily feed the Atlantic basin, while the Ross and Adélie regions feed the Indian and Pacific basins (Solodoch et al., 2022). North of the ACC, AABW is seen moving north in all ocean basins along deep western boundary currents and recirculating into the interior of these basins (Reid, 1989; Reid, 1994; Reid, 1997; Purkey et al., 2018). Along its northward pathway, AABW encounters sills and narrow passages, and its properties are further modified by mixing (Bryden and Nurser, 2003). This mixing causes AABW to become more buoyant (Figure 3A) and warmer (Figure 3B) as it spreads northward.

AABW has been historically challenging to monitor. The remote location of Antarctica and its harsh weather conditions imply long, expensive, often risky, and logistically demanding expeditions to collect *in situ* measurements. Oceanographic campaigns are further hampered by sea ice cover over the polar Southern Ocean (south of approximately 60°S) during austral winter and in many Antarctic coastal regions during austral summer (see Figure 2A). Sea ice cover also limits the ability of satellites to measure ocean surface properties. Similar and further limitations apply north of the seasonal sea ice zone, where AABW is found below ~2 km depth. At these depths, ocean properties can be neither directly measured by satellites nor reached by regular Argo floats (Riser et al., 2016). Observation of AABW thus has mostly relied on *in situ* measurements requiring time-consuming and expensive oceanographic expeditions.

Here, we review progress made during the past decades in measuring AABW, from its formation around Antarctica to its northward transport through the Southern Ocean. In Section 2, we describe observations in the open ocean through ship-based surveys, through moorings, and within the ice shelf cavities through bore holes. Section 3 introduces new tools developed in recent years, while Section 4 illustrates indirect approaches that can be used to monitor AABW. In each section, we outline important

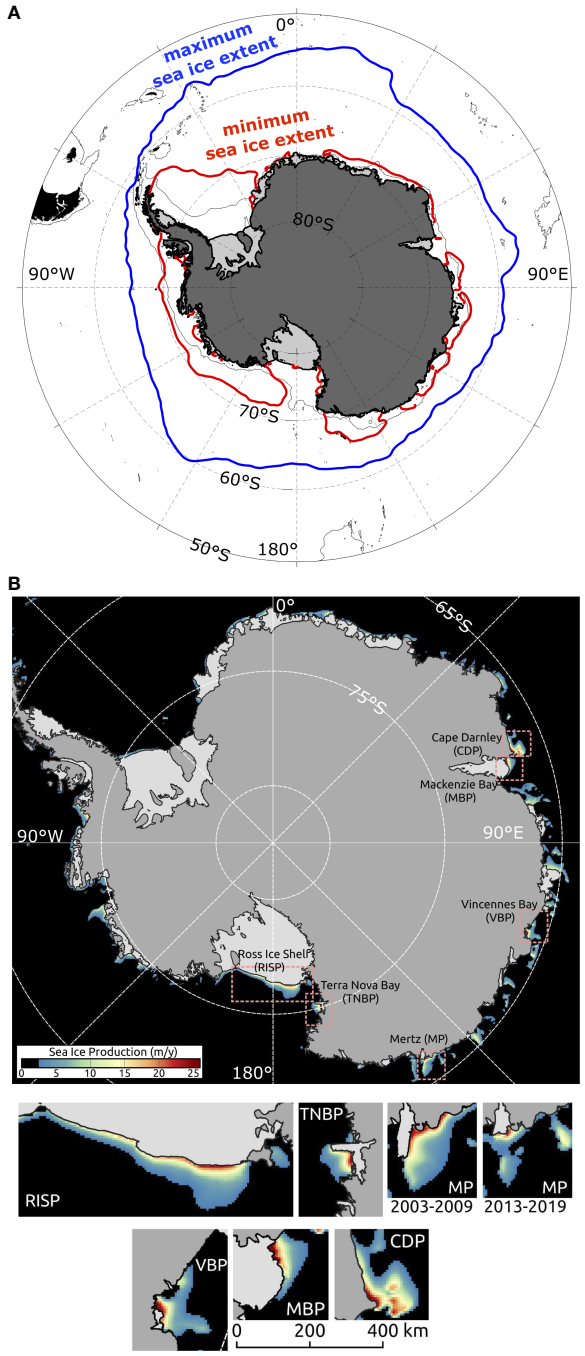

FIGURE 2
Maps showing Antarctic sea ice coverage and production. **(A)** Map of summer minimum (February, red line) and winter maximum (September, blue line) Antarctic sea ice extent (defined by the 15% sea ice concentration threshold from the 1978–2018 climatological sea ice values; Meier et al., 2017). **(B)** Map of annual sea ice production (m/year) during the freezing period (March–October) averaged over the period 2003–2019, updated by Nakata et al. (2021). The lower panels are close-up maps for the polynyas (red dashed rectangles in the main panel) that can create Antarctic Bottom Water (AABW) dense precursors.

scientific discoveries associated with the different tools. Section 5 delineates knowledge gaps in understanding AABW and the observational needs required to address them. Section 6 provides concluding remarks.

2 Multidecadal *in situ* observations

2.1 Ship-based hydrography

This section describes hydrographic (i.e., temperature and salinity) measurements of shelf and abyssal waters collected by ships in the Southern Ocean. We begin with early expeditions from the 18th century that spanned almost three centuries of ocean explorations. We then focus on more recent observations from the second half of the 20th century to the present, which have collected measurements on the continental shelf and in the deep Southern Ocean (i.e., equatorward of the continental shelf break).

2.1.1 Early measurements

While ocean surface currents have been known since the days when sailing ships formed the basis of trade (more than 1,000 years ago) and refined during the 15th to 17th centuries of exploration, little was known about the ocean properties or circulation below the surface. From the 18th century, this started to change (Wüst, 1964; Wüst, 1968; Warren, 1981). In 1750, Captain Henri Ellis, aboard the *Earl of Halifax*, found that there were indications of cold water below the subtropical Atlantic sea surface. By extrapolation to the sea floor, J. Otto in 1800 and A. von Humboldt in 1814 speculated that near the deep seafloor, the temperature would be approximately 0°C and of polar origin. Wüst (1968) reported that this was partially verified in 1837 with an observation of 1.7°C water at 3,741 m depth in the tropical Pacific made by the French frigate *Venus*. During the same period, in 1800, Count Rumford proposed a meridional circulation of the ocean whereby water sinks near the poles and rises near the equator, a view shared later by E. von Lenz in 1845.

Systematic study of the ocean below the surface began with the *Challenger* expedition (1873 to 1876; Thompson and Murray, 1895), which is considered the start of the "Era of Exploration" (1873 to 1914). The *Challenger* expedition, with widely spaced stations in each ocean basin, produced the first large-scale coherent picture of the water masses in the deep ocean. Other expeditions during this exploration era coarsely revealed the spatial pattern of ocean circulation within its deep and abyssal parts.

The hemispheric abyssal circulation pattern (sinking at the poles and upwelling at the equator) of von Lenz in the 19th century was still in vogue 50 years later in 1902. At this time, G. Schott published a diagram of the oceanic meridional circulation of the Atlantic Ocean based on the *Valdivia* Expedition (1898 to 1899), including cross-equator flow from south to north below 2,000 m (Richardson, 2008; Figure 4A). In the 1920s, a more complete view of the meridional exchange emerged. Analyses by Brennecke (1921); Merz and Wüst (1922), and Merz (1925) revealed the asymmetry of the North and South Atlantic Oceans.

In 1925, an "Era of National Systematic and Dynamic Ocean Surveys" began and lasted until 1940 (Wüst, 1964). This era was initiated with a new and detailed view of the South Atlantic stratification from the German Atlantic Expedition on the Research Vessel *Meteor* in the period 1925 to 1927. This expedition collected sections of closely spaced hydrographic

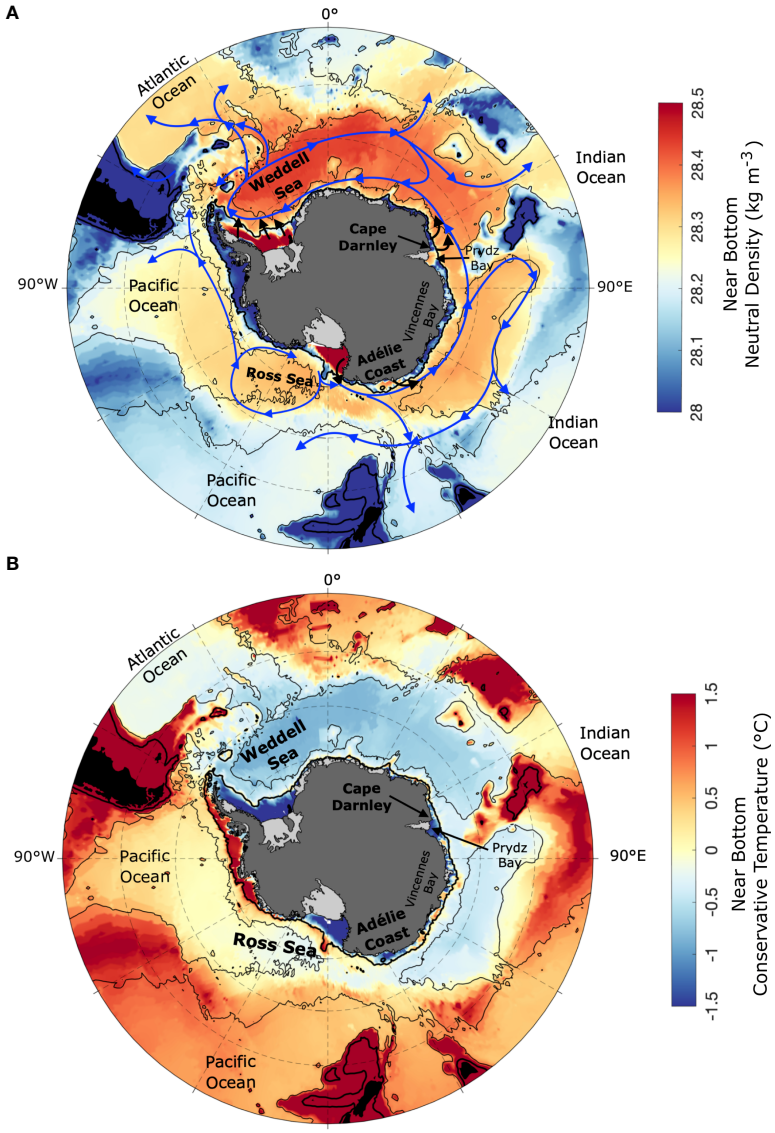

FIGURE 3
Maps of Antarctic Bottom Water (AABW) properties and spreading in the Southern Ocean. Climatological near bottom **(A)** neutral density (kg/m^3) and **(B)** conservative temperature (°C) derived from the World Ocean Experiment (WOCE; Gouretski and Koltermann, 2004). AABW formation regions are highlighted in **(A)** by black arrows, while blue arrows show the main pathways of AABW through the Southern Ocean (from Orsi et al., 1999; Talley, 2013; Van Sebille et al., 2013; Purkey et al., 2018; Solodoch et al., 2022). AABW and its precursor DSW are characterized by dense (red in panel **A**) and cold (blue in panel **B**) water properties near the seafloor. The 1,000-m isobath is in thick black and roughly delimits the continental shelf, while the 4,000-m isobath is in thin black (Gouretski and Koltermann, 2004). The Antarctic coastline is from BedMachine (Morlighem et al., 2020).

stations across the Atlantic Ocean between 20°N and 65°S, with subsurface observations reaching the deep seafloor up to 6 km deep. Based on the *Meteor* expedition and other hydrographic data, Wüst (1935) produced schematics of the spreading of the sub-thermocline circulation of the Atlantic Ocean between 60°S and 60°N, including AABW (Figure 4B), which remain qualitatively similar to modern schematics of the deep Atlantic circulation (Talley, 2013).

Circum-Antarctic surveys in the 1920s and 1930s conducted under the auspices of the *Discovery* investigations (Deacon, 1937) and 1960s and 1970s by the *Eltanin* (Gordon, 2012) provided new details of the formation sites of AABW along the continental margins of Antarctica and its spreading across the ACC into the major ocean basins. Combining observations from these expeditions and others around the world ocean, Lynn and Reid (1968) provided a global overview of the characteristics of abyssal waters.

The International Geophysical Year (1957 to 1959) marked the beginning of a new era of observational ocean research, providing a transition from a more-or-less independent national research work of one ship to systematic multi-ship, multi-national surveys. A notable example is the World Ocean Circulation Experiment (WOCE) surveys that covered the global ocean during the 1990s, producing an atlas series that included detailed views of the bottom

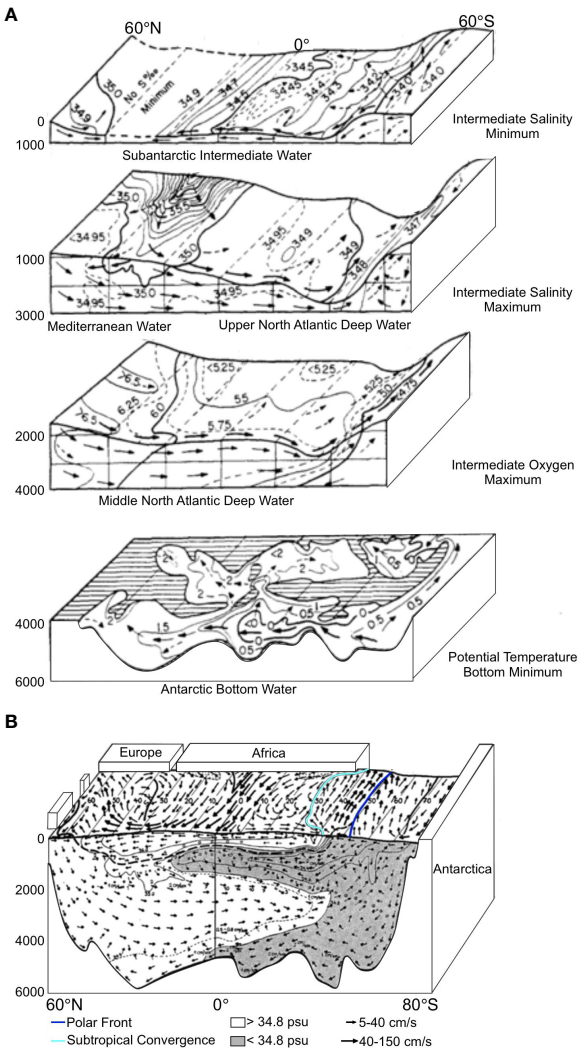

FIGURE 4
Schematic diagrams showing meridional spreading of water mass in the Atlantic Ocean. **(A)** Spreading of main water masses of the Atlantic Ocean in four core layers adapted from Wüst, 1964. **(B)** Surface currents, salinity contours, and the meridional circulation along a section in the western Atlantic by Wüst (1935); Wüst (1949). Small numbers are geostrophic speeds in cm/s. Dashed line is the 9° C boundary between warm and cold layers. Polar Front and Subtropical Convergence are depicted as blue and cyan lines, respectively. Adapted from Richardson (2008).

water characteristics and the extent of interocean exchange (Orsi and Whitworth, 2005).

As described below, with the expansion of observations from ships, moorings, Argo floats, and new platforms along with geochemical tracers, we now have a much more refined view of the spatio-temporal variability of AABW along with estimates of ventilation times associated with its spread across the global ocean. Wüst (1964) said of ocean research: "As in all sciences, progress is not continuous. Most of the ideas, instruments and methods influencing research work in the laboratories are conceived in the preparation and in the accomplishment of great expeditions. At the same time new theoretical concepts are also formed." So it is today, as we can now view in increasing detail, the cold waters near the seafloor that emanate from Antarctica.

2.1.2 Antarctic continental shelf

Here, we focus on the four main continental shelf regions around Antarctica where AABW originates (Weddell Sea, Ross Sea, Adélie Coast, and Prydz Bay/Cape Darnley).

2.1.2.1 Weddell Sea

Ship-based hydrographic observations in the southern and western Weddell Sea are hampered year-round due to a vast sea ice cover (Figure 2A). Thus, observations are austral summer-biased and limited (with a few exceptions) to areas around the Filchner Trough, near the tip of the Antarctic Peninsula, and to coastal polynyas formed by offshore winds across the ice shelf fronts. The first systematic observations were collected in the 1970s during Norwegian expeditions (Foldvik et al., 1985a) and continued in the following decades, including multiple hydrographic surveys on the southern continental shelf by German-led expeditions onboard the RVIB *Polarstern* (Janout et al., 2021). The multiple conductivity–temperature–depth (CTD) surveys provide information about the variability, pathways, and modifications of the shelf water masses (HSSW, ISW, and modified Circumpolar Deep Water (mCDW), with the latter resulting from the mixing of CDW with cooler and fresher waters near the coast) all contributing to the AABW formation (see Nicholls et al., 2009, for a comprehensive review). ISW forms beneath the Filchner-Ronne Ice Shelf and is transported toward the continental slope in the Filchner Trough on the south-eastern continental shelf. Multidecadal observations have shown that while ISW exhibits considerable variability in temperature and salinity (depending on the ice shelf cavity circulation), its density has remained stable over the past five decades (Figure 5E).

On the western Weddell Sea shelf (i.e., north of the Ronne Ice Shelf), heavy sea ice conditions and icebergs (Rackow et al., 2017) have precluded systematic surveys. Measurements from opportunistic surveys during favorable sea ice conditions or from drift experiments such as Ice Station Weddell-1 (ISW-1; Gordon and Ice Station Weddell Group of Principal Investigators and Chief Scientists, 1993) and Ice Station POLarstern (ISPOL; Hellmer et al., 2008; Huhn et al., 2008) provide evidence of HSSW near the shelf break, confirming the western Weddell Sea as a source of AABW.

2.1.2.2 Ross Sea

HSSW in the Ross Sea is mainly produced in two coastal polynyas in the western sector of the continental shelf: the Terra Nova Bay and Ross Ice Shelf Polynyas. Summer hydrographic measurements of these water masses started in 1957 (Jacobs et al., 2022) and were conducted in most subsequent years near Ross Island during expeditions by the United States, New Zealand, and South Korea (see Figure 5E). Key locations of repeated measurements are Terra Nova Bay, Hayes Bank, and Bay of Whales (Jacobs et al., 2022). In Terra Nova Bay, oceanographic observations began in 1978 with the United States icebreaker USCGC *Burton Island* (Jacobs et al., 2022) and since 1994 have been continued almost yearly by the Italian Antarctic Program (Castagno et al., 2019; Silvano et al., 2020). Systematic observations have been carried out by the South Korean Antarctic Program since 2014 as well, in both the Ross (Yoon et al., 2020) and Amundsen

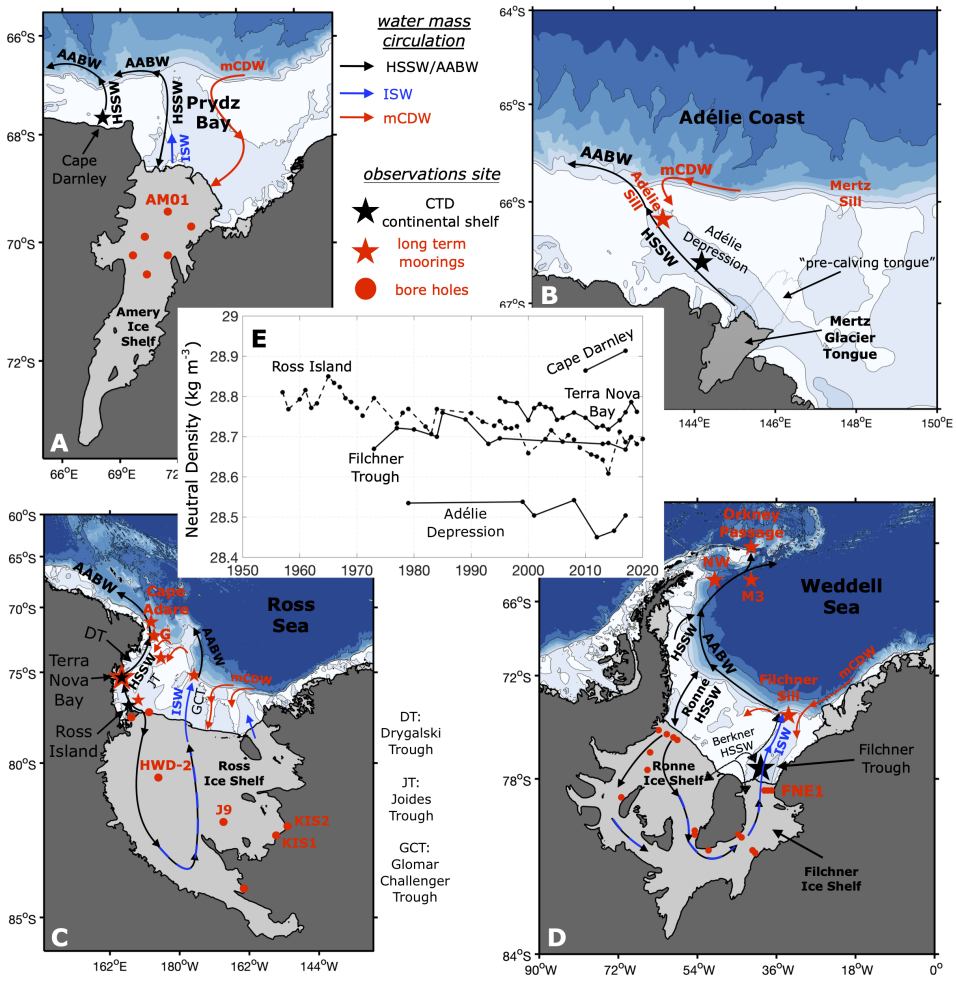

FIGURE 5
Maps showing circulation in **(A)** Prydz Bay, **(B)** Adélie Coast, **(C)** Ross Sea, and **(D)** Weddell Sea **(D)**. Circulation of water masses and locations of oceanographic measurements are depicted by arrows, dots, and stars (according to the legend). **(E)** Time series of neutral density (kg/m^3) observed near the seafloor in the main areas of high-salinity shelf water (HSSW)/Ice Shelf Water (ISW) sourcing Antarctic Bottom Water (AABW). mCDW refers to modified Circumpolar Deep Water. From lighter to denser: Adélie Depression (location is indicated by the black star in panel **B**), Filchner Trough (black star in panel **D**), Terra Nova Bay/Ross Island (black stars in panel **C**), and Cape Darnley (black star in panel **A**).

Seas (Kim et al., 2021; Yang et al., 2022). These long time series have reported both statistically significant long-term decreasing trends for salinity and density (Jacobs and Giulivi, 2010; Jacobs et al., 2022) and interannual variability of these parameters with 5-year to 10-year fluctuations and a strong rebound after 2014 (Castagno et al., 2019; Silvano et al., 2020; Yoon et al., 2020; Figure 5E). Furthermore, ship-based hydrographic observations have provided significant insights into the processes involved in the production, pathways, and outflow of HSSW, ISW, and AABW (Bergamasco et al., 2002; Budillon et al., 2003; Gordon et al., 2004; Smethie and Jacobs, 2005; Whitworth and Orsi, 2006; Gordon et al., 2009; Orsi and Wiederwohl, 2009; Budillon et al., 2011; Rusciano et al., 2013; Gordon et al., 2015; Castagno et al., 2017). HSSW directly contributes to AABW formation, escaping the continental shelf primarily through the Drygalski Trough, while ISW formed beneath the Ross Ice Shelf contributes by being exported via the Glomar Challenger Trough.

2.1.2.3 Prydz Bay/Cape Darnley

AABW originates from the Cape Darnley Polynya, located to the northwest of Prydz Bay (Ohshima et al., 2013), and to a lesser extent from the McKenzie Bay Polynya within Prydz Bay (Williams et al., 2016). Compared to the Weddell and Ross Sea continental shelves, detailed hydrographic observations started relatively late around Prydz Bay. After the early cruises by the Soviet Union, Australian cruises in the 1980s established the general circulation pattern in Prydz Bay (Smith et al., 1984; Nunes Vaz and Lennon, 1996). Australian hydrographic projects further clarified the water mass structure (Herraiz-Borreguero et al., 2015; Herraiz-Borreguero et al., 2016). From the 2000s, Japanese, Chinese, Russian, and Indian voyages collected hydrographic observations in most years (e.g., Yabuki et al., 2006; Antipov and Klepikov, 2017; Liu et al., 2018). Off Cape Darnley, a series of hydrographic and mooring observations have been made intermittently since the 2010s by the Japanese Antarctic Research Expedition (Aoki et al., 2020a; Aoki et al., 2022).

No statistically significant long-term trends have been reported for temperature and salinity so far (Schmidtko et al., 2014), although trends and interannual/decadal variability may emerge as more data are collected and the time series are extended (Figure 5E).

2.1.2.4 Adélie Land/George V Land

Oceanographic sampling along the Adélie Land and George V Land coasts completed by the USNS *Eltanin* in 1969 showed that a relatively fresh AABW variety was formed in the region and could be tracked offshore (Gordon and Tchernia, 1972). The continental shelf was rarely visited in following years, with the notable exception of the GLACIER79 voyage (Jacobs and Haines, 1982), until the World Ocean Circulation Experiment program began in the early 1990s. Rintoul (1998) brought together the new WOCE measurements and historical data to show that dense water exported from the Adélie Depression made a substantial contribution to the abyssal waters of the Australian Antarctic Basin. From the 1990s, French (e.g., Lacarra et al., 2011; Martin et al., 2017), American (e.g., Sambrotto et al., 2003), Japanese (e.g., Aoki et al., 2017), and Australian (e.g., Rintoul, 2007; Williams et al., 2010; Snow et al., 2018) expeditions completed comprehensive sampling of the Adélie continental shelf, including a rare mid-winter expedition to the Mertz Polynya (Williams and Bindoff, 2003). The multidecadal record has provided evidence of changes in HSSW properties over time (Aoki et al., 2005; Rintoul, 2007; Jacobs and Giulivi, 2010; Aoki et al., 2013), most notably a sharp reduction in salinity following calving of the Mertz Glacier Tongue (Shadwick et al., 2013; Lacarra et al., 2014; Aoki et al., 2017; Snow et al., 2018) (Figure 5E).

2.1.3 "Deep" Southern Ocean

In this section, we focus on *in situ* hydrographic observations collected in the polar Southern Ocean (south of approximately 60° S) and within/north of the ACC. These observations of AABW have begun to reveal how it has changed over recent decades.

2.1.3.1 Polar Southern Ocean

Over the polar Southern Ocean, multidecadal changes have been observed in the Weddell Sea, Ross Sea, and offshore East Antarctica thanks to a combination of early expeditions in the 1960s and 1970s and reoccupations of select hydrographic sections through the Global Ocean Ship-Based Hydrographic Investigation Program (GO-SHIP). Within the Weddell Basin, three hydrographic transects have been particularly frequently occupied over the past 30 years: A23 extends from the northern Weddell to South Georgia (Meredith et al., 2014), SR4 crosses the Weddell Sea from Cape Norvegia on the coast of Queen Maud Land to Joinville Island off the tip of Antarctic Peninsula (Fahrbach et al., 2004; Kerr et al., 2009; Kerr et al., 2018), and A12 sits along the Prime Meridian (Fahrbach et al., 2011). Outside of the Weddell Basin, two repeated transects capture long-term property changes in AABW sourced from the Weddell Sea: section SR1b spanning eastern Drake Passage south of Falkland Islands (Cunningham et al., 2003) and in the Vema Channel connecting the Argentine Basin and Brazil Basin (Campos et al., 2021). Abrahamsen et al. (2019) computed the AABW area along three hydrographic transects (A23, SR4, and SR1b) and identified a decadal decline of the dense water mass volume from the early 1990s to the mid-2010s, followed by a brief 4-year recovery until 2018. The most recent occupations at A23 and SR4 show that the decline of the AABW area has resumed (Zhou et al., 2023; Figure 6B). AABW warming has been detected in the Weddell Sea as well as freshening, even though the temperature signal is stronger in the densest waters (Figure 6A; Azaneu et al., 2013; Jullion et al., 2013; Zhou et al., 2023).

Directly downstream from the Ross Sea continental shelf, AABW has shown variability in volume, temperature, and salinity. A repeated hydrographic zonal section at 62°S (S4P) capturing the outflow from Cape Adare showed strong freshening between the 1990s and 2000s (Swift and Orsi, 2012). Subsequently, all repeated meridional GO-SHIP sections south of the Antarctic-Pacific ridge show the fresh anomaly being carried around the Ross Gyre and into the Bellingshausen Basin (Purkey and Johnson, 2013; Purkey et al., 2019). In addition, warming and a decrease in AABW volume were observed across the deep southern basin, possibly at an accelerated rate between the 2000s and 2010s (Purkey and Johnson, 2010; Desbruyères et al., 2016; Purkey et al., 2019). Recent observations at S4P show a recovery in AABW volume and salinity since 2018 near Cape Adare (Aoki et al., 2020b; Silvano et al., 2020; Gunn et al., 2023).

Offshore East Antarctica, varieties of AABW originate from the Adélie Coast, off Cape Darnley/Prydz Bay, and, possibly and to a lesser extent, from Vincennes Bay (Kitade et al., 2014; see Figure 3 for location). Several transects of precise, top-to-bottom observations were obtained from the *Eltanin* and *Conrad* from the late 1960s to the 1970s. GO-SHIP sections I06, I08, I09, SR3, P15, and SR4, as well as projects such as BROKE/BROKE-West (Bindoff et al., 2000; Meijers et al., 2010), extended the time series from the 1990s. In the Australian Antarctic Basin, AABW freshened during the period 1970s–1990s, and the freshening accelerated from the 1990s to the 2000s (Shimada et al., 2012; van Wijk and Rintoul, 2014; Menezes et al., 2017). From the mid-2010s, the freshening changed to salinification due to changes in the bottom water formed upstream in the Ross Sea (Aoki et al., 2020b; Silvano et al., 2020; Figure 6D). Changes in AABW layer thickness have closely followed those in salinity, with contraction between the 1970s and the 2000s and a rebound in the 2010s (Figure 6E). AABW warming has been observed over recent decades (Couldrey et al., 2013; van Wijk and Rintoul, 2014; Katsumata et al., 2015), concurrent with full-depth warming due to a multidecadal poleward shift of the ACC's southern branch (Yamazaki et al., 2021). There is a gap between I06 (30°E) and I08 (~80°E), and observations are less systematic. However, the southern tip of I7 (~60°E) was occupied in 2013, and the full section was completed in 2019/20, revealing a weak freshening of AABW over the continental slope (Aoki et al., 2020c; Anilkumar et al., 2021; Yamazaki et al.[1]). The observed

1 Yamazaki, K., Katsumata, K., Hirano, D., Nomura, D., Sasaki, H., Murase, H., et al. Revisiting circulation and water masses over the East Antarctic margin (80-150°E). *Progr. Oceanogr.* (In review).

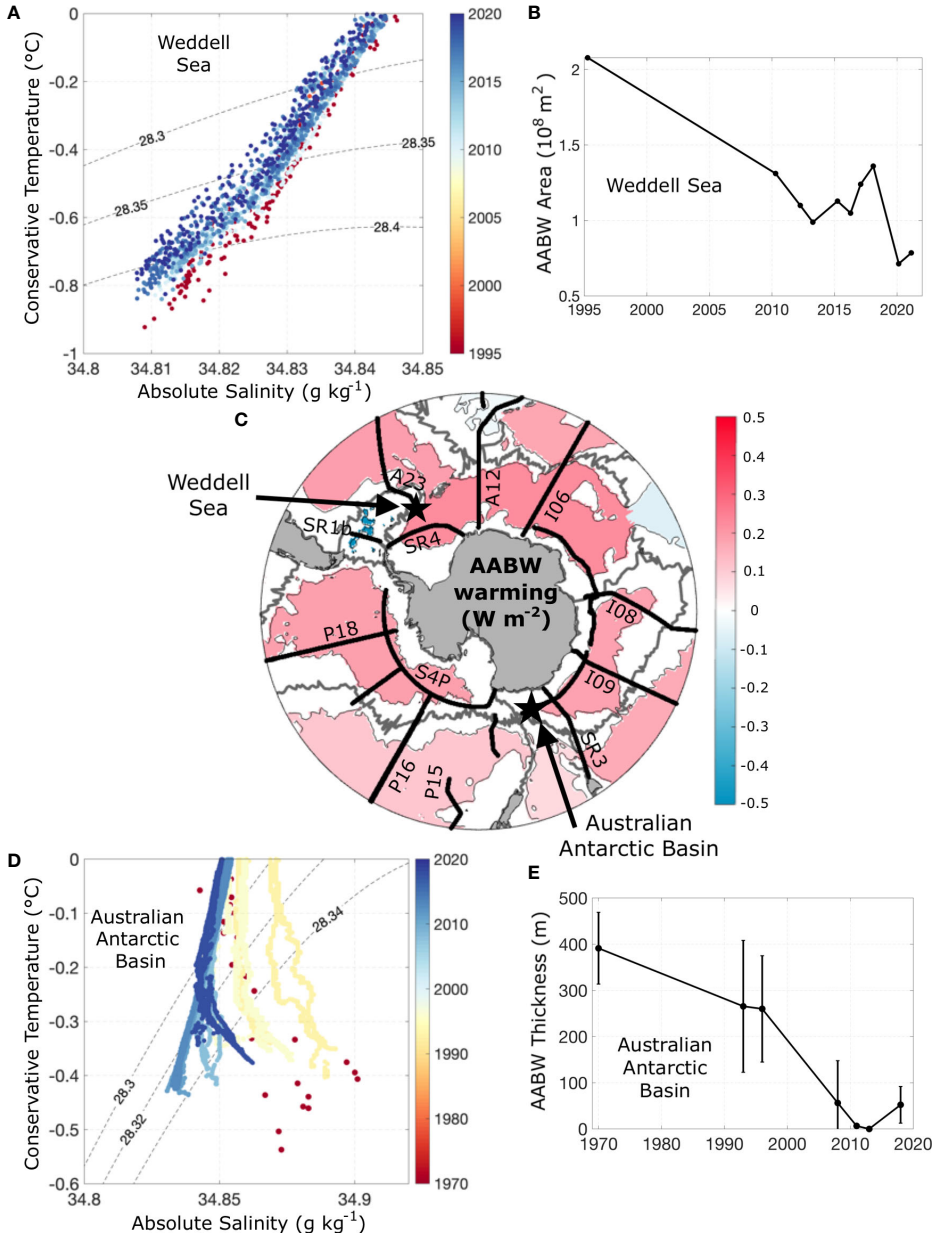

FIGURE 6
Decadal variability of Antarctic Bottom Water (AABW) properties from repeat hydrographic data. **(A)** Conservative temperature (°C) versus absolute salinity (g/kg) diagram in the Weddell Sea from measurements collected along the A23 line south of 60°S (see black star in panel C for location). **(B)** AABW area (m2) along the A23 line south of 60°S (Abrahamsen et al., 2019; Zhou et al., 2023; neutral density >28.4 kg/m^3). **(C)** AABW warming (W/m^2) between the 1990s and the 2010s (see Purkey and Johnson, 2010, for methodology; >4,000 m depth). **(D)** Conservative temperature versus absolute salinity plot in the Australian Antarctic Basin obtained by observations along the P11S line at 150°E (see black star in panel **C** for location). **(E)** AABW (neutral density >28.34 kg/m^3; Silvano et al., 2020) thickness (m) along 150°E. AABW density varies in different sectors and therefore AABW definitions change accordingly. GO-SHIP sections are depicted in black in **(C)**.

warming and freshening might be associated with the shoaling of the deep ventilation from East Antarctica (Shimada et al., 2022).

2.1.3.2 Antarctic Circumpolar Current and north

The hydrographic properties of AABW in the ACC region and to the north have been observed, mapped, and monitored from ship-based observations for decades. Reoccupations of GO-SHIP sections have revealed warming within AABW around the globe, accounting for ~10% of the total increase in ocean heat content (Purkey and Johnson, 2010; Desbruyères et al., 2016) plausibly owing to a decrease in AABW production rates (Masuda et al., 2010; Purkey and Johnson, 2012; Li et al., 2023). Within the Southern Ocean (Figure 6C), deep warming and declining AABW volume were noted as early as the 1980s in the western South Atlantic basin and continued through the 2020s (Coles et al., 1996; Johnson and Doney, 2006; Purkey and Johnson, 2010; Johnson et al., 2014; Desbruyères et al., 2016; Johnson, 2022). Similarly, deep warming over the past three decades has been observed in the Indian and

Pacific sectors (Fukasawa et al., 2004; Kawano et al., 2006; Johnson et al., 2007; Purkey and Johnson, 2010; Kouketsu et al., 2011; Desbruyères et al., 2016) with possible acceleration of the warming rate in the Southwest Pacific basin over the last decade (Johnson et al., 2019; Purkey et al., 2019).

2.2 Long-term moorings

Long-term moorings have been deployed in the Weddell Sea, Ross Sea, and Adélie Coast to observe shelf and bottom waters. Here, we report results from sustained programs that span decades of observations.

2.2.1 Weddell Sea

ISW formed beneath the Filchner-Ronne Ice Shelf escapes the cavity and flows northward through the Filchner Trough, spills over the Filchner Sill, and descends the continental slope forming AABW (e.g., Foldvik et al., 2004). The first hydrographic and current meter moorings aimed at monitoring the flow of ISW at the continental shelf break were deployed in 1968 by the Norwegians. The moorings were successfully recovered 5 years later. Year-long time series of velocities and temperature were obtained, but unfortunately, the mooring was placed outside the ISW plume (Foldvik et al., 1985b). At that time, the existence of an ISW plume was a theory only. The plume was first discovered in 1977, and moorings were deployed at its core at the Filchner Sill (Foldvik et al., 1985c). The position of Sill moorings (Figure 5D) proved to be a key site for monitoring the flux of ISW overflow (Foldvik et al., 2004). Renewal of the Sill moorings continues to extend this gappy but exceptionally long oceanographic time series from Antarctica (Figure 7A). These observations highlight the complex time variability in the ISW overflow, which is influenced by tides, mixing, and topographic waves (e.g., Semper and Darelius, 2017; Daae et al., 2019). Today, the ISW overflow is monitored by means of an array of subsurface instrumented moorings operated in cooperation between Norway, France, Germany, and the UK.

AABW originated from the south-western Weddell Sea is also monitored as part of a German observational effort. Since 1989, the Alfred Wegener Institute maintains a mooring array located in a cross-slope transect off the tip of the Antarctic Peninsula (NW moorings; see Figure 5D) that allows to study the time evolution of the dense plumes flowing along the continental slope in the northwestern Weddell Sea (Fahrbach et al., 2001; Llanillo et al., 2023). Further downstream, the US Lamont-Doherty Earth Observatory maintains moorings south of the South Orkney Islands (Figure 5D) that record two decades (since 1999) of AABW temperature and salinity properties exported from the western boundary of the Weddell Sea. The combination of these off-shelf moorings has allowed us to better understand Southern Ocean ventilation and its relation to the global climate system. Hydrographic properties and circulation of AABW can be altered by local changes in atmospheric, ice shelf, and sea ice characteristics and by shifts in large-scale wind stress patterns such as those

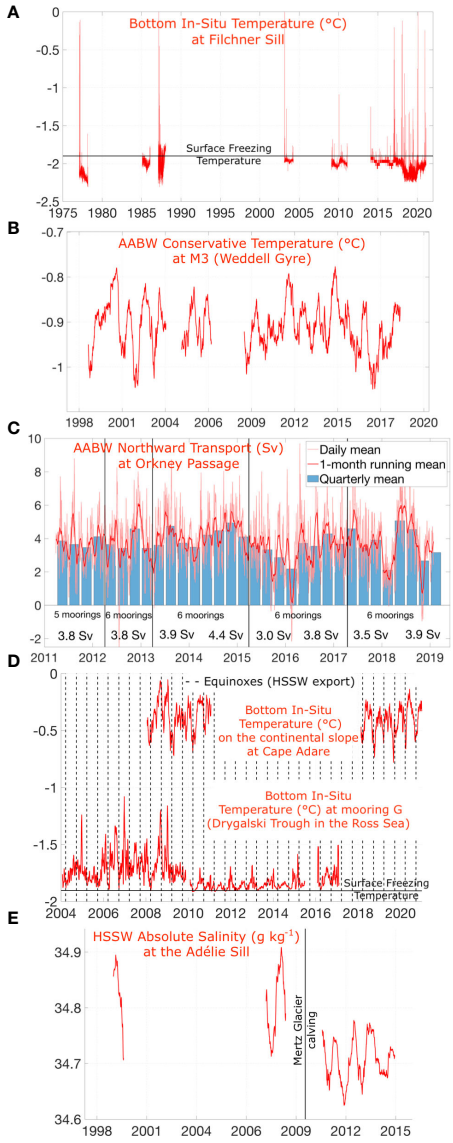

FIGURE 7
Temporal variability of Antarctic Bottom Water (AABW) properties from long-term mooring data. **(A)** *In situ* temperature (°C) observed near the seafloor at ~550 m depth at the Filchner Sill, Weddell Sea. Surface freezing temperature for a salinity of 34.7 g/kg is shown in solid black for reference. **(B)** AABW conservative temperature (°C) measured at ~4,500 m depth along the northern limb of the Weddell Gyre (M3 in Figure 5D). **(C)** Northward transport (10^6 m^3/s; Sverdrup (Sv)) of AABW through Orkney Passage (Abrahamsen et al., 2019; Spingys et al., 2021; AABW defined here in the density class $28.26 < \gamma^n < 28.40$ kg/m^3). The light red line indicates daily averages of transport through the mooring array, the thick red line is the 1-month running mean, and the blue bars are quarterly averages. Vertical black lines indicate mooring cruises to the area; the annual (April 1–March 31) mean AABW transport through the array is indicated at the bottom of the graph. **(D)** *In situ* temperature observed near the seafloor at ~ 500 m depth at mooring G in the Drygalski Trough and at Cape Adare (both in the Ross Sea near the shelf break and on the continental slope, respectively). Weak tides during equinoxes (dashed black lines) allow cold high-salinity shelf water (HSSW) to be exported from the shelf break (Bowen et al., 2023). Surface freezing temperature for a salinity of 34.9 g/kg is shown in solid black for reference. **(E)** HSSW absolute salinity (g/kg) at the Adélie Sill observed near the seafloor at ~600 m depth. Black line indicates the calving time of the Mertz Glacier Tongue (February 2010), after which HSSW salinity showed a decline (Snow et al., 2018). Locations of all moorings are shown in Figure 5 by red stars.

associated with the Southern Annular Mode (SAM) and El Niño/Southern Oscillation (ENSO) (McKee et al., 2011; Gordon et al., 2020; Llanillo et al., 2023; Zhou et al., 2023). AABW export detected since February 1999 reveals a distinct seasonal cycle as well as interannual variability (Figure 7B). The seasonal variability is associated with the shifting of the front located along the Antarctic Slope (Gordon et al., 2010). The interannual AABW variability is linked to the regional wind field, which varies with ENSO and SAM phases (McKee et al., 2011; Gordon et al., 2020; Llanillo et al., 2023).

Finally, since 2004, moorings have been deployed as part of the Lamont-Doherty Earth Observatory CORC-ARCHES (Consortium on the Ocean's Role in Climate—AbRupt climate CHangE Studies) project and more recently by the British Antarctic Survey in the Orkney Passage (Figure 5D), which has been identified as a key export region of AABW from the Weddell Sea (e.g., Naveira Garabato et al., 2002). The first 3 years consisted of temperature and salinity measurements at a single point. In 2007–2011, moorings that included current meters were deployed along the western flank of the passage, with five to six UK moorings covering the AABW layer across the full passage since 2011 and providing a sustained time series of AABW export from the Weddell Gyre (Figure 7C; Abrahamsen et al., 2019).

2.2.2 Ross Sea

In the Ross Sea, the first attempt to obtain a year-long time series of salinity, temperature, and currents was made in 1978. A mooring was deployed close to the Ross Ice Shelf to capture the ISW outflow, resulting in a 7-month record (Jacobs and Haines, 1982). A second successful attempt near this ice shelf was made in 1983 with an array of four moorings (Pillsbury and Jacobs, 1985). In 1994, the Italian CLIMA project deployed the first mooring to monitor HSSW in Terra Nova Bay. This mooring is still operating and is the longest mooring-based time series registered in the Ross Sea. It is part of a five-mooring array maintained by the Italian Marine Observatory on the continental shelf and positioned in Terra Nova Bay as well as close to the shelf break in three different troughs (see Figure 5C for location). The Korea Polar Research Institute (KOPRI) has been also operating moorings in Terra Nova Bay to study HSSW since 2014 in collaboration with New Zealand.

Since the early 1990s, in the Ross Sea, long-term moorings have been deployed mostly in the western sector to investigate HSSW and AABW formation processes, the seasonal cycle, and long-term variability of the water properties, along with the outflow of these dense waters from the continental shelf (Budillon et al., 2002; Buffoni et al., 2002; Whitworth and Orsi, 2006; Gordon et al., 2009; Muench et al., 2009; Padman et al., 2009; Budillon et al., 2011; Rusciano et al., 2013; Gordon et al., 2015; Castagno et al., 2017; Le Bel et al., 2021; Bowen et al., 2023). In Terra Nova Bay, the resulting time series have documented convection processes that occur during sea ice formation and showed the HSSW seasonal cycle and its link to atmospheric forcing (Buffoni et al., 2002; Rusciano et al., 2013; Le Bel et al., 2021) and glacier tongue effects (Stevens et al., 2017). Moorings positioned at the shelf break and on the continental slope by US (CALM and ANSLOPE), Italian (CLIMA and MORSea), and New Zealand (Ross Sea outflow experiment; Bowen et al., 2021; Bowen et al., 2023) programs have increased our understanding of the processes involved in AABW formation and export. Tides have been shown to be particularly important in both stages, acting on daily, seasonal (see Figure 7D), and potentially longer time scales (Whitworth and Orsi, 2006; Gordon et al., 2009; Muench et al., 2009; Padman et al., 2009; Castagno et al., 2017; Bowen et al., 2021; Bowen et al., 2023).

2.2.3 Adélie Land/George V Land

The first moorings sampling AABW formed on the Adélie coast on the continental slope were deployed by Japan in the period 1995 to 1996, revealing a seasonally varying plume of bottom water descending the slope (Fukamachi et al., 2000). French scientists deployed moorings in the polynya in Commonwealth Bay between 2008 and 2012 (Lacarra et al., 2014) and near the Mertz Glacier Tongue between 2008 and 2010 (Martin et al., 2017). The moored time series confirmed the production of a particularly salty variety of HSSW in Commonwealth Bay and helped resolve the seasonal and interannual variability of shelf water salinity. Australian moorings were deployed in the Mertz Polynya and across the Adélie Sill (see Figure 5B for location), an export pathway for HSSW, beginning in 1998: Williams et al. (2008) used moored time series from 1998 to 2000 to document the seasonal cycle of HSSW formation, export, and re-stratification and to provide the first direct estimates of the export of dense water from the continental shelf to the deep ocean. Snow et al. (2018) used 8 years of moored measurements at the Adélie Sill to quantify the impact of calving of the Mertz Glacier Tongue on HSSW formation and export (Figure 7E). The salinity and density of dense water leaving the shelf decreased immediately after the calving event and caused a reduction in AABW density and volume off-shelf, illustrating the rapid response of the deep ocean to local forcing anomalies on the continental shelf. The proximity of the Adélie Land region to the south magnetic pole makes direct velocity estimates challenging, requiring creative approaches to infer current direction (Williams et al., 2008; Marouchos et al., 2013; Martin et al., 2017).

2.3 Ice shelf cavities

While there is generally a focus on ice shelf basal melting in glaciological and sea-level-rise studies, the fate of glacial meltwater is of direct relevance to AABW production, as it helps set the conditions for the formation of (or lack thereof) Dense Shelf Waters (including ISW and HSSW; Herraiz-Borreguero et al., 2016; Williams et al., 2016; Silvano et al., 2018; Li et al., 2023). This dependence emphasizes the need for a better understanding of ice shelf basal melting, cavity circulation, and internal mixing (e.g., Foster, 1983; Stevens et al., 2020) as well as the need for year-round observations. Basal melting can be inferred from satellite estimates of ice thickness and flow (e.g., Moholdt et al., 2014) and downward-looking radar (autonomous phase-sensitive radio echosounders

(ApRES)) deployed on the ice surface (Brennan et al., 2013; Nicholls et al., 2015). Direct observations of ocean conditions and basal melting beneath the ice shelf can be obtained using a hot-water drill to gain access to the underlying water column (Makinson and Anker, 2014). Typical instruments used in this environment include cameras, sediment corers, water samplers, CTD, current meters, turbulence sensors, and hydrographic time series moorings. Here, we briefly review *in situ* observations collected through bore holes beneath the three largest ice shelves in Antarctica (the Ross, Filchner-Ronne, and Amery ice shelves), where ice–ocean processes are pivotal to the properties of AABW spread throughout the global ocean.

2.3.1 Filchner-Ronne Ice Shelf

The Filchner-Ronne Ice Shelf is the second-largest ice shelf by area (having an area of ~450,000 km^2) and the largest by volume. Since the late 1980s, hot-water drills have been used to make access holes at a variety of locations on the Ronne Ice Shelf (e.g., Nicholls et al., 2009), and, more recently on the Filchner Ice Shelf (Huhn et al., 2018; Hattermann et al., 2021), through ice thicknesses from 300 m up to 940 m (Figure 5D shows locations of the boreholes). These observations have allowed inference of the cavity circulation, ISW formation processes, and outflow from the cavity (Figure 5D depicts the circulation pathways within the cavity). HSSW formed in the polynya north of the Ronne Ice Shelf front descends along the southward deepening bathymetry (Johnson and Smith, 1997) to drive an anti-cyclonic thermohaline circulation. As a result of the pressure dependence of the melting point of ice, HSSW can drive basal melting over the deepest parts of the ice shelf, creating a colder, but fresher, and therefore slightly less dense ISW. As the ISW ascends the ice base and the pressure reduces, some refreezing takes place in the center of the ice shelf. ISW leaves the cavity primarily via the Filchner Trough, which connects the ice shelf cavity with the deep ocean (Foldvik et al., 1985a). The exact rates and time scales of these processes depend on a complex interplay between the buoyancy-driven circulation, strong tides (Makinson and Nicholls, 1999) that contribute to advection and drive mixing processes, and freshwater runoff from beneath the grounded ice sheet that causes further water mass transformations within the cavity (Huhn et al., 2018). Ice-cavity observations combined with historical measurements at the ice shelf front also revealed the presence of two distinct modes (Figure 8A), in which water masses in Filchner Trough were dominated by either Ronne HSSW-derived ISW (Ronne mode) or more locally derived Berkner-HSSW (Berkner mode) (Hattermann et al., 2021; Janout et al., 2021). On a multi-year time scale, the outflows in the Filchner Trough respond to variability in sea ice formation rates in the Ronne Polynya (Hattermann et al., 2021).

2.3.2 Ross Ice Shelf

The Ross Ice Shelf is the largest ice shelf by area (approximately 470,000 km^2). It is fed from both East and West Antarctica, and so, in terms of glaciology and sedimentology, it is often thought of as having two distinct sides (Rignot et al., 2013; Tinto et al., 2019). Its cavity was one of the first to be directly observed, at J9 during a multi-year borehole initiative in the late 1970s (Jacobs et al., 1979). Subsequent hydrographic borehole expeditions have included those in support of the 2002 Andrill project in Windless Bight (Robinson et al., 2010) and at Coulman High from 2010 to 2014 (Stewart et al., 2019; see Figure 5C for the location of boreholes in the northwestern sector of the ice shelf). The Windless Bight observations underpinned studies of the ISW plume exiting the

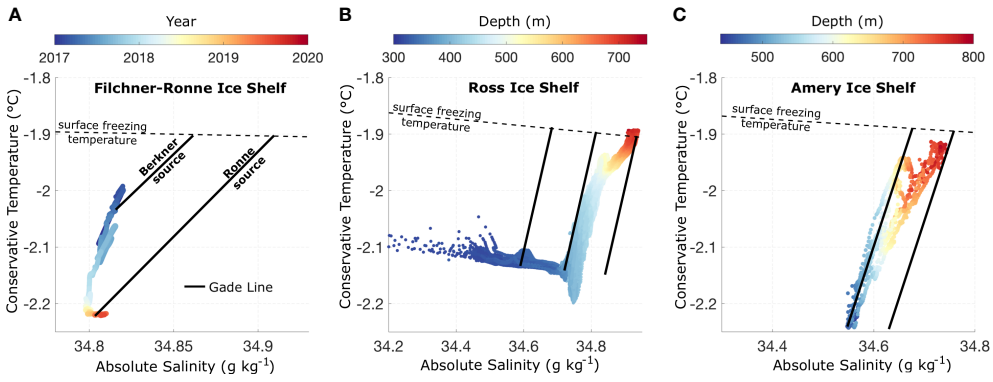

FIGURE 8
Variability of Ice Shelf Water (ISW) properties from data collected under ice shelves. **(A)** Conservative temperature (°C)–absolute salinity (g/kg) diagram for the Filchner-Ronne Ice Shelf cavity at FNE1 at the lowest instrument (960 m depth; Hattermann et al., 2021), color-coded according to the time of measurements. Between 2017 and 2019, ISW transitioned from Berkner to Ronne source as highlighted by the Gade Line (i.e., the mixing line between ISW properties and ISW source at the surface freezing temperature; Gade, 1979). **(B)** Conservative temperature–absolute salinity plot for the Ross Ice Shelf cavity at HWD-2, color-coded according to depth (m) (Stevens et al., 2020). By extrapolating the Gade Line from the ISW properties to the surface freezing temperature, we can infer that different sources with different salinity (range >0.2 g/kg) can drive melting. **(C)** Conservative temperature–absolute salinity diagram in the cavity of the Amery Ice Shelf at AM01, color-coded according to depth (Herraiz-Borreguero et al., 2013). The ISW source is water with salinity between approximately 34.65 and 34.75 g/kg. Locations of all sites are shown in Figure 5. The dashed black line represents the surface freezing temperature according to salinity.

Ross/McMurdo cavity and flowing northward, possibly sufficiently far north to influence the Terra Nova Bay Polynya (Robinson et al., 2014; Stevens et al., 2017). Such ISW outflows, both in McMurdo Sound and further to the east, are likely to influence sea ice production in the Ross Ice Shelf Polynya (Langhorne et al., 2015; Dale et al., 2017) and associated HSSW production.

The southernmost extent of the cavity was occupied in 2014 as part of the WISSARD program (Begeman et al., 2018). More recently, a sequence of borehole experiments and hydrographic moorings in the center (HWD; Stevens et al., 2020) and along the Kamb Ice Stream (KIS1 and KIS2; see Figure 5C for location; Lawrence et al., 2023) have sampled the oceanographic conditions in conjunction with glaciological and sedimentological studies, showing the vertical structure and illustrating how waters of different salinity drive basal melting of the Ross Ice Shelf (Figure 8B). The addition of hydrographic mooring data revealed the importance of tidal and convective mixing as an influence on cavity circulation.

2.3.3 Amery Ice Shelf

The Amery Ice Shelf, with an area of approximately 62,000 km^2, is the third largest embayed ice shelf in Antarctica. The deepest part of the southern grounding line is approximately 2.5 km below sea level (Fricker et al., 2002) where relatively high basal melt rates are observed (>2 m/year; Adusumilli et al., 2020). Approximately 25% of basal melt is thought to refreeze as marine ice (Wen et al., 2010; Galton-Fenzi et al., 2012). The Amery Ice Shelf system has long been a focus of Australian Antarctic research since the 1960s (e.g., Budd, 1966). During the 21st century, the importance of ice–ocean interactions beneath this ice shelf became fully apparent, leading to the establishment of the "Amery Ice Shelf Ocean Research (AMISOR)" project. This multidisciplinary project had overall aims of quantifying interactions between the ocean and the ice shelf and determining the implications for grounded ice discharge and water mass modification. The AMISOR project successfully drilled six boreholes (see Figure 5A for location). The hot-water drilling started in 2001 and concluded in 2006. Each borehole had a mooring with three microCATs measuring temperature, salinity, and pressure, distributed vertically to cover the whole water column. The complete AMISOR time series spans from 2001 to 2013 and provides one of the longest time series of ocean properties ever recorded from the cavity of an ice shelf. Under-ice shelf measurements reveal that ISW originates from HSSW of salinity between approximately 34.65 and 34.75 g/kg (Figure 8C) and that the formation of the marine ice layer is subject to seasonal variability in the HSSW inflow into the cavity (Herraiz-Borreguero et al., 2013). Between July and November, HSSW inflow causes a re-stratification of the water column within 80 km of the ice shelf front, steepening the density surfaces and allowing ISW to upwell and reach a new *in situ* freezing temperature. It is during this period that frazil ice formation and deposition occur (Herraiz-Borreguero et al., 2013). The timing and duration of ISW outflow play a critical role in conditioning the water column within the Mackenzie Bay Polynya prior to the start of sea ice formation (Herraiz-Borreguero et al., 2015; Herraiz-Borreguero et al., 2016). The outflow of ISW limits the efficiency of the Mackenzie Bay Polynya to form HSSW, affecting the final HSSW temperature and salinity and ultimately AABW formation (Williams et al., 2016). In fact, the outflow of ISW delays the onset of deep convection on the continental shelf by 2 to 6 months (Herraiz-Borreguero et al., 2016).

2.4 Tracers

Several tracers have been used to track the formation and spreading of AABW. The most widely used have been chlorofluorocarbons (CFCs), but several others have been employed (sea water isotopes, dissolved oxygen, radiocarbon, noble gases, and nutrients). Here, we provide a brief overview starting with CFCs.

2.4.1 CFCs

Since the 1930s, atmospheric concentrations of chlorofluorocarbons (CFC-11 and CFC-12) and sulfur hexafluoride (SF6) have varied following their usage as industrial compounds. These known time-dependent atmospheric concentrations, coupled with their conservative nature in the ocean interior, have made them an excellent tool for tracing AABW formation and pathways throughout the abyssal ocean (Fine, 2011; Purkey et al., 2018; Ohashi et al., 2022). Furthermore, CFC observations have been used to quantify AABW contribution to the sequestration of anthropogenic carbon in the deep ocean, highlighting its increase in AABW in recent decades in all ocean basins (e.g., Matear and McNeil, 2003; Ríos et al., 2012; Murata et al., 2019; Mahieu et al., 2020) and for validating AABW formation and pathways in ocean models (e.g., Sasai et al., 2004; Müller et al., 2006; Solodoch et al., 2022).

Circumpolar analyses of CFC concentrations within the deep Southern Ocean capture AABW formation and outflow from the Weddell Sea, Ross Sea, and Adélie Coast (Figure 9 illustrates CFC-11 map in 2021) and have been used to infer a net AABW production rate of 8.1 Sv (1 Sv = 10^6 m^3/s) considering a layer of neutral density >28.27 kg/m^3 (Orsi et al., 1999). This inferred transport is consistent with the 5- to 15-Sv estimated rates from hydrographic observations, despite large uncertainties and slightly different definitions of AABW (Gill, 1973; Carmack, 1977; Jacobs et al., 1985). A broader definition of northward-flowing AABW that includes a mixture with the overlying CDW adds an extra 9.4 Sv (Orsi et al., 2001; Orsi et al., 2002), leading to a total estimated transport of 17.5 Sv (Orsi et al., 2002). Outside the Southern Ocean, local maxima in CFCs highlight deep western boundary currents carrying AABW north in the Indian, Pacific, and Atlantic Oceans (Purkey et al., 2018).

Within AABW formation regions, CFCs have been used to study the dynamics of AABW formation and quantify regional AABW formation rates. Orsi et al. (1999) indicated that 60% (4.1 Sv) of AABW originates in the Atlantic sector of the Southern Ocean and 40% (3.2 Sv) in the Indian-Pacific sector. In the Ross Sea, CFCs within shelf waters suggest that 0.88 Sv of HSSW is converted to ISW in 4 to 7 years while circulating under the glacial ice before flowing off the continental shelf (Smethie and Jacobs, 2005; Loose et al., 2009; Rivaro et al., 2015). The CFC-tagged shelf water reveals

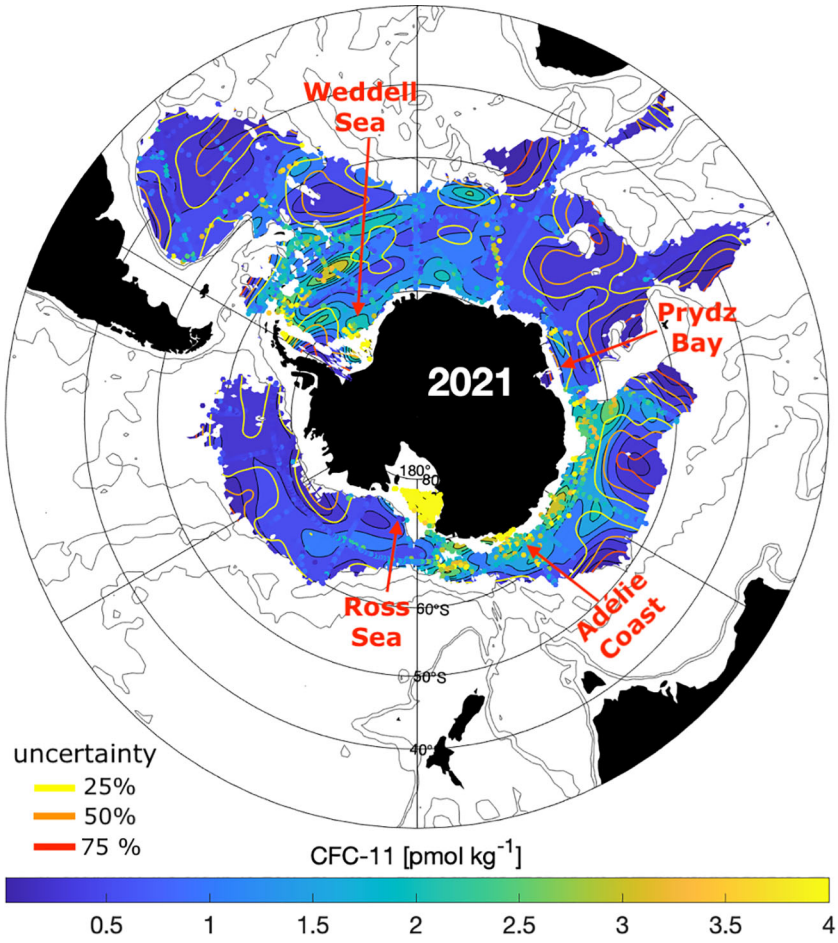

FIGURE 9
CFC-11 used as a tracer to map Antarctic Bottom Water (AABW). Reconstructed map of CFC-11 concentration in 2021 for water denser than 28.27 kg/m^3 (i.e., AABW). Objective mapping following Cimoli et al. (2023). Dots indicate available observations, whereas solid lines indicate uncertainty in the reconstruction (color-coded as shown in the legend). Note that in large areas of the Southern Ocean, the uncertainty is over 50%, as very few CFC data are available. Red arrows show the main areas of AABW formation.

dual locations of deep water production, with a larger production on the west side of the Ross Basin and a more moderate production from the Glomar Challenger Trough (Gordon et al., 2009) with a high-CFC signature seen in the plume of shelf water flowing into the deep currents along the continental slope (Purkey et al., 2018). CFC concentrations revealed a similar dual production of deep water along the Adélie–George V Coast, with high- and low-salinity abyssal waters being exported from the Adélie and Mertz Sills, respectively (Williams et al., 2010). In the Weddell Sea, CFC-based estimates suggest at least 3.5 Sv of AABW production (Mensch et al., 1996; Meredith et al., 2001a), with discrepancies in estimates of the contributions reaching the Atlantic and Indian Oceans. Haine et al. (1998) estimated 0.8 to 1.6 Sv of AABW transport into the South Indian Ocean, while Meredith et al. (2001a) estimated 3.2 Sv into the Indian Ocean and 0.9 Sv into the South Atlantic. Furthermore, repeated CFC observations have suggested a 15% to 21% decline in ventilation rates of bottom waters in the Weddell Gyre in the 27-year long period from 1984 to 2011 (Huhn et al., 2013). Finally, Meredith et al. (2013) used CFCs and SF6 to demonstrate the trapping and retention of AABW in deep trenches as it flows northward from source regions in the Weddell Sea, creating remarkably strong deep stratification due to temporal changes in the unimpeded waters flowing above. In general, comparison between different regional estimates of AABW formation rates is challenging, as AABW is defined in different ways in different studies, typically based on neutral density or temperature (e.g., neutral density >28.27 kg/m^3 in Orsi et al., 1999; potential temperature<0°C in Meredith et al., 2001a).

2.4.2 Other tracers

In addition to CFCs, other tracers can be used to investigate AABW in terms of both freshwater input (oxygen isotopes and noble gases) and abyssal ventilation (dissolved oxygen and radiocarbon).

The motivation to use stable oxygen isotopes of seawater ($\delta^{18}O$, the ratio between $H_2{}^{18}O$ and $H_2{}^{16}O$) along with hydrographic parameters arises from the need to disentangle freshwater sources that ultimately control abyssal water properties. Continental ice is very isotopically light (depleted in the $H_2{}^{18}O$ molecule and thus with low $\delta^{18}O$ values), and this signal is transferred into shelf waters

through glacial melt input during processes at the ice shelf/iceberg–ocean boundary (Weiss et al., 1979; Schlosser et al., 1991; Weppernig et al., 1996; Akhoudas et al., 2020). Oceanic measurements of $\delta^{18}O$ can thus reveal in striking detail how abyssal water masses form by using simple mass balance calculations in which water mass concentrations including glacial melt can be computed (Meredith et al., 2001b; Meredith et al., 2008). In "cold" regime areas of Antarctica such as the Weddell and Ross Seas, where HSSW flows into ice shelf cavities and gains glacial meltwater, the resulting ISW that is exported northward is easily discernable by its depleted isotopic signature and is composed of up to 8% of glacial melt (Schlosser et al., 1990; Loose et al., 2009; Akhoudas et al., 2020). Compiling $\delta^{18}O$ observations from 1973 to 2017 in the Weddell Gyre, Figure 10A shows the isotopic signature of the bottom water layer and clearly highlights the newly ventilated dense waters from the shelf becoming isotopically enriched (i.e., higher $\delta^{18}O$ values) as they entrain the old CDW along the continental slope; this process is critical to the production of AABW and feeds the along-slope current. The distribution of meltwater links the rate of ice melting to the bottom water formation with an AABW production of ~8 Sv in the Weddell Sea, including 55% of newly ventilated HSSW and ISW (Akhoudas et al., 2021). Noble gases such as helium and neon can also be used to trace glacial meltwater in Antarctica (e.g., Huhn et al., 2018). Noble gases are typically present in low concentrations in oceanic waters, and a high excess of helium and neon can be used to estimate fractions of glacial meltwater in polar oceans. While glacial meltwater only represents a small proportion of waters sourced in the southern high latitudes, increasing glacial melt content in shelf waters has the potential to decrease their salinity, slowing their formation with consequences on the AABW export (Silvano et al., 2018).

Other dissolved gases can also act as dye tracers that help to define and identify water masses (Talley et al., 2011; Rae and Broecker, 2018; Liu and Tanhua, 2021). Once waters descend below the ocean surface, they carry a signature of gases taken up by surface waters when in contact with the atmosphere. In the cold Antarctic seas, the capability for water to absorb atmospheric gases is relatively high, although the sea ice cover can partially impede air–sea exchanges (Watts et al., 2022). Spatial variations in the efficiency of air–sea gas exchange and ocean circulation patterns confer AABW with a clear signature in several gases, including dissolved oxygen and radiocarbon. The global spatial distribution of dissolved gases has played an important role in identifying the sources and pathways of AABW in the modern ocean (e.g., Sverdrup et al., 1942; GO-SHIP; de Lavergne et al., 2017; Purkey

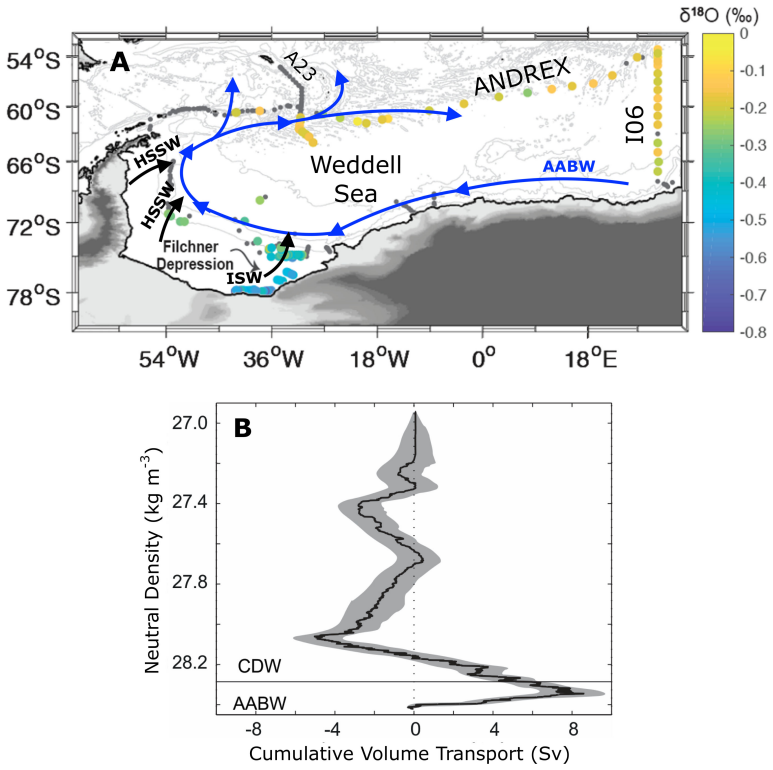

FIGURE 10
$\delta^{18}O$ and inverse modeling to quantify Antarctic Bottom Water (AABW) formation processes. **(A)** Spatial map of observed AABW $\delta^{18}O$ in the Weddell Sea. $\delta^{18}O$ is shown on the 28.37 kg/m^3 neutral density surface to capture the densest AABW variety that originates on the continental shelf of the south-western Weddell Sea. Gray dots represent profiles where density near the bottom is less dense than 28.37 kg/m^3. AABW circulation is shown by blue arrows, while areas of high-salinity shelf water (HSSW) and Ice Shelf Water (ISW) export are in black. Repeated GO-SHIP sections I06, A23, and ANDREX (Jullion et al., 2014) are highlighted. **(B)** Accumulated volume transport across the combined ANDREX–I06 section (positive is transport directed out of the Weddell Sea; see **(A)** for location; Naveira Garabato et al., 2016). Uncertainty is shown in gray. Related calculations indicate 13.3 ± 3.2 Sv of Circumpolar Deep Water (CDW) and AABW less dense than 28.345 ± 0.008 kg/m^3 are transformed into both denser AABW by downslope convection around the gyre's south-western rim (8.4 ± 2.0 Sv) and upper ocean waters less dense than 28.061 ± 0.011 kg/m^3 by upwelling within the Weddell Gyre (4.9 ± 2.0 Sv). The value 28.27 kg/m^3 is included for reference (horizontal black line).

et al., 2018; Rae and Broecker, 2018) and in the "paleo ocean" (e.g., Williams et al., 2019; Glasscock et al., 2020; Rafter et al., 2022). Such tracers have also begun to provide information about the causes of AABW variability, including its production rate, and how it ventilates the deep ocean (van Wijk and Rintoul, 2014; Katsumata et al., 2015; Gunn et al., 2023). With continuing data collection and increased availability, improved techniques (e.g., Cimoli et al., 2023), and combination with synthetic tracers from models (e.g., Solodoch et al., 2022), dissolved gases can provide further insight into the variability of AABW over the past century.

3 New observing systems

3.1 Profiling floats

Profiling floats are part of the Argo program and have revolutionized the field of oceanography and the ability to monitor the ocean since the 2000s (Riser et al., 2016). Such floats were designed to autonomously measure ocean properties (temperature, salinity, and pressure) between the surface and 2,000 m depth, usually every 10 days, and in areas not covered by sea ice. This design precluded monitoring of AABW and its source waters on the Antarctic continental shelf. However, over the last decade, new technological developments have enabled profiling floats to sample under sea ice (Klatt et al., 2007; Riser et al., 2016) on the Antarctica continental shelf and below 2,000 m depth ("Deep Argo" floats).

Profiling floats have been deployed on the Antarctic continental shelf since the 2010s (see Figure 11A). These floats are designed not to surface when a specified threshold is reached (for example, when the ocean temperature falls below a certain value) in order to avoid sea ice encounters. This threshold can be chosen depending on the environmental setting and experimental design. As the position of the floats is unknown when sea ice is present, different interpolation schemes and acoustic tracking methods have been employed to reconstruct the under-sea ice trajectories. These include simple linear interpolation between known positions or more sophisticated

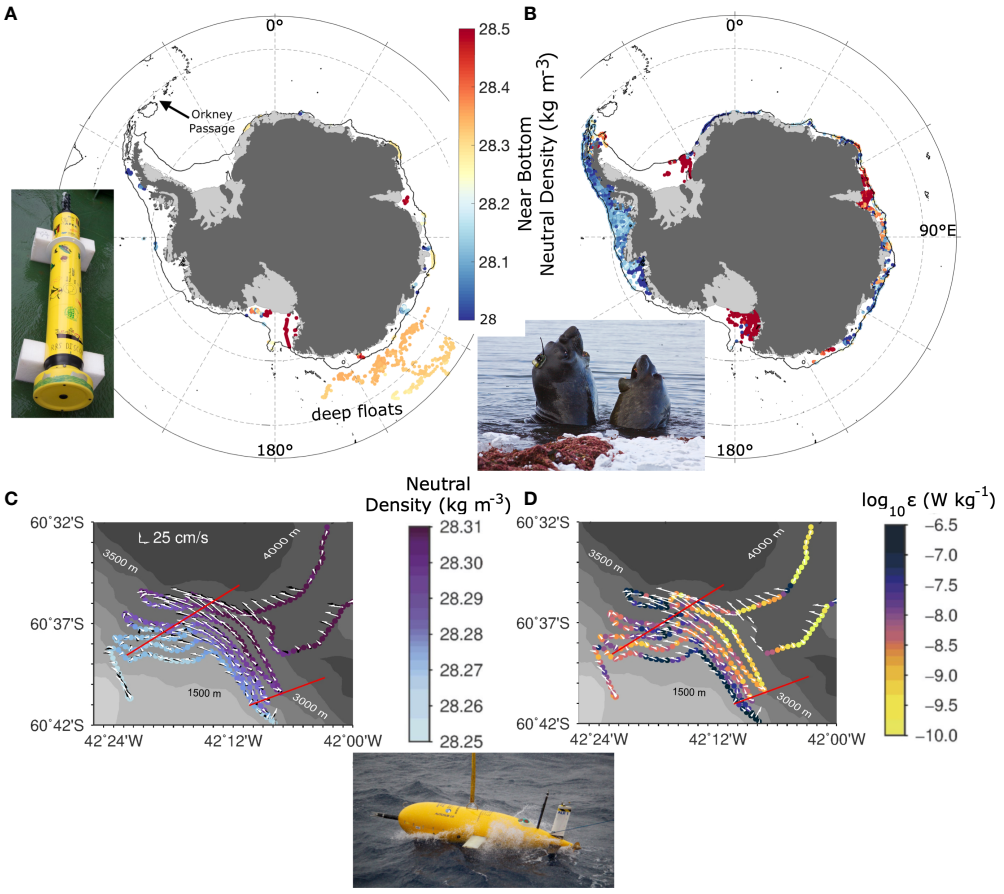

FIGURE 11
(A) Examples of new observing systems that can map Antarctic Bottom Water (AABW). Near-bottom neutral density (kg/m^3) obtained by profiling floats (on the continental shelf) and by deep floats (off the continental shelf). **(B)** Neutral density extracted by conductivity–temperature–depth (CTD)-instrumented seals at the deepest level reached at each location. The black line in panels **A** and **B** indicates the 1,000-m isobath, delimiting the continental shelf. Maps of **(C)** neutral density and **(D)** the rate of turbulent kinetic energy dissipation (W/kg), which quantifies mixing, measured by Autosub Long Range at ~90 m above the sea floor in the Orkney Passage (color). See **(A)** for location of Orkney Passage. Horizontal velocity averaged over 50–75 m (black vectors) and 125–150 m (white vectors) above the sea floor, bathymetry (gray shading), and two high-resolution CTD sections (red lines labeled B3 and B4), are shown in both **(C, D)** Adapted from Naveira Garabato et al. (2019). Images of a profiling float (P. Abrahamsen), CTD-instrumented seal (C. R. McMahon, IMOS Animal Tagging), and Autosub Long Range (A. Naveira Garabato) are shown in **(A-D)**, respectively.

methods that consider bathymetry, potential vorticity, sea level, and ocean density (Wallace et al., 2020; Yamazaki et al., 2020; Oke et al., 2022). It is also common to park floats at the seafloor between consecutive profiles to avoid strong drifting along and away from the continental shelf (e.g., Porter et al., 2019; Silvano et al., 2019; Wallace et al., 2020; van Wijk et al., 2022). These floats have been deployed in many locations around Antarctica, providing new insights into the seasonality of the mixed layer and its impact on shelf properties (e.g., Porter et al., 2019; Silvano et al., 2020).

Deep Argo floats, with the ability to profile to either 4,000 m or 6,000 m depth and under sea ice, can provide year-round observations of the abyssal ocean. Presently, the floats have been deployed in regional pilot arrays in specific basins where changes in bottom water had been previously observed through traditional shipboard hydrographic surveys. The arrays of Deep Argo floats simultaneously sample AABW throughout these basins at a significantly higher frequency than repeat hydrographic sections (every 10 days compared to years apart), thus providing a new perspective of AABW variability and circulation. The first array was deployed in the Southwest Pacific basin, with original test deployments in 2014 and deployment of a more complete array in 2016. The resulting data allowed for the quantification of recent AABW warming (Johnson et al., 2019) and abyssal transport (Zilberman et al., 2020) in that basin. In 2018, the first Antarctic pilot array was deployed in the Australian Antarctic Basin (see Figure 11A), and in 2019, another pilot array was deployed in the Brazil Basin. These floats are already providing new information about the pathways and variability of AABW (Johnson et al., 2020; Thomas et al., 2020; Foppert et al., 2021). The Deep Argo floats have offered a new perspective on AABW, despite the technology still being relatively new, and they are poised to transform our understanding of AABW variability and circulation as the pilot arrays transform into a global fleet.

3.2 Seals

Marine mammals, in particular Elephant (Southern *Mirounga leonina*) and Weddell (*Leptonychotes weddellii*) seals, equipped with biological and physical electronic sensors, such as CTD instruments (Nicholls et al., 2008; Roquet et al., 2013), have provided unique observations in the Southern Ocean (see McMahon et al. (2021) for a full discussion). Seals have the ability to dive to the seafloor (up to ~2,000 m depth for elephant seals) and under sea ice, providing year-round observations in regions hard to reach (such as the Antarctic continental shelf; see Figure 11B), especially in the winter months. Temperature and salinity profiles collected by seals have delivered new insights into the formation of dense waters on the Antarctic continental shelf (e.g., Nicholls et al., 2008; Ohshima et al., 2013; Kitade et al., 2014; Williams et al., 2016; Portela et al., 2021). These data have highlighted factors limiting dense water formation, including intrusions of warm CDW onto the shelf (Ribeiro et al., 2021; Herraiz-Borreguero and Naveira Garabato, 2022) and glacial meltwater input from melting ice shelves (Williams et al., 2016; Silvano et al., 2018; Ribeiro et al., 2021).

3.3 AUVs and gliders

Recent advances in long-endurance autonomous robotic technologies are beginning to open up new avenues for AABW observation. In particular, the advent of deep ocean gliders (Osse and Eriksen, 2007; Testor et al., 2019) and autonomous underwater vehicles (AUVs; Furlong et al., 2012; Roper et al., 2021) capable of measuring in waters as deep as 6,000 m over distances of up to several thousand kilometers and periods of several months are enabling the controlled, spatially targeted observation of AABW properties and flow with fine spatio-temporal resolution—reaching areas that are difficult to access with ship-deployed instrumentation or drifting platforms. Examples include AUV (Jenkins et al., 2010; Davis et al., 2022; Davis et al., 2023) and glider (Nelson et al., 2017; Friedrichs et al., 2022) missions under Antarctic ice shelves, as well as glider campaigns on the continental shelf (Kohut et al., 2013) and AUV deployments in the abyssal Southern Ocean (Naveira Garabato et al., 2019).

The potential of these technologies to advance understanding of processes relevant to AABW is illustrated by measurements of the flow through the Orkney Passage, a key chokepoint in the equatorward export of the AABW formed in the Weddell Sea (Naveira Garabato et al., 2002; Jullion et al., 2014). During a 3-day mission, the AUV Autosub Long Range (Figures 11C, D) acquired hydrographic, velocity, and turbulent microstructure data within 100 m of the seafloor along a ~180-km track, with an along-track resolution of a few meters (Naveira Garabato et al., 2019). This new mode of AABW observation unveiled the occurrence of important, previously undocumented submesoscale dynamics, suggested to be centrally implicated in the wind-forced regulation of the deep ocean heat budget of the South Atlantic (Meredith et al., 2011; Naveira Garabato et al., 2019). Autonomous robotic missions have also been deployed under ice shelves, including the Filchner-Ronne Ice Shelf (AUV; Davis et al., 2022) and Ross Ice Shelf (gliders; Nelson et al., 2017). As the endurance and robustness of autonomous robotic assets expand in coming years, it is expected that the AABW observing system will increasingly rely on these technologies for process-understanding and monitoring AABW characteristics across key circulation pathways.

4 Indirect approaches

4.1 Inverse modeling

Inverse modeling has, to date, been the most widely used indirect approach to quantitatively determine AABW circulation on regional-to-basin scales. In their most common form, inverse models (Wunsch, 1996; McIntosh and Rintoul, 1997) enable the assessment of the "steady state" ocean circulation that is consistent with both observations (e.g., measurements of hydrographic and biogeochemical variables along transects bounding a closed box) and fundamental dynamical and thermodynamical constraints (e.g., hydrostatic and geostrophic balance; conservation of mass, heat, and salt). Inverse models of this type (commonly referred to as

"box-inverse models") are formally underdetermined (Wunsch, 1996). As they have an infinite number of possible solutions, generating a realistic and physically insightful circulation requires that the models' initial conditions and uncertainties be defined judiciously under firm guidance from observations and sound physical principles.

The view of AABW circulation emerging from box-inverse models spanning the circumpolar domain (Ganachaud and Wunsch, 2000; Sloyan and Rintoul, 2001; Lumpkin and Speer, 2007; Naveira Garabato et al., 2014) is one of significant AABW production within, and equatorward export along, each of the three major Southern Hemisphere basins. AABW denser (neutral density) than 28.27 kg/m^3 is assessed by these models to form at a circumpolar rate of approximately 7 to 20 Sv, with the factor of three variations being attributed to uncertainties associated with differing model formulations (e.g., different assumed flow-governing physics or locations of observational transects). At the regional scale, inverse modeling has been performed in the Weddell Sea, providing an estimate of AABW production in the south-western Weddell Sea of 8 Sv (Jullion et al., 2014; Naveira Garabato et al., 2016; see Figure 10B).

4.2 Remote sensing

The many observational challenges associated with direct observation of AABW, noted in previous sections, have motivated efforts to indirectly observe AABW, for example, using remote sensing technologies. To date, the only aspect of AABW that has been systematically estimated via remote measurements is the rate of sea ice formation in coastal polynyas around Antarctica (Tamura et al., 2008; Tamura et al., 2016). These studies developed a thin ice thickness algorithm using Special Sensor Microwave Imager (SSM/I) and estimated sea ice formation from a heat budget analysis with the assumption that all the heat loss is used for ice formation. Higher spatial resolution estimates by Nihashi and Ohshima (2015) used the Advanced Microwave Scanning Radiometer-EOS (AMSR-E) data.

Recent work highlights the importance of underwater frazil ice production in Antarctic coastal polynyas (Thompson et al., 2020; Ohshima et al., 2022). The underwater frazil ice formation prevents heat-insulating surface-cover ice from forming, thereby enabling efficient ice production. A thin ice algorithm that detects active frazil, a mixture of frazil/pancake ice and open water, has been developed for AMSR-E (Nakata et al., 2019) and SSM/I (Kashiwase et al., 2021), which provides a more accurate estimation of sea ice formation. Figure 2B shows the updated map of sea ice formation based on that algorithm. The three polynyas exhibiting the highest sea ice formation rate (Ross Ice Shelf Polynya, Cape Darnley Polynya, and Mertz Polynya) correspond to three of the four major AABW formation sites. Sea ice formation in the Mertz Polynya, however, abruptly decreased due to the glacier calving in 2010 (see the lower panels in Figure 2B), resulting in a decrease in AABW formation (Aoki et al., 2013; Snow et al., 2018). This example demonstrates that the variability of AABW is closely linked to sea ice formation in coastal polynyas. In addition, recent changes in AABW formed in the Ross Sea have also been suggested to be associated with variability in sea ice formation (Silvano et al., 2020).

While satellite-derived estimates of sea ice formation provide useful information on AABW formation and variability, surface freshwater/buoyancy fluxes do not directly quantify the rate of dense water formation, as the transformation rate also depends on the surface density gradients (Abernathey et al., 2016; Groeskamp et al., 2019). The rate of AABW formation also depends critically on the entrainment/mixing occurring over the continental shelf and slope (e.g., Akhoudas et al., 2021; Bowen et al., 2021). After forming and descending the Antarctic continental slope, AABW spreads at depths that are not directly observable using remote sensing techniques. However, there is precedent for observing components of the ocean's overturning circulation indirectly via satellite measurements of sea surface height (SSH; Chelton et al., 2001), sea surface temperature (SST; Deser et al., 2010), and ocean bottom pressure (OBP; Tapley et al., 2019). Indeed, there is now a substantial body of research devoted to the identification of "fingerprints" of Atlantic Meridional Overturning Circulation (AMOC) variability in SSH and SST and to the use of SSH and OBP measurements for reconstruction of subsurface meridional transports in the North Atlantic (see Frajka-Williams et al., 2019, and references therein).

Recent studies have explored the possibility of using satellite measurements to observe the circulation of AABW. All of these studies are founded on the dynamical link between the meridional geostrophic transport of AABW and the zonal momentum balance, as indicated schematically in Figure 12A. Zonal momentum input from surface winds is removed at the sea floor via topographic form stress (TFS) (see, e.g., Olbers et al., 2004). The geostrophic meridional transport of AABW, T_{AABW}, is exactly related to the difference between the interfacial form stress (IFS) at the isopycnal upper bound of the AABW layer and the TFS at the sea floor (Stewart and Hogg, 2017; Stewart et al., 2021).

$$|f|\rho T_{AABW} = IFS - TFS, \quad (1)$$

where f is the Coriolis parameter and ρ is a reference density. Assuming that IFS varies slowly, Eq. (1) implies that variations in TFS, expressed as changes in OBP (Olbers et al., 2004), control AABW transport. The equivalent barotropic structure of the ACC means that these TFS changes may have an expression in SSH.

For example, Mazloff and Boening (2016) used the Southern Ocean State Estimate (SOSE; Section 4.3) to show that variability in the deep, geostrophic flow of AABW into the Pacific could be inferred from OBP measurements. Mizobata et al. (2020) combined SSH measurements with *in situ* hydrography to compute the export of AABW by a series of standing eddies in the Indian sector of the Southern Ocean and showed that the velocity structure is amenable to indirect inference from satellite observations alone. Stewart and Hogg (2017) performed controlled experiments using an idealized high-resolution channel model of the ACC to show that changes in the multi-annual-mean export of AABW lead to potentially measurable signatures in SSH and OBP. Figure 12C schematically

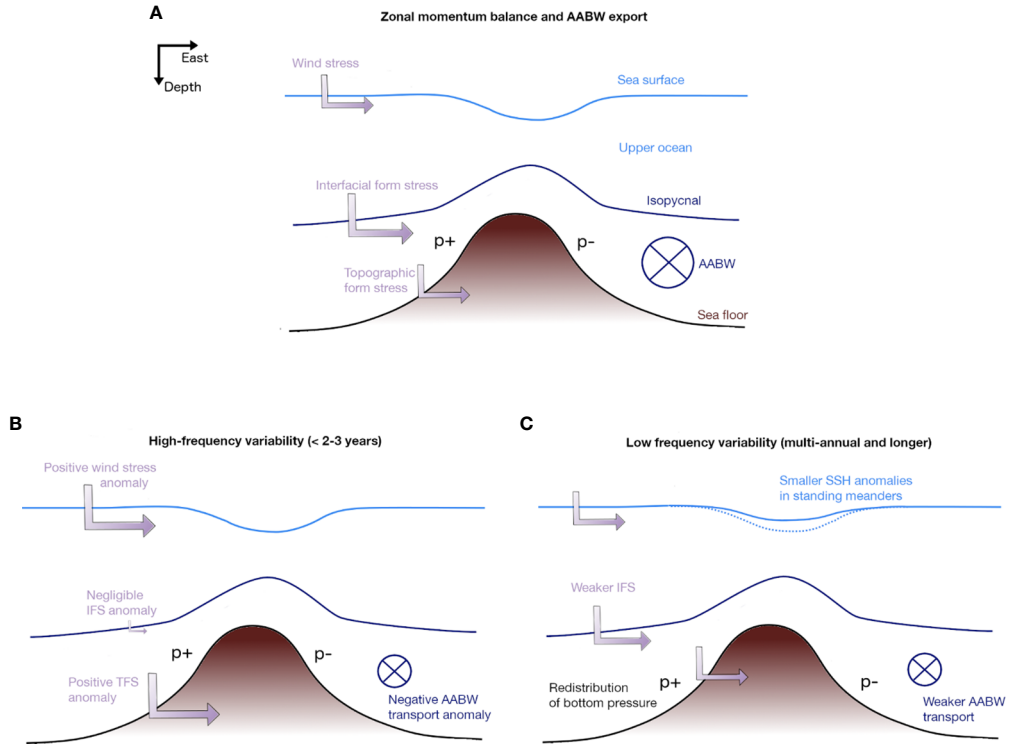

FIGURE 12
Schematic of dynamical links with Antarctic Bottom Water (AABW) transport variability, offering potential approaches to indirect observation of AABW circulation. **(A)** Mean northward flow of AABW across the Southern Ocean abyss (dark blue) and mean zonal momentum balance (purple arrows/labels). The AABW flow and momentum balance are linked via geostrophy in the AABW layer, which requires that the interfacial form stress (IFS) at the top of the AABW layer exceeds the topographic form stress (TFS). **(B)** Regarding time scales shorter than a few years, zonal wind stress fluctuations induce a primarily barotropic response and thus fluctuations in the TFS but are too rapid to produce a substantial baroclinic response and adjustments of the IFS (Ward and Hogg, 2011). Consequently, AABW transport fluctuations on these time scales are primarily due to wind variability (Stewart et al., 2021). **(C)** On multi-annual time scales, temporal fluctuations in AABW transport lead to fluctuations in sea surface height in the ACC's standing meanders and in the distribution of bottom pressure (Stewart and Hogg, 2017).

illustrates the suggested correspondence between deep AABW outflows across the Southern Ocean and anomalies in SSH and OBP that might be leveraged to indirectly observe its transport. Changes in the surface circulation of the standing meanders in the ACC may also be expected to produce a signature in SST, but the potential for indirectly observing AABW transport via SST remains to be explored.

It may also be possible to observe dense water overflows at the shelf break closer to the source from satellite-observed SSH. Modeling work has shown that simulated dense water overflow pulses in cross-slope canyons in the Ross Sea are associated with a negative steric height anomaly (Morrison et al., 2020). A similar signal is seen in the North Atlantic, where dense overflow variability has been detected in concurrent observations of satellite SSH and *in situ* mooring data (Høyer and Quadfasel, 2001). It has been proposed that the Denmark Strait overflow transport variability may be able to be monitored solely from satellite data (Lea et al., 2006). However, Haine (2010) concluded that SSH measurement noise in altimetry data available in 2010 was too large to allow for accurate detection of Denmark Strait overflow variability. An additional challenge for observing Antarctic overflows from satellites is the presence of sea ice. However, with the development of methods to detect SSH beneath sea ice (e.g., Armitage et al., 2018; Auger et al., 2022) and additional recent altimetry missions, the possibility of detecting Antarctic overflows from satellites warrants further investigation.

Recent works have drawn additional links between the deep circulation of AABW and near-surface winds. Tandon et al. (2020) showed that winds drive substantial fluctuations (several Sverdrups) in the Indo-Pacific overturning streamfunction, due to the long time scale over which the stratification adjusts to wind forcing, associated with the westward propagation of baroclinic Rossby waves. Stewart et al. (2021) showed that a similar phenomenon occurs at high southern latitudes (south of 30°S). Regarding time scales shorter than a few years, the baroclinic (IFS) component of the zonal momentum balance responds negligibly to wind fluctuations, whereas the barotropic (TFS) component adjusts to compensate for the wind changes (see Figure 12B). This leads to AABW northward transport fluctuations that are approximately equal in magnitude and opposite in sign to wind-driven surface Ekman transport fluctuations on time scales shorter than a few years. This finding potentially allows high-frequency variability in AABW transport to be indirectly observed/reconstructed from the zonal surface wind stress, which can be calculated from reanalysis products or surface pressure measurements. However, such high-frequency fluctuations pose a challenge for efforts to measure

AABW export from the Antarctic continental shelf across the Southern Ocean, which likely manifests as interannual-to-decadal fluctuations in AABW transport (Abrahamsen et al., 2019; Silvano et al., 2020).

4.3 Data assimilation modeling

Data assimilation products have the potential to add value to sparse observations by filling data gaps with dynamically realistic models. Data assimilation acts to "nudge" a model toward observational constraints. Similarly, a state estimate is produced by obtaining the least squares fit of a forward-running ocean model to a wide range of available observations to produce a temporally evolving three-dimensional field (e.g., Wunsch and Heimbach, 2007). In contrast, inverse models, as discussed in Section 4.1, usually lack temporal resolution and primarily incorporate only hydrographic section data.

A recent intercomparison project compared the global performance of 26 ocean data assimilation products (Balmaseda et al., 2015), highlighting the recent advancement of such products. However, only a few of these data assimilation models are evaluated for AABW formation and circulation. For example, Azaneu et al. (2014) showed that AABW in the ECCO2 reanalysis is formed by deep convection in the Weddell Sea rather than by on-shelf dense water production and subsequent descent down the continental slope (Menemenlis et al., 2008). A range of data assimilation products (ECMWF-ORAS4 (Balmaseda et al., 2013), CFSR (Saha et al., 2010), MyOcean-UR025.4 (Ferry et al., 2012), ECCO2 (Menemenlis et al., 2008), ECCOV4r4 (Forget et al., 2015), SODA 2.2.4 (Carton and Giese, 2008; Giese and Ray, 2011, and SOSE (Mazloff et al., 2010)) are compared in Dotto et al. (2014); Aguiar et al. (2017), and Bailey et al. (2023). While some of these reanalyses formed AABW at realistic rates (e.g., ECCOV4r4, SODA, and SOSE), all of the models did not well capture the spatial distribution and variability of AABW compared with observations. Despite this discrepancy between data assimilation models and observations, a few studies have utilized data assimilation products to study the hydrography and circulation of AABW (e.g., Mazloff et al., 2013; Van Sebille et al., 2013; Abernathey et al., 2016; Cessi, 2019; Rousselet et al., 2021; Stewart et al., 2021).

The physics of AABW formation and export are thus rarely well captured in forward ocean models (Renner et al., 2009; Kerr et al., 2012; Heuzé, 2021), whether or not they assimilate hydrographic observations. In the rare cases where AABW processes are better captured (e.g., ACCESS-OM2-01; Kiss et al., 2020; Solodoch et al., 2022), it is clearly dependent on high resolution (Mensah et al., 2021) and thus comes at a computational expense that restricts the length of simulations. These limitations hamper our ability to characterize the role of AABW in global ocean ventilation. The Ocean Circulation Inverse Model (OCIM; DeVries and Primeau, 2011), which is a three-dimensional dynamical ocean model optimized to fit a wide range of relevant hydrographic observations, provides an alternative tool to characterize AABW pathways. This circulation estimate is steady and has a relatively low spatial resolution (2° in the horizontal, 48 layers in the vertical; Holzer et al., 2021). However, because it assimilates six tracers (temperature, salinity, CFC-11, CFC-12, radiocarbon, and Helium-3) whose distributions are reproduced with high accuracy, it allows faithful quantification of ventilation rates and pathways in the global deep ocean (DeVries and Holzer, 2019; Holzer et al., 2021). For example, the Ocean Circulation Inverse Model has provided revised estimates of the strength (approximately 8 Sv) and structure (confined to depths > 2.5 km) of the abyssal overturning in the Pacific Ocean (Holzer et al., 2021). These estimates reflect a modern mean state; changes in AABW cannot be assessed with this tool.

5 Future directions

Since the 19th century and more systematically after the 1960s, observations in the Southern Ocean have progressively transformed our understanding of AABW. In recent decades, observations also revealed clear trends in AABW: 1) AABW volume reduction, 2) AABW warming, and 3) AABW salinity changes (e.g., Purkey et al., 2018; Silvano et al., 2020). However, the causes of these changes remain uncertain due to the paucity of *in situ* data, and several aspects of AABW formation and spreading remain poorly known. Below we highlight some of the outstanding questions in AABW processes and outline which observing system will be required in coming years and decades to tackle them.

5.1 Outstanding questions

Q1) **What is the contribution of AABW to the lower limb of the meridional overturning circulation?**

Box-inverse models provide a wide range of AABW formation rates (7–20 Sv; Section 4.1). The weaker estimates (<10 Sv) are consistent with diagnostics from CFCs (Orsi et al., 1999) but are difficult to reconcile with direct measurements of the northward export of AABW at selected chokepoints, such as the Orkney Passage (through which 4–6 Sv of AABW has been shown to leave the Weddell Sea; Naveira Garabato et al., 2002; Jullion et al., 2014; Abrahamsen et al., 2019) and the deep boundary current to the east of the Kerguelen Plateau (via which ~12 Sv has been observed to flow equatorward; Fukamachi et al., 2010). These comparisons suggest that AABW production is potentially in line with, or may possibly even exceed, the highest inverse model estimates and signal the robust quantification of circumpolar AABW formation as well as mixing as a major outstanding challenge.

Coupled with this problem, there is a long-standing discussion on the relative contributions of different Southern Ocean sectors to AABW production and northward export, ranging from a view of the dominance of the Weddell region (e.g., Lumpkin and Speer, 2007) to another of approximate equipartition between the Atlantic, Indian and Pacific sectors (e.g., Naveira Garabato et al., 2014), as also suggested by recent modeling work (Solodoch et al., 2022). Settling this issue will entail gaining a greater quantitative understanding of zonal, inter-sector exchanges of AABW. It is plausible that the Weddell's disproportionate importance as an

AABW formation hotspot suggested by some works may reflect the accumulation in, and subsequent export from, the Weddell Sea of AABW produced in the Indian and Pacific sectors (Jullion et al., 2014), which may be promoted by the westward flow prevalent along much of the Antarctic continental slope (Naveira Garabato et al., 2014; Solodoch et al., 2022).

Q2) What is the role of AABW in ocean heat storage and biogeochemical cycles?

AABW plays an important role in storing heat in the ocean abyss, thus affecting the planetary heat budget as well as the sea level (Purkey and Johnson, 2013). Moreover, AABW supplies oxygen and "preformed" nutrients to the global ocean abyss, thus affecting marine ecosystems and the carbon cycle (Marinov et al., 2006; Henley et al., 2020). However, very little is known about the impact of AABW changes on deep ocean heat and carbon storage as well as deep ocean oxygenation. Historically, abyssal biogeochemical properties have been less observed than physical properties, hampering our knowledge of the full climatic impact of AABW and its changes.

Q3) What are the temporal changes in AABW formation and how are they driven?

Observations during the past decades have detected temporal changes in AABW formation. However, relatively short, sparse, and intermittent observations prevent us from capturing all time scales of AABW variability. At interannual to multidecadal time scales, several forcing mechanisms have been shown to regulate AABW formation variability. These include atmospheric variability associated with climate modes, sea ice formation, ice sheet melting, iceberg calving, and tides (e.g., Gordon et al., 2009; Snow et al., 2018; Silvano et al., 2020; Hattermann et al., 2021; Jacobs et al., 2022; Bowen et al., 2023). However, the paucity of observations prevents us from 1) fully capturing the dynamics behind these forcing mechanisms, 2) quantifying their relative roles at different time scales, and 3) verifying whether their impact changes spatially.

Q4) What regulates AABW transport through the Southern Ocean?

Even less is known about what controls AABW transport through the Southern Ocean and its changes. Only a few mooring-based estimates of flow are available (Fukamachi et al., 2010; Abrahamsen et al., 2019). In addition, a limited understanding of AABW mixing processes in the deep Southern Ocean hampers quantification of AABW's contribution to tracer transports and budgets.

Q5) What is the role of seasonal processes on AABW formation and circulation?

Seasonal variability (in particular wintertime processes) remains poorly understood. Our knowledge of key processes such as sea ice formation, convection, cross-shelf exchange, and gravity currents relies on very few observations collected in rare winter expeditions, mooring deployments, (deep and ice-capable) Argo floats, and seals.

Q6) **How do AABW anomalies form and propagate?**

AABW has warmed, freshened, and contracted over past decades within the Southern Ocean and to its north (e.g., Purkey and Johnson, 2010). However, the mechanisms responsible for these trends are not fully understood. The relative roles of changes in the source waters of AABW, waves, advection, mixing, and past offshore polynya events (e.g., the Weddell Polynya in the 1970s) in regulating multidecadal trends in AABW properties need further examination.

Q7) **What is the role of small-scale ocean dynamics on the formation and export of AABW?**

While recent advances in microstructure measurements, AUVs, and gliders have started to show the importance of sub-mesoscale and turbulent processes in AABW-related processes (Naveira Garabato et al., 2019; Spingys et al., 2021), a global quantification of their impact is missing. The multiscale nature of the lower limb of the global overturning circulation is only starting to emerge now from an observational point of view.

5.2 The need for an AABW observing system

To address the outstanding questions highlighted above, an internationally coordinated and strategically designed observing system is required. Here, we suggest some priorities for an AABW observing system (summarized in Figure 13), taking into consideration what has been measured in the past:

1) Continue long-term summertime time series of HSSW and ISW properties in the Ross Sea, Weddell Sea, and Adélie Land (Section 2.1.2) and initiate repeat measurements in Prydz Bay and Cape Darnley (**Q3**).

2) Design targeted campaigns in poorly sampled coastal regions using the latest technologies in measuring ocean properties, including biogeochemical parameters, under ice. These areas include the south-western Weddell Sea, eastern Ross Sea/western Amundsen Sea, and several regions around East Antarctica where only seals have been able to provide *in situ* observations (**Q1**, **Q2**, **Q3**, and **Q5**).

3) Maintain monitoring by moorings in key regions of AABW formation: Ross Sea, Weddell Sea, and Adélie Land (Section 2.2). Sustain mooring observations in Prydz Bay and Cape Darnley. Moorings should ideally cover continental shelf, shelf break, and slope to capture processes involved in AABW formation and could be extended to also include biogeochemical sensors that measure additional ocean properties and provide new insight (**Q2**, **Q3**, and **Q5**).

4) Sustain long-term mooring observations of AABW variability and export to other ocean basins (Weddell Gyre and Orkney Passage; Section 2.2) and establish new long-term (i.e., decadal) mooring systems in key chokepoints such as east of the Kerguelen, South Sandwich Trench, and Campbell Plateau (**Q1**, **Q2**, **Q4**, **Q5**, and **Q6**).

5) Repeat Southern Ocean GO-SHIP transects (Section 2.1.3) at least once every 10 years and prioritize the annual/biannual occupations of more frequent sections (e.g., A23, SR1b, SR3, and SR4) (**Q2**, **Q3**, **Q4**, and **Q6**).

6) Sustain under-ice shelf measurements at the Ross and Filchner-Ronne Ice Shelves and possibly re-establish a program at the Amery Ice Shelf (Section 2.3; **Q3**, **Q5**, and **Q7**).

7) Tracer measurements should become standard in every oceanographic campaign (Section 2.4). In particular, CFCs and

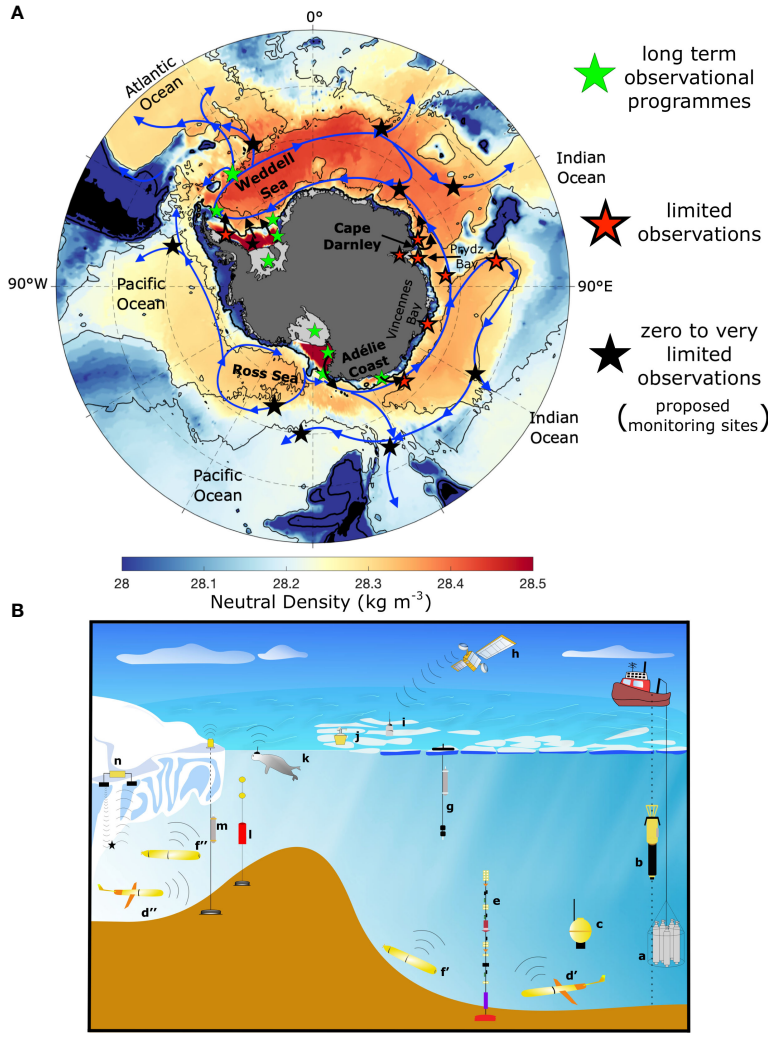

FIGURE 13
Antarctic Bottom Water (AABW) observing system. **(A)** Climatological near-bottom neutral density (kg/m^3) highlighting high values (red to yellow) in AABW formation regions (black arrows) and along the main AABW pathways through the Southern Ocean (blue arrows); same as Figure 3A. Overlaid are stars highlighting key areas to monitor AABW (see Section 5). Green stars represent locations where sustained (either established long-term moorings or repeated ship-based surveys) observations are ongoing. Red stars are locations where observations are more sporadic or relatively recent (less than approximately a decade) and need to be sustained over the coming decades. Black stars are instead regions where nearly no observations are available and an international effort to fill these gaps is envisaged. **(B)** AABW observational tools building on Newman et al. (2019): (a) ship-based conductivity–temperature–depth (CTD) combined with multiple sensors such as dissolved oxygen and velocity as well as water samples to measure tracers (e.g., oxygen isotopes and CFCs); (b) microstructure profilers to measure turbulence; (c) deep (>2,000 m depth) Argo floats; gliders to measure the deep ocean (d′) and collect observations on the continental shelf/slope and in ice shelf cavities (d′′); (e) Moorings to measure physical and biogeochemical variables, with potential to use fiber optics; autonomous underwater vehicles (AUVs) capable of reaching the deep ocean (>2,000 m depth; f′) and ice shelf cavities (f′′); (g) ice-tethered profiler (ITP); (h) satellite observations of ocean, sea ice, and ice sheet properties; (i) under-sea ice profiling floats; (j) buoys; (k) animal borne ocean sensors; (l) sound sources for acoustic locating floats, AUVs, and gliders under sea ice and ice shelves; (m) moorings deployed through boreholes to measure properties within ice shelf cavities; (n) downward-looking radars (autonomous phase-sensitive radio echosounders (ApRES)) to measure rates of ice shelf basal melt.

oxygen isotope measurements should be prioritized given their ability to provide essential information on AABW ventilation, freshwater sources, and anthropogenic imprint. Careful consideration is needed to avoid mismatches between different laboratories when processing oxygen isotope samples (**Q1**, **Q2**, **Q3**, **Q4**, **Q5**, **Q6**, and **Q7**).

8) Further, strengthen the array of (ice-capable and deep) profiling floats and seals measuring ocean physical and biogeochemical properties on the Antarctic continental shelf and in the abyssal Southern Ocean (Sections 3.1, 3.2). Development of more sensors to be installed on these platforms (e.g., microstructure) would be highly beneficial (**Q2**, **Q3**, **Q5**, **Q6**, and **Q7**).

9) Design and deliver new missions with AUVs and gliders (Section 3.3) for multi-month, high vertical and horizontal resolution observations in the Southern Ocean (**Q2**, **Q4**, **Q5**, and **Q7**).

10) Further develop box-inverse and data assimilation models, including at a regional scale. The combination of different observationally guided modeling approaches is essential given

their strengths and weaknesses (Sections 4.1, 4.3; **Q1**, **Q2**, **Q3**, **Q4**, **Q5**, **Q6**, and **Q7**).

11) Further refine remote sensing approaches to estimating sea ice formation rates from satellites (e.g., Tamura et al., 2008; Ohshima et al., 2022; see Section 4.2). Further work on indirect observations of AABW circulation through satellite-derived SSH, SST, and OBP needs to be progressed beyond theory, except in a few specific regions (Mazloff and Boening, 2016; Mizobata et al., 2020; see Section 4.2) (**Q3**, **Q4**, **Q5**, and **Q6**).

12) Develop and deploy new technologies. One example of (relatively) low-cost, autonomous tools that can be used to monitor conditions (e.g., on the Antarctic continental shelf) is recording "pop-up" buoys (e.g., Long Term Underwater Sensing bottom landers, LoTUS, and T-pops). The buoys register temperature during a pre-set time interval (years) after which they let go of their anchor and "pop up" to the surface. They are designed to survive in and below sea ice and to transfer data via satellite once out of the ice. Similarly, ice-tethered profilers employed in the Arctic (Toole et al., 2011) can be deployed in Antarctic coastal regions to collect year-round high-resolution observations near the surface.

A further opportunity for sustained low-cost observations at high space-time resolution (meter to centimeter, minute to millisecond) is presented by distributed fiber optic sensing (Hartog et al., 2018). This technology can be utilized in a wide range of marine environments using dedicated and legacy cables to measure temperature (Selker et al., 2006), including in Antarctic environments (e.g., Kobs et al., 2014). Additionally, recent studies have demonstrated the potential of utilizing strain to observe ocean properties (Williams et al., 2022; Spingys et al.[2]). Finally, further development and deployment of sound sources for under-ice navigation are envisaged, especially on continental shelves and under-ice shelves.

13) Machine learning can be used in several ways to help address AABW-related questions. For example, a possible means of circumventing the limitations of satellite-derived proxies of AABW circulation (SSH, SST, and OBP; see Section 4.2) is to leverage machine learning techniques, which have been used, e.g., to infer subsurface velocity fields (Chapman and Charantonis, 2017) and subsurface meridional heat transport/overturning from SSH (George et al., 2021; Solodoch et al., 2023).

6 Conclusions

This review outlines the different techniques used to observe AABW from beneath the Antarctic ice shelves to the north of the ACC. These techniques have shaped our current understanding of the polar and abyssal oceans. However, despite the continuous development of observational tools, a robust quantification of AABW's capacity to take up and store heat and carbon in the abyssal ocean, as well as of the mechanisms involved, is missing. This inadequate understanding limits our ability to predict heat and carbon partitioning between atmosphere and ocean on multidecadal and longer time scales, hampering long-term projections of global climatic change.

Designing an observing system capable of assessing outstanding questions in "AABW research", as highlighted in Section 5 and Figure 13, is key to addressing this fundamental gap in our understanding of the Earth system. The AABW observing system can build on the legacy of decades of pioneering expeditions and measurements in the Southern Ocean as well as experience in monitoring the AMOC (Frajka-Williams et al., 2019), providing a framework for future generations of environmental scientists. This observing system will also serve other areas of active research, including Antarctic Ice Sheet and sea level rise (through observations of ocean properties near Antarctic glaciers), Southern Ocean ecosystem dynamics (through analysis of ocean conditions both near the coast and in the abyssal Southern Ocean), and oceanographic technology (by improving observing capabilities in polar and abyssal environments). The further development of autonomous (e.g., AUVs and gliders) and remote (satellite) tools will be essential to reduce the environmental impact of operations both in the Southern Ocean and in other ocean basins. International programs, such as the Southern Ocean Observing System (SOOS), could provide the framework for designing, implementing, and sustaining the AABW observing system along with national research programs.

Author contributions

ASi conceived the review on observing AABW and led the writing. All co-authors contributed to the writing and provided data and expertise. All authors contributed to the article and approved the submitted version.

Funding

The author(s) declare financial support was received for the research, authorship, and/or publication of this article. ASi acknowledges funding from NERC (NE/V014285/1). MB, CSt, and DF acknowledge funding from the New Zealand Strategic Science Investment Fund: Antarctic Science Platform Contract ANTA1801. SR and AF were supported by the Australian Antarctic Program Partnership (AAPP) through grant funding from the Australian Government as part of the Antarctic Science Collaboration Initiative program. AKM was supported by the Australian Research Council (ARC) Australian Centre for Excellence in Antarctic Science (SR200100008) and by the ARC Discovery Project DP190100494. EA, AJSM, MM acknowledge NERC grants NE/N018095/1 (ORCHESTRA), NE/V013254/1 (ENCORE), and NE/W004933/1 (BIOPOLE). This project has received funding from the European Union's Horizon 2020 research and innovation program under grant agreement no. 821001. This research was supported by OCEAN:ICE, which is co-funded by the European Union, Horizon Europe Funding Programme for research and innovation under grant agreement no. 101060452 and by UK Research and Innovation. O:I Contribution number 1. FH was supported by the European Union (ERC, VERTEXSO, 101041743) and the Initiative and Networking Fund of

2 Spingys, C., Naveira Garabato, A. C., and Belal, M. Distributed fibre optic sensing for high space-time resolution ocean velocity observations: A Case study from a macrotidal channel. *Earth Space Sci.* (Submitted).

the Helmholtz Association (Grant Number: VH-NG-19-33). WL was supported by the Korea Institute of Marine Science & Technology Promotion (KIMST) funded by the Ministry of Oceans and Fisheries (RS-2023-00256677; PM23020).

Acknowledgments

We thank the constructive comments from the reviewers that helped improve the manuscript. We also thank the key support of the SCAR-SCOR initiative Southern Ocean Observing System (SOOS; https://www.soos.aq) over the years, which provided an excellent platform for data sharing, expertise exchange, international coordination of Southern Ocean measurements, and organization of meetings (both online and in person; https://soos.aq/soos-symposium-2023). This review has also been informed by the SCAR program INSTANT (Instabilities and thresholds in Antarctica, https://www.scar-instant.org). C. Ofelio designed the schematics in Figures 1, 13B.

Conflict of interest

The authors declare that the research was conducted in the absence of any commercial or financial relationships that could be construed as a potential conflict of interest.

Publisher's note

References

Abernathey, R. P., Cerovecki, I., Holland, P. R., Newsom, E., Mazloff, M., and Talley, L. D. (2016). Water-mass transformation by sea ice in the upper branch of the Southern Ocean overturning. *Nat. Geosci.* 9, 596–601. doi: 10.1038/ngeo2749

Abrahamsen, E. P., Meijers, A. J. S., Polzin, K. L., Naveira Garabato, A. C., King, B., Firing, Y. L., et al. (2019). Stabilization of dense Antarctic water supply to the Atlantic Ocean overturning circulation. *Nat. Clim. Change* 9, 742–746. doi: 10.1038/s41558-019-0561-2

Adusumilli, S., Fricker, H. A., Medley, B., Padman, L., and Siegfried, M. R. (2020). Interannual variations in meltwater input to the Southern Ocean from Antarctic ice shelves. *Nat. Geosci.* 13, 616–620. doi: 10.1038/s41561-020-0616-z

Aguiar, W., Mata, M. M., and Kerr, R. (2017). On deep convection events and Antarctic Bottom Water formation in ocean reanalysis products. *Ocean Sci.* 13, 851–872. doi: 10.5194/os-13-851-2017

Akhoudas, C., Sallée, J.-B., Reverdin, G., Aloisi, G., Benetti, M., Vignes, L., et al. (2020). Ice shelf basal melt and influence on dense water outflow in the Southern Weddell Sea. *J. Geophys. Res.: Oceans* 125, e2019JC015710. doi: 10.1029/2019JC015710

Akhoudas, C. H., Sallée, J. B., Haumann, F. A., Meredith, M. P., Naveira Garabato, A. C., Reverdin, G., et al. (2021). Ventilation of the abyss in the Atlantic sector of the Southern Ocean. *Sci. Rep.* 11, 1–13. doi: 10.1038/s41598-021-86043-2

Anilkumar, N., Jena, B., George, J. V., Sabu, P., Kshitija, S., and Ravichandran, M. (2021). Recent freshening, warming, and contraction of the antarctic bottom water in the Indian sector of the southern ocean. *Front. Mar. Sci.* 8. doi: 10.3389/fmars.2021.730630

Antipov, N. N., and Klepikov, A. V. (2017). Interannual variability of water masses in the area of bottom water formation in Prydz Bay. *Arctic Antarctic Res.* 3, 87–106. doi: 10.30758/0555-2648-2017-0-3-87-106

Aoki, S., Katsumata, K., Hamaguchi, M., Noda, A., Kitade, Y., Shimada, K., et al. (2020c). Freshening of antarctic bottom water off cape darnley, east Antarctica. *J. Geophys. Res.: Oceans* 125, e2020JC016374. doi: 10.1029/2020JC016374

Aoki, S., Kitade, Y., Shimada, K., Ohshima, K. I., Tamura, T., Bajish, C. C., et al. (2013). Widespread freshening in the seasonal ice zone near 140°E off the Adélie Land Coast, Antarctica, from 1994 to 2012. *J. Geophys. Res.: Oceans* 118, 6046–6063. doi: 10.1002/2013JC0090009

Aoki, S., Kobayashi, R., Rintoul, S. R., Tamura, T., and Kusahara, K. (2017). Changes in water properties and flow regime on the continental shelf off the Adélie/George V Land coast, East Antarctica, after glacier tongue calving. *J. Geophys. Res.: Oceans* 122, 6277–6294. doi: 10.1002/2017JC012925

Aoki, S., Ono, K., Hirano, D., and Tamura, T. (2020a). Continuous winter oceanic profiling in the Cape Darnley Polynya, East Antarctica. *J. Oceanogr.* 76 (5), 365–372. doi: 10.1007/s10872-020-00550-w

Aoki, S., Rintoul, S. R., Ushio, S., Watanabe, S., and Bindoff, N. L. (2005). Freshening of the adélie land bottom water near 140°E. *Geophys. Res. Lett.* 32, L23601. doi: 10.1029/2005GL024246

Aoki, S., Takahashi, T., Yamazaki, K., Hirano, D., Ono, K., Kusahara, K., et al. (2022). Warm surface waters increase Antarctic ice shelf melt and delay dense water formation. *Commun. Earth Environ.* 3, 142. doi: 10.1038/s43247-022-00456-z

Aoki, S., Yamazaki, K., Hirano, D., Katsumata, K., Shimada, K., Kitade, Y., et al. (2020b). Reversal of freshening trend of Antarctic Bottom Water in the Australian-Antarctic Basin during 2010s. *Sci. Rep.* 10 (1), 1–8. doi: 10.1038/s41598-020-71290-6

Armitage, T. W., Kwok, R., Thompson, A. F., and Cunningham, G. (2018). Dynamic topography and sea level anomalies of the southern ocean: variability and teleconnections. *J. Geophys. Res.* 123, 613–630. doi: 10.1002/2017JC013534

Auger, M., Prandi, P., and Sallée, J.-B. (2022). Southern ocean sea level anomaly in the sea ice-covered sector from multimission satellite observations. *Sci. Data* 9 (1), 70. doi: 10.1038/s41597-022-01166-z

Azaneu, M., Kerr, R., and Mata, M. M. (2014). Assessment of the representation of Antarctic Bottom Water properties in the ECCO2 reanalysis. *Ocean Sci.* 10, 923–946. doi: 10.5194/os-10-923-2014

Azaneu, M., Kerr, R., Mata, M. M., and Garcia, C. A. (2013). Trends in the deep southern ocean, (1958–2010): Implications for Antarctic Bottom Water properties and volume export. *J. Geophys. Res. Oceans* 118, 4213–4227. doi: 10.1002/jgrc.20303

Bailey, S. T., Jones, C. S., Abernathey, R. P., Gordon, A. L., and Yuan, X. (2023). Water mass transformation variability in the Weddell Sea in ocean reanalyses. *Ocean Sci.* 19 (2), 381–402. doi: 10.5194/os-19-381-2023

Balmaseda, M. A., Hernandez, A., Storto, M. D., Palmer, O., Alves, L., and Shi, G. C. (2015). The ocean reanalyses intercomparison project (ORA-IP). *J. Operat. Oceanogr.* 8 (Suppl. 1), s80–s97. doi: 10.1080/1755876X.2015.1022329

Balmaseda, M. A., Mogensen, K., and Weaver, A. T. (2013). Evaluation of the ECMWF ocean reanalysis system ORAS4. *Q. J. R. Meteorol. Soc* 139, 1132–1161. doi: 10.1002/qj.2063

Begeman, C. B., Tulaczyk, S. M., Marsh, O. J., Mikucki, J. A., Stanton, T. P., Hodson, T. O., et al. (2018). Ocean stratification and low melt rates at the Ross Ice Shelf grounding zone. *J. Geophys. Res.: Oceans* 123, 7438–7452. doi: 10.1029/2018JC013987

Bergamasco, A., Defendi, V., Zambianchi, E., and Spezie, G. (2002). Evidence of dense water overflow on the Ross Sea shelf - break. *Antarct. Sci.* 14, 271–277. doi: 10.1017/S0954102002000068

Bindoff, N. L., Rosenberg, M. A., and Warner, M. J. (2000). On the circulation and water masses over the antarctic continental slope and rise between 80 and 150°. *Deep-Sea Res. Part II: Topical Stud. Oceanogr.* 47, 2299–2326. doi: 10.1016/S0967-0645(00)00038-2\

Bowen, M. M., Fernandez, D., Forcen-Vazquez, A., Gordon, A. L., Huber, B., Castagno, P., et al. (2021). The role of tides in bottom water export from the western Ross Sea. *Sci. Rep.* 11, 2246. doi: 10.1038/s41598-021-81793-5

Bowen, M. M., Fernandez, D., Gordon, A. L., Huber, B., Castagno, P., Falco, P., et al. (2023). Tides regulate the flow and density of Antarctic Bottom Water from the western Ross Sea. *Sci. Rep.* 13, 3873. doi: 10.1038/s41598-023-31008-w

Brennan, P. V., Lok, L., Nicholls, K. W., and Corr, H. F. J. (2013). Phase-sensitive FMCW radar system for high-precision Antarctic ice shelf profile monitoring. *IET Radar Sonar Navig.* 8 (7), 776–786. doi: 10.1049/iet-rsn.2013.0053

Brennecke, W. (1921). *Die ozeanographischen Arbeiten der Deutschen Antarktischen Expedition 1911-1912* (Hamburg: University of California Libraries).

Bryden, H. L., and Nurser, A. J. (2003). Effects of strait mixing on ocean stratification. *J. Phys. Oceanogr.* 33 (8), 1870–1872. doi: 10.1175/1520-0485(2003)033<1870:EOSMOO>2.0.CO;2

Budd, W. (1966). The dynamics of the amery ice shelf. *J. Glaci.* 6 (45), 335–358. doi: 10.3189/S0022143000019456

Budillon, G., Castagno, P., Aliani, S., Spezie, G., and Padman, L. (2011). Thermohaline variability and Antarctic Bottom Water formation at the Ross Sea shelf break. *Deep. Sea. Res. Part I. Oceanogr. Res. Pap.* 58, 1002–1018. doi: 10.1016/j.dsr.2011.07.002

Budillon, G., Cordero, S. G., and Salusti, E. (2002). On the dense water spreading off the Ross Sea shelf (Southern Ocean). *J. Mar. Syst.* 35, 207–227. doi: 10.1016/S0924-7963(02)00082-9

Budillon, G., Pacciaroni, M., Cozzi, S., Rivaro, P., Catalano, G., Ianni, C., et al. (2003). An optimum multiparameter mixing analysis of the shelf waters in the Ross sea. *Antar. Sci.* 15 (1), 105–118. doi: 10.1017/S095410200300110X

Buffoni, G., Cappelletti, A., and Picco, P. (2002). An investigation of thermohaline circulation in Terra Nova Bay polynya. *Ant. Sci.* 14 (1), 83–92. doi: 10.1017/S0954102002000615

Campos, E. J., Van Caspel, M. C., Zenk, W., Morozov, E. G., Frey, D. I., Piola, A. R., et al. (2021). Warming trend in antarctic bottom water in the vema channel in the South Atlantic. *Geophys. Res. Lett.* 48 (2021), e2021GL094709. doi: 10.1029/2021GL094709

Carmack, E. C. (1977). "Water characteristics of the Southern Ocean south of the Polar Front," in *A voyage of discovery, george deacon 70th anniversary volume*. Ed. M. Angel (Oxford: Pergamon Press), 15–41.

Carton, J. A., and Giese, B. S. (2008). A reanalysis of ocean climate using Simple Ocean Data Assimilation (SODA). *Mon. Weather Rev.* 136, 2999–3017. doi: 10.1175/2007MWR1978.1

Castagno, P., Falco, P., Dinniman, M. S., Spezie, G., and Budillon, G. (2017). Temporal variability of the Circumpolar Deep Water infow onto the Ross Sea continental shelf. *J. Mar. Syst.* 166, 37–49. doi: 10.1016/j.jmarsys.2016.05.006

Castagno, P., Rintoul, S. R., Capozzi, V., Ditullio, G. R., Spezie, G., Budillon, G., et al. (2019). Rebound of shelf water salinity in the Ross Sea. *Nat. Commun.* 10, 1–6. doi: 10.1038/s41467-019-13083-8

Cessi, P. (2019). The global overturning circulation. *Ann. Rev. Mar. Sci.* 11, 249–270. doi: 10.1146/annurev-marine-010318-095241

Chapman, C., and Charantonis, A. A. (2017). Reconstruction of subsurface velocities from satellite observations using iterative self-organizing maps. *IEEE Geosci Rem. Sens. Lett.* 14 (5), 617–620. doi: 10.1109/LGRS.2017.2665603

Chelton, D. B., Ries, J. C., Haines, B. J., Fu, L.-L., and Callahan, P. S. (2001). "Satellite altimetry," in *Satellite altimetry and earth sciences*, vol. 69 . Eds. L. Fu and A. Cazenave (New York, NY: Elsevier), 1–131.

Cimoli, L., Gebbie, G., Purkey, S. G., and Smethie, W. M. (2023). Annually resolved propagation of CFCs and $_{SF6}$ in the global ocean over eight decades. *J. Geophys. Res.: Oceans* 128, e2022JC019337. doi: 10.1029/2022JC019337

Coles, V. J., McCartney, M. S., Olson, D. B., and Smethie, W. M. (1996). Changes in the Antarctic Bottom Water properties in the western South Atlantic in the late 1980s. *J. Geophys. Res.* 101, 8957–8970. doi: 10.1029/95JC03721

Couldrey, M. P., Jullion, L., Naveira Garabato, A. C., Rye, C., Herraiz-Borreguero, L., Brown, P. J., et al. (2013). Remotely induced warming of Antarctic Bottom Water in the eastern Weddell gyre. *Geophys. Res. Lett.* 40, 2755–2760. doi: 10.1002/grl.50526

Cunningham, S. A., Alderson, S. G., King, B. A., and Brandon, M. A. (2003). Transport and variability of the antarctic circumpolar current in drake passage. *J. Geophys. Res.: Oceans* 108, 8084. doi: 10.1029/2001JC001147

Daae, K., Fer, I., and Darelius, E. (2019). Variability and mixing of the Filchner overflow plume on the continental slope, Weddell Sea. *J. Phys. Oceanogr.* 49 (1), 3–20. doi: 10.1175/JPO-D-18-0093.1

Dale, E. R., McDonald, A. J., Coggins, J. H. J., and Rack, W. (2017). Atmospheric forcing of sea ice anomalies in the Ross Sea Polynya region. *Cryosphere* 11 (1), 1–21. doi: 10.5194/tc-2016-89

Davis, P. E. D., Jenkins, A., Nicholls, K. W., Dutrieux, P., Schröder, M., Janout, M. A., et al. (2022). Observations of modified warm deep water beneath ronne ice shelf, Antarctica, from an autonomous underwater vehicle. *J. Geophys. Res. Oceans* 127, e2022JC019103. doi: 10.1029/2022JC019103

Davis, P. E. D., Nicholls, K. W., Holland, D. M., Schmidt, B. E., Washam, P., Riverman, K. L., et al. (2023). Suppressed basal melting in the eastern Thwaites Glacier grounding zone. *Nature* 614 (7948), 479–485. doi: 10.1038/s41586-022-05586-0

Deacon, G. E. R. (1937). The hydrology of the southern ocean. *Discovery Rep. XV*, 1–124.

de Lavergne, C., Madec, G., Roquet, F., Holmes, R. M., and McDougall, T. J. (2017). Abyssal ocean overturning shaped by seafloor distribution. *Nature* 551, 181–186. doi: 10.1038/nature24472

Desbruyères, D. G., Purkey, S. G., McDonagh, E. L., Johnson, G. C., and King, B. A. (2016). Deep and abyssal ocean warming from 35 years of repeat hydrography. *Geophys. Res. Lett.* 43, 10,356–10,365. doi: 10.1002/2016GL070413

Deser, C., Alexander, M. A., Xie, S.-P., and Phillips, A. S. (2010). Sea surface temperature variability: patterns and mechanisms. *Ann. Rev. Mar. Sci.* 2, 115–143. doi: 10.1146/annurev-marine-120408-151453

DeVries, T., and Holzer, M. (2019). Radiocarbon and helium isotope constraints on deep ocean ventilation and mantle-3He sources. *J. Geophys. Res.* 124, 3036–3057. doi: 10.1029/2018jc014716

DeVries, T., and Primeau, F. (2011). Dynamically and observationally constrained estimates of water-mass distributions and ages in the global ocean. *J. Phys. Oceanogr.* 41, 2381–2401. doi: 10.1175/jpo-d-10-05011.1

Dotto, T. S., Kerr, R., Mata, M. M., Azaneu, M., Wainer, I. E. K. C., Fahrbach, E., et al. (2014). Assessment of the structure and variability of Weddell Sea water masses in distinct ocean reanalysis products. *Ocean Sci.* 10 (3), 523–546. doi: 10.5194/os-10-523-2014

Fahrbach, E., Harms, S., Rohardt, G., Schröder, M., and Woodgate, A. R. (2001). Flow of bottom water in the northwestern Weddell Sea. *J. Geophys. Res.* 106 (C2), 2761–2778. doi: 10.1029/2000jc900142

Fahrbach, E., Hoppema, M., Rohardt, G., Boebel, O., Klatt, O., and Wisotzki, A. (2011). Warming of deep and abyssal water masses along the Greenwich meridian on decadal time scales: the weddell gyre as a heat buffer. *Deep Sea Res. Part II: Top. Stud. Oceanogr.* 58, 2509–2523. doi: 10.1016/j.dsr2.2011.06.007

Fahrbach, E., Hoppema, M., Rohardt, G., Schröder, M., and Wisotzki, A. (2004). Decadal-scale variations of water mass properties in the deep Weddell Sea. *Ocean Dyn.* 54, 77–91. doi: 10.1007/s10236-003-0082-3

Ferrari, R., Jansen, M. F., Adkins, J. F., Burke, A., Stewart, A. L., and Thompson, A. F. (2014). Antarctic sea ice control on ocean circulation in present and glacial climates. *Proc. Natl. Acad. Sci. U.S.A.* 111 (24), 8753–8758. doi: 10.1073/pnas.1323922111

Ferry, N., Barnier, B., Garric, G., Haines, K., Masina, S., Parent, L., et al. (2012). Nemo: The modelling engine of global ocean reanalysis. *Mercator Ocean Q. Newslett.* 46–59, 201.

Fine, R. A. (2011). Observations of CFCs and SF6 as ocean tracers. *Annu. Rev. Mar. Sci.* 3, 173–119. doi: 10.1146/annurev.marine.010908.163933

Foldvik, A., Gammelsrød, T., Østerhus, S., Fahrbach, E., Rohardt, G., Schröder, M., et al. (2004). Ice shelf water overflow and bottom water formation in the southern Weddell Sea. *J. Geophys. Res.* 109, C02015. doi: 10.1029/2003JC002008

Foldvik, A., Gammelsrød, T., and Tørresen, T. (1985a). "Circulation and water masses on the southern Weddell Sea shelf," in *Oceanology of the Antarctic continental shelf, Antarctic research series*, vol. 43 . Ed. S. S. Jacobs (American Geophysical Union), 5–20. doi: 10.1029/AR043p000

Foldvik, A., Gammelsrød, T., and Tørresen, T. (1985b). Hydrographic observations from the Weddell Sea during the Norwegian Antarctic Research Expedition 1976/77. *Polar Res.* 3, 177–193. doi: 10.1111/j.1751-8369.1985.tb00506.x

Foldvik, A., Gammelsrød, T., and Tørresen, T. (1985c). Physical Oceanography studies in the Weddell Sea during the Norwegian Antarctic Research Expedition 1978/79. *Polar Res.* 3 (2), 195–207. doi: 10.3402/polar.v3i2.6952

Foppert, A., Rintoul, S. R., Purkey, S. G., Zilberman, N., Kobayashi, T., Sallée, J. B., et al. (2021). Deep Argo reveals bottom water properties and pathways in the Australian-Antarctic Basin. *J. Geophys. Res.: Oceans* 126, 1–18. doi: 10.1029/2021JC017935

Forget, G., Campin, J. M., Heimbach, P., Hill, C. N., Ponte, R. M., and Wunsch, C. (2015). ECCO version 4: an integrated framework for non-linear inverse modeling and global ocean state estimation. *Geosci. Model. Dev.* 8, 3071–3104. doi: 10.5194/gmd-8-3071-2015

Foster, T. D. (1983). The temperature and salinity fine-structure of the ocean under the Ross Ice Shelf. *J. Geophys. Res.* 88, 2556–2564. doi: 10.1029/JC088iC04p02556

Frajka-Williams, E., Ansorge, I. J., Baehr, J., Bryden, H. L., Chidichimo, M. P., Cunningham, S. A., et al. (2019). Atlantic Meridional Overturning Circulation: observed transport and variability. *Front. Mar. Sci.* 6. doi: 10.3389/fmars.2019.00260

Fricker, H. A., Allison, I., Craven, M., Hyland, G., Ruddell, A., Young, N., et al. (2002). Redefinition of the Amery ice shelf, East Antarctica, grounding zone. *J. Geophys. Res.* 107 (B5), 2092. doi: 10.1029/2001JB000383

Friedrichs, D. M., McInerney, J. B. T., Oldroyd, H. J., Lee, S., Yun, S., Yoon, S. T., et al. (2022). Observations of submesoscale eddy-driven heat transport at an ice shelf calving front. *Commun. Earth Environ.* 3, 140. doi: 10.1038/s43247-022-00460-3

Fukamachi, Y., Rintoul, S. R., Church, J. A., Aoki, S., Sokolov, S., Rosenberg, M. A., et al. (2010). Strong export of Antarctic bottom water east of the Kerguelen plateau. *Nat. Geosci.* 3 (5), 327–331. doi: 10.1038/ngeo842

Fukamachi, Y., Wakatsuchi, M., Taira, K., Kitagawa, S., Ushio, S., Takahashi, A., et al. (2000). Seasonal variability of bottom water properties off Adélie Land, Antarctica. *J. Geophys. Res.* 105 (C3), 6531–6540. doi: 10.1029/1999JC900292

Fukasawa, M., Freeland, H., Perkin, R., Watanabe, T., Uchida, H., and Nishina, A. (2004). Bottom water warming in the North Pacific Ocean. *Nature* 427, 825–827. doi: 10.1038/nature02337

Furlong, M. E., Paxton, D., Stevenson, P., Pebody, M., McPhail, S. D., and Perrett, J. (2012). "Autosub long range: a long range deep diving AUV for ocean monitoring," in *Autonomous Underwater Vehicles (AUV), 2012 IEEE/OES*(Southampton), 1–7. doi: 10.1109/AUV.2012.6380737

Gade, H. G. (1979). Melting of ice in sea water: a primitive model with application to the Antarctic ice shelf and icebergs. *J. Phys. Oceanogr.* 9, 189–198. doi: 10.1175/1520-0485(1979)009<0189:MOIISW>2.0.CO;2

Galton-Fenzi, B. K., Hunter, J. R., Coleman, R., Marsland, S. J., and Warner, R. C. (2012). Modeling the basal melting and marine ice accretion of the Amery Ice Shelf. *J. Geophys. Res.* 117, C09031. doi: 10.1029/2012JC008214

Ganachaud, A., and Wunsch, C. (2000). Improved estimates of global ocean circulation, heat transport and mixing from hydrographic data. *Nature* 408, 453–456. doi: 10.1038/35044048

George, T. M., Manucharyan, G. E., and Thompson, A. F. (2021). Deep learning to infer eddy heat fluxes from sea surface height patterns of mesoscale turbulence. *Nat. Commun.* 12, 1–11. doi: 10.1038/s41467-020-20779-9

Giese, B. S., and Ray, S. (2011). El Niño variability in simple ocean data assimilation (SODA), 1871–2008. *J. Geophys. Res.* 116, C02024. doi: 10.1029/2010JC006695

Gill, A. E. (1973). Circulation and bottom water production in the Weddell Sea. *Deep-Sea Res.* 20 (2), 111–140. doi: 10.1016/0011-7471(73)90048-X

Glasscock, S. K., Hayes, C. T., Redmond, N., and Rohde, E. (2020). Changes in Antarctic Bottom Water formation during interglacial periods. *Paleoceanogr. Paleoclimatol.* 35, e2020PA003867. doi: 10.1029/2020PA003867

Gordon, A. L. (1978). Deep Antarctic convection west of Maud Rise. *J. Phys. Oceanogr.* 8, 600–612. doi: 10.1175/1520-0485(1978)008<0600:DACWOM>2.0.CO;2

Gordon, A. L. (2012). Circumpolar view of the Southern ocean from 1962 to 1992. *Oceanography* 25 (3), 18–23. doi: 10.5670/oceanog.2012.69

Gordon, A. L. (2013). "Bottom water formation," in *Encyclopedia of ocean sciences, 2nd edn*, vol. 1 . Eds. J. H. Steele, S. A. Thorpe and K. K. Turekian (London: Academic Press), 415–421.

Gordon, A. L., Huber, B. A., and Abrahamsen, E. P. (2020). Interannual variability of the outflow of Weddell Sea Bottom Water. *Geophys. Res. Lett.* 47 (4), 1–9. doi: 10.1029/2020GL087014

Gordon, A. L., Huber, B. A., and Busecke, J. (2015). Bottom water export from the western Ross Sea 2007 through 2010. *Geophys. Res. Lett.* 42, 5387–5394. doi: 10.1002/2015GL064457

Gordon, A. L., Huber, B., McKee, D., and Visbeck, M. (2010). A seasonal cycle in the export of bottom water from the Weddell Sea. *Nat. Geosci.* 3 (8), 551–556. doi: 10.1038/ngeo916

Gordon, A. L., Ice Station Weddell Group of Principal Investigators and Chief Scientists (1993). Weddell Sea exploration from ice station. *Eos Trans. AGU* 74 (11), 121–126. doi: 10.1029/93EO00260

Gordon, A. L., Orsi, A. H., Muench, R., Huber, B. A., Zambianchi, E., and Visbeck, M. (2009). Western Ross Sea continental slope gravity currents. *Deep-Sea Res. II* 56 (13–14), 796–817. doi: 10.1016/j.dsr2.2008.10.037

Gordon, A. L., and Tchernia, P. (1972). *Waters of the continental margin off Adélie Coast, Antarctica. Antarctic Oceanology II: The Australian-New Zealand Sector, Antarct. Res. Ser* Vol. 19. Ed. D. E. Hayes (Washington, D. C: AGU), 59–69. doi: 10.1029/AR019p0059

Gordon, A. L., Zambianchi, E., Orsi, A., Visbeck, M., Giulivi, C. F., Whitworth, T., et al. (2004). Energetic plumes over the western Ross Sea continental slope. *Geophys. Res. Lett.* 31, L21302. doi: 10.1029/2004gl020785

Gouretski, V., and Koltermann, K. P. (2004). WOCE global hydrographic climatology. *Berichte Des. BSH* 35, 1–52.

Groeskamp, S., Griffies, S. M., Iudicone, D., Marsh, R., Nurser, A. J., and Zika, J. D. (2019). The water mass transformation framework for ocean physics and biogeochemistry. *Annu. Rev. Mar. Sci.* 11, 271–305. doi: 10.1146/annurev-marine-010318-095421

Gunn, K. L., Rintoul, S. R., England, M. H., and Bowen, M. M. (2023). Recent reduced abyssal overturning and ventilation in the Australian Antarctic Basin. *Nat. Clim. Change* 13, 1–8. doi: 10.1038/s41558-023-01667-8

Haine, T. W. N. (2010). High-frequency fluctuations in Denmark Strait transport. *Geophys. Res. Lett.* 37, L14601. doi: 10.1029/2010GL043272

Haine, T. W. N., Watson, A. J., Liddicoat, M. I., and Dickson, R. R. (1998). The flow of Antarctic bottom water to the southwest Indian Ocean estimated using CFCs. *J. Geophys. Res. Ocean.* 103, 27637–27653. doi: 10.1029/98JC02476

Hartog, A. H., Belal, M., and Clare, M. A. (2018). Advances in distributed fiber-optic sensing for monitoring marine infrastructure, measuring the deep ocean, and quantifying the risks posed by seafloor hazards. *Mar. Technol. Soc J.* 52, 58–73. doi: 10.4031/MTSJ.52.5.7

Hattermann, T., Nicholls, K. W., Hellmer, H. H., Davis, P. E. D., Janout, M. A., Østerhus, S., et al. (2021). Observed interannual changes beneath Filchner-Ronne Ice Shelf linked to large-scale atmospheric circulation. *Nat. Commun.* 12 (1), 1–11. doi: 10.1038/s41467-021-23131-x

Hellmer, H. H., Schröder, M., Haas, C., Dieckmann, G. S., and Spindler, M. (2008) The ISPOL drift experiment. *Deep Sea Res. II* 55, 913–917. doi: 10.1016/j.dsr2.2008.01.001

Henley, S. F., Cavan, E. L., Fawcett, S. E., Kerr, R., Monteiro, T., Sherrell, R. M., et al. (2020). Changing biogeochemistry of the Southern Ocean and its ecosystem implications. *Front. Mar. Sci.* 7. doi: 10.3389/fmars.2020.00581

Herraiz-Borreguero, L., Allison, I., Craven, M., Nicholls, K. W., and Rosenberg, M. A. (2013). Ice shelf/ocean interactions under the Amery Ice Shelf: seasonal variability and its effect on marine ice formation. *J. Geophys. Res. Oceans* 118, 7117–7131. doi: 10.1002/2013jc009158

Herraiz-Borreguero, L., Church, J. A., Allison, I., Peña-Molino, B., Coleman, R., Tomczak, M., et al. (2016). Basal melt, seasonal water mass transformation, ocean current variability, and deep convection processes along the Amery Ice Shelf calving front, East Antarctica. *J. Geophys. Res.: Oceans* 121, 4946–4965. doi: 10.1002/2016jc011858

Herraiz-Borreguero, L., Coleman, R., Allison, I., Rintoul, S. R., Craven, M., and Williams, G. D. (2015). Circulation of modifed Circumpolar Deep Water and basal melt beneath the Amery Ice Shelf, East Antarctica. *J. Geophys. Res.: Oceans* 120, 3098–3112. doi: 10.1002/2015JC010697

Herraiz-Borreguero, L., and Naveira Garabato, A. C. (2022). Poleward shift of Circumpolar Deep Water threatens the East Antarctic Ice Sheet. *Nat. Clim. Change* 12 (8), 728–734. doi: 10.1038/s41558-022-01424-3

Heuzé, C. (2021). Antarctic bottom water and north Atlantic deep water in CMIP6 models. *Ocean Sci.* 17, 59–90. doi: 10.5194/os-17-59-2021

Holzer, M., DeVries, T., and de Lavergne, C. (2021). Diffusion controls the ventilation of a Pacific Shadow Zone above abyssal overturning. *Nat. Commun.* 12 (1), 1–13. doi: 10.1038/s41467-021-24648-x

Høyer, J. L., and Quadfasel, D. (2001). Detection of deep overflows with satellite altimetry. *Geophys. Res. Lett.* 28 (8), 1611–1614. doi: 10.1029/2000GL012549

Huhn, O., Hattermann, T., Davis, P. E. D., Dunker, E., Hellmer, H. H., Nicholls, K. W., et al. (2018). Basal melt and freezing rates from first noble gas samples beneath an ice shelf. *Geophys. Res. Lett.* 45, 8455–8461. doi: 10.1029/2018GL079706

Huhn, O., Hellmer, H. H., Rhein, M., Rodehacke, C., Roether, W., Schodlok, M. P., et al. (2008). Evidence of deep- and bottom-water formation in the western Weddell Sea. *Deep. Res. Part II* 55 (8–9), 1098–1116. doi: 10.1016/j.dsr2.2007.12.015

Huhn, O., Rhein, M., Hoppema, M., and van Heuven, S. (2013). Decline of deep and bottom water ventilation and slowing down of anthropogenic carbon storage in the Weddell Sea 1984–2011. *Deep Sea Res. Part I: Oceanographic Res. Pap.* 76, 66–84. doi: 10.1016/j.dsr.2013.01.005

Jackett, D. R., and McDougall, T. J. (1997). A neutral density variable for the world's oceans. *J. Phys. Oceanogr.* 27, 237–263. doi: 10.1175/1520-0485(1997)027andlt;0237:ANDVFTandgt;2.0.CO;2

Jacobs, S. S., Fairbanks, R. G., and Horibe, Y. (1985). "Origin and evolution of water masses near the Antarctic continental margin: Evidence from H218O/H216O ratios in sea water," in *Antarctic research series*, vol. 43 . Ed. S. S. Jacobs (Washington, DC: American Geophysical Union), 59–85.

Jacobs, S. S., and Giulivi, C. F. (2010). Large Multidecadal salinity trends near the Pacifc-Antarctic Continental Margin. *J. Clim.* 23, 4508–4524. doi: 10.1175/2010JCLI3284.1

Jacobs, S. S., Giulivi, C. F., and Dutrieux, P. (2022). Persistent Ross Sea freshening from imbalance West Antarctic ice shelf melting. *J. Geophys. Res.: Oceans.* 127, e2021JC017808. doi: 10.1029/2021JC017808

Jacobs, S. S., Gordon, A. L., and Ardai, J. (1979). Circulation and melting beneath the Ross Ice Shelf. *Science* 203 (4379), 439–443. doi: 10.1126/science.203.4379.439

Jacobs, S. S., and Haines, W. E. (1982). "Ross ice shelf project, lamont-doherty geological observatory, & United States Antarctic research program," in *Oceanographic data in the Ross Sea and along George V Coast 1976-1979* (Palisades, N.Y: Lamont-Doherty Geological Observatory of Columbia University).

Janout, M. A., Hellmer, H. H., Hattermann, T., Huhn, O., Sültenfuss, J., Østerhus, S., et al. (2021). Fris revisited in 2018: On the circulation and water masses at the Filchner and Ronne ice shelves in the southern Weddell Sea. *J. Geophys. Res.: Oceans* 126, 1–19. doi: 10.1029/2021JC017269

Jenkins, A., Dutrieux, P., Jacobs, S. S., McPhail, S. D., Perrett, J. R., Webb, A. T., et al. (2010). Observations beneath pine island glacier in West Antarctica and implications for its retreat. *Nat. Geosci.* 3, 468–472. doi: 10.1038/ngeo890

Johnson, G. C. (2008). Quantifying antarctic bottom water and north atlantic deep water volumes. *J. Geophys. Res.: Oceans* 113, 1–13. doi: 10.1029/2007JC004477

Johnson, G. C. (2022). Antarctic Bottom Water warming and circulation slowdown in the Argentine Basin from analyses of Deep Argo and historical shipboard temperature data. *Geophys. Res. Lett.* 49, e2022GL100526. doi: 10.1029/2022GL100526

Johnson, G. C., Cadot, C., Lyman, J. M., McTaggart, K. E., and Steffen, E. L. (2020). Antarctic bottom water warming in the Brazil basin: 1990s through 2020, from WOCE to deep argo. *Geophys. Res. Lett.* 47, e2020GL089191. doi: 10.1029/2020GL089191

Johnson, G. C., and Doney, S. C. (2006). Recent western South Atlantic bottom water warming. *Geophys. Res. Lett.* 33, L14614. doi: 10.1029/2006GL026769

Johnson, G. C., McTaggart, K. E., and Wanninkhof, R. (2014). Antarctic Bottom Water temperature changes in the western South Atlantic from 1989 to 2014. *J. Geophys. Res.: Oceans* 119, 8567–8577. doi: 10.1002/2014JC010367

Johnson, G. C., Mecking, S., Sloyan, B. M., and Wijffels, S. E. (2007). Recent bottom water warming in the Pacific Ocean. *J. Climate* 20, 537165–535375. doi: 10.1175/2007JCLI1879.1

Johnson, G. C., Purkey, S. G., Zilberman, N. V., and Roemmich, D. (2019). Deep Argo quantifies bottom water warming rates in the Southwest Pacific Basin. *Geophys. Res. Lett.* 46 (5), 2662–2669. doi: 10.1029/2018gl081685

Johnson, M. R., and Smith, A. M. (1997). Seabed topography under the southern and western Ronne Ice Shelf from seismic surveys. *Antarct. Sci.* 92, 201–208. doi: 10.1017/s0954102097000254

Jullion, L., Garabato, A. C. N., Bacon, S., Meredith, M. P., Brown, P. J., Torres-Valdés, S., et al. (2014). The contribution of the Weddell Gyre to the lower limb of the

Global Overturning Circulation. *J. Geophys. Res.: Oceans* 119, 3357–3377. doi: 10.1002/2013JC009725

Jullion, L., Naveira Garabato, A. C., Meredith, M. P., Holland, P. R., Courtois, P., and King, B. A. (2013). Decadal freshening of the Antarctic Bottom Water exported from the Weddell Sea. *J. Clim.* 26, 8111–8125. doi: 10.1175/JCLI-D-12-00765.1e

Kashiwase, H., Ohshima, K. I., Nakata, K., and Tamura, T. (2021). Improved SSM/I thin ice algorithm with ice type discrimination in coastal polynyas. *J. Atm. Ocean. Tech.* 38 (4), 823–835. doi: 10.1175/JTECH-D-20-0145.1

Katsumata, K., Nakano, H., and Kumamoto, Y. (2015). Dissolved oxygen change and freshening of Antarctic Bottom water along 62°S in the Australian-Antarctic Basin between 1995/1996 and 2012/2013. *Deep-Sea Res. Part II: Topical Stud. Oceanogr.* 114, 27–38. doi: 10.1016/J.DSR2.2014.05.016

Kawano, T., Fukasawa, M., Kouketsu, S., Uchida, H., Doi, T., Kaneko, I., et al. (2006). Bottom water warming along the pathway of lower circumpolar deep water in the Pacific ocean. *Geophys. Res. Lett.* 33, 23, L23613. doi: 10.1029/2006GL027933

Kerr, R., Dotto, T. S., Mata, M. M., and Hellmer, H. H. (2018). Three decades of deep water mass investigation in the Weddell Sea, (1984–2014): Temporal variability and changes. *Deep-Sea Res. Part II: Topical Stud. Oceanogr.* 149, 70–83. doi: 10.1016/j.dsr2.2017.12.002

Kerr, R., Heywood, K. J., Mata, M. M., and Garcia, C. A. E. (2012). On the outflow of dense water from the Weddell and Ross Seas in OCCAM model. *Ocean Sci.* 8(3), 369–388. doi: 10.5194/os-8-369-2012

Kerr, R., Mata, M. M., and Garcia, C. A. (2009). On the temporal variability of the Weddell Sea Deep Water masses. *Antarct. Sci.* 21, 383. doi: 10.1017/S0954102009001990

Kim, T.-W., Yang, H. W., Dutrieux, P., Wåhlin, A. K., Jenkins, A., Kim, Y. G., et al. (2021). Interannual variation of modified circumpolar deep water in the Dotson-Getz trough, West Antarctica. *J. Geophys. Res.: Oceans* 126 (12), e2021JC017491. doi: 10.1029/2021jc017491

Kiss, A. E., Hogg, A. M., Hannah, N., Boeira Dias, F., Brassington, G., Chamberlain, M. A., et al. (2020). ACCESS-OM2 V1.0: A global ocean-sea ice model at three resolutions. *Geosci. Model. Dev.* 13, 401–442. doi: 10.5194/gmd-13-401-2020

Kitade, Y., Shimada, K., Tamura, T., Williams, G. D., Aoki, S., Fukamachi, Y., et al. (2014). Antarctic bottom water production from the Vincennes Bay Polynya, East Antarctica. *Geophys. Res. Lett.* 41, 2014GL059971. doi: 10.1002/2014GL059971

Klatt, O., Boebel, O., and Fahrbach, E. (2007). A profiling float's sense of ice. *J. Atmos. Ocean. Technol.* 24, 1301–1308. doi: 10.1175/JTECH2026.1

Kobs, S., Holland, D. M., Zagorodnov, V., Stern, A., and Tyler, S. W. (2014). Novel monitoring of Antarctic ice shelf basal melting using a fiber-optic distributed temperature sensing mooring. *Geophys. Res. Lett.* 41, 6779–6786. doi: 10.1002/2014GL061155

Kohut, J., Hunter, E., and Huber, B. (2013). Small-scale variability of the cross-shelf flow over the outer shelf of the Ross Sea. *J. Geophys. Res.: Oceans* 118, 1863–1876. doi: 10.1002/jgrc.20090

Kouketsu, S., Doi, T., Kawano, T., Masuda, S., Sugiura, N., Sasaki, Y., et al. (2011). Deep ocean heat content changes estimated from observation and reanalysis product and their influence on sea level change. *J. Geophys. Res.* 116, C03012. doi: 10.1029/2010JC006464

Lacarra, M., Houssais, M.-N., Herbaut, C., Sultan, E., and Beauverger, M. (2014). Dense shelf water production in the Adélie Depression, East Antarctica 2004–2012: impact of the mertz glacier calving. *J. Geophys. Res.: Oceans* 119, 5203–5220. doi: 10.1002/2013JC009124

Lacarra, M., Houssais, M.-N., Sultan, E., Rintoul, S. R., and Herbaut, C. (2011). Summer hydrography on the shelf off Terre Adélie/George V Land based on the ALBION and CEAMARC observations during the IPY. *Pol. Sci.* 5 (2), 88–103. doi: 10.1016/j.polar.2011.04.008

Langhorne, P. J., Hughes, K. G., Gough, A. J., Smith, I. J., Williams, M. J. M., Robinson, N. J., et al. (2015). Observed platelet ice distributions in Antarctic sea ice: An index for ocean-ice shelf heat flux. *Geophys. Res. Lett.* 42, 5442–5451. doi: 10.1002/2015GL064508

Lawrence, J. D., Washam, P. M., Stevens, C., Hulbe, C., Horgan, H. J., Dunbar, G., et al. (2023). Crevasse refreezing and signatures of retreat observed at Kamb Ice Stream grounding zone. *Nat. Geosci.* 16, 238–243. doi: 10.1038/s41561-023-01129-y

Lea, D., Haine, T., and Gasparovic, R. (2006). Observability of the Irminger Sea circulation using variational data assimilation. *Q. J. R. Meteorol. Soc* 132, 1545–1576. doi: 10.1256/qj.05.77

Le Bel, D. A., Zappa, C. J., Budillon, G., and Gordon, A. L. (2021). Salinity response to atmospheric forcing of the Terra Nova Bay polynya, Antarctica. *Ant. Sci.* 33 (3), 318–331. doi: 10.1017/S0954102021000146

Li, Q., England, M. H., Hogg, A. M., Rintoul., S. R., and Morrison, A. K. (2023). Abyssal ocean overturning slowdown and warming driven by Antarctic meltwater. *Nature* 615, 841–847. doi: 10.1038/s41586-023-05762-w

Liu, M., and Tanhua, T. (2021). Water masses in the Atlantic ocean: characteristics and distributions. *Ocean Sci.* 17, 463–486. doi: 10.5194/os-17-463-2021

Liu, C., Wang, Z., Cheng, C., Wu, Y., Xia, R., Li, B., et al. (2018). On the modified Circumpolar Deep Water upwelling over the Four Ladies Bank in Prydz Bay, East Antarctica. *J. Geophys. Res.: Oceans* 123, 7819–7838. doi: 10.1029/2018JC014026

Llanillo, P. J., Kanzow, T., Janout, M. A., and Rohardt, G. (2023). The deep-water plume in the northwestern Weddell Sea, Antarctica: Mean state, seasonal cycle and interannual variability influenced by climate modes. *J. Geophys. Res.: Oceans* 128, e2022JC019375. doi: 10.1029/2022JC019375

Loose, B., Schlosser, P., Smethie, W. M., and Jacobs, S. S. (2009). An optimized estimate of glacial melt from the Ross Ice Shelf using noble gases, stable isotopes and CFC transient tracers. *J. Geophys. Res.* 114, C08007. doi: 10.1029/2008JC005048

Lumpkin, R., and Speer, K. (2007). Global ocean meridional overturning. *J. Phys. Oceanogr.* 37, 2550–2562. doi: 10.1175/JPO3130.1

Lynn, R. J., and Reid, J. L. (1968). Characteristics and circulation of deep and abyssal waters. *Deep Sea Res. Oceanogr. Abstr.* 15, 577–598. doi: 10.1016/0011-7471(68)90064-8

Mahieu, L., Lo Monaco, C., Metzl, N., Fin, J., and Mignon, C. (2020). Variability and stability of anthropogenic CO 2 in Antarctic bottom water observed in the Indian sector of the Southern Ocean 1978–2018. *Ocean Sci.* 16 (6), 1559–1576. doi: 10.5194/os-16-1559-2020

Makinson, K., and Anker, P. G. D. (2014). The BAS ice-shelf hot-water drill: design, methods and tools. *Ann. Glaciol.* 55, 44–52. doi: 10.3189/2014aog68a030

Makinson, K., and Nicholls, K. W. (1999). Modeling tidal currents beneath Filchner-Ronne Ice Shelf and on the adjacent continental shelf: Their effect on mixing and transport. *J. Geophys. Res.: Oceans* 104, 13449–13465. doi: 10.1029/1999jc900008

Marinov, I., Gnanadesikan, A., Toggweiler, J. R., and Sarmiento, J. L. (2006). The Southern Ocean biogeochemical divide. *Nature* 441 (7096), 964–967. doi: 10.1038/nature04883

Marouchos, A., Sherlock, M., Rintoul, S., and Pender, L. (2013). A system for correcting ADCP heading on moorings at high latitudes. *OCEANS*, 1–4. doi: 10.23919/OCEANS.2013.6741100

Martin, A., Houssais, M.-N., le Goff, H., Marec, C., and Dausse, D. (2017). Circulation and water mass transports on the East Antarctic shelf in the Mertz Glacier region. *Deep. Res. Part I* 126, 1–20. doi: 10.1016/j.dsr.2017.05.007

Marzocchi, A., and Jansen, M. F. (2019). Global cooling linked to increased glacial carbon storage via changes in Antarctic sea ice. *Nat. Geosci.* 12 (12), 1001–1005. doi: 10.1038/s41561-019-0466-8

Masuda, S., Awaji, T., Sugiura, N., Matthews, J. P., Toyoda, T., Kawai, Y., et al. (2010). Simulated rapid warming of abyssal North Pacific Waters. *Science* 329, 319–322. doi: 10.1126/science.1188870

Matear, R. J., and McNeil, B. I. (2003). Decadal accumulation of anthropogenic CO_2 in the Southern Ocean: A comparison of CFC-age derived estimates to multiple-linear regression estimates. *Global Biogeochem. Cycles* 17 (4), 1113. doi: 10.1029/2003GB002089

Mazloff, M. R., and Boening, C. (2016). Rapid variability of Antarctic Bottom Water transport into the Pacific Ocean inferred from GRACE. *Geophys. Res. Lett.* 43, 3822–3829. doi: 10.1002/2016GL068474

Mazloff, M. R., Ferrari, R., and Schneider, T. (2013). The force balance of the Southern Ocean Meridional Overturning Circulation. *J. Phys. Oceanogr.* 43 (6), 1193–1208. doi: 10.1175/jpo-d-12-069.1

Mazloff, M. R., Heimbach, P., and Wunsch, C. (2010). An eddy-permitting southern ocean state estimate. *J. Phys. Oceanogr.* 40, 880–899. doi: 10.1175/2009JPO4236.1

McIntosh, P. C., and Rintoul, S. R. (1997). Do box inverse models work? *J. Phys. Oceanogr.* 27 (2), 291–308. doi: 10.1175/1520-0485(1997)027<0291:dbimw>2.0.co;2

McKee, D. C., Yuan, X., Gordon, A. L., Huber, B. A., and Dong, Z. (2011). Climate impact on interannual variability of Weddell Sea bottom water. *J. Geophys. Res.* 116 (5), 1–17. doi: 10.1029/2010JC006484

McMahon, C. R., Roquet, F., Baudel, S., Belbeoch, M., Bestley, S., Blight, C., et al. (2021). Animal borne ocean sensors – aniBOS – an essential component of the global ocean observing system. *Front. Mar. Sci.* 8. doi: 10.3389/fmars.2021.751840

Meier, W. N., Fetterer, F., Savoie, M., Mallory, S., Duerr, R., and Stroeve, J. (2017). *NOAA/NSIDC climate data record of passive microwave sea ice concentration, version 3* (Boulder, Colorado USA: National Snow and Ice Data Center). doi: 10.7265/N59P2ZTG

Meijers, A. J. S., Klocker, A., Bindoff, N. L., Williams, G. D., and Marsland, S. J. (2010). The circulation and water masses of the Antarctic shelf and continental slope between 30 and 80°E. *Deep Sea Res. II Top. Stud. Oceanogr.* 57, 723–737. doi: 10.1016/j.dsr2.2009.04.019

Menemenlis, D., Campin, J. M., Heimbach, P., Hill, C., Lee, T., Nguyen, A., et al. (2008). ECCO2: high resolution global ocean and sea ice data synthesis. *Mercator Ocean Q. Newslett.*, 13–21.

Menezes, V. V., Macdonald, A. M., and Schatzman, C. (2017). Accelerated freshening of Antarctic Bottom Water over the last decade in the Southern Indian Ocean. *Sci. Adv.* 3, e1601426. doi: 10.1126/sciadv.1601426

Mensah, V., Nakayama, Y., Fujii, M., Nogi, Y., and Ohshima, K. I. (2021). Dense water downslope flow and AABW production in a numerical model: Sensitivity to horizontal and vertical resolution in the region off Cape Darnley polynya. *Ocean Model.* 165, 101843. doi: 10.1016/j.ocemod.2021.101843

Mensch, M., Bayer, R., Bullister, J., Schlosser, P., and Weiss, R. (1996). The distribution of tritium and CFCs in the Weddell Sea during the mid-1980s. *Prog. Oceanogr.* 38 (4), 377–415. doi: 10.1016/S0079-6611(97)00007-4

Meredith, M. P., Brandon, M. A., Wallace, M. I., Clarke, A., Leng, M. J., Renfrew, I. A., et al. (2008). Variability in the freshwater balance of northern Marguerite Bay,

Antarctic Peninsula: results from delta O-18. *Deep Sea Res. Part II* 55, 309–322. doi: 10.1016/j.dsr2.2007.11.005

Meredith, M. P., Brown, P. J., Naveira Garabato, A. C., Jullion, L., Venables, H. J., and Messias, M. J. (2013). Dense bottom layers in the Scotia Sea, Southern Ocean: Creation, lifespan and destruction. *Geophys. Res. Lett.* 40, 933–936. doi: 10.1002/grl.50260

Meredith, M. P., Gordon, A. L., Naveira Garabato, A. C., Abrahamsen, E. P., Huber, B. A., Jullion, L., et al. (2011). Synchronous intensification and warming of Antarctic Bottom Water outflow from the Weddell Gyre. *Geophys. Res. Lett.* 38, L03603. doi: 10.1029/2010GL046265

Meredith, M. P., Heywood, K. J., Dennis, P. F., Goldson, L. E., White, R. M. P., Fahrbach, E., et al. (2001b). Freshwater fluxes through the western Fram Strait. *Geophys. Res. Lett.* 28, 1615–1618. doi: 10.1029/2000GL011992

Meredith, M. P., Jullion, L., Brown, P. J., Naveira Garabato, A. C., and Couldrey, M. P. (2014). Dense waters of the Weddell and Scotia Seas: Recent changes in properties and circulation. *Philos. Trans. R. Soc London Ser. A* 372, 20130041. doi: 10.1098/rsta.2013.0041

Meredith, M. P., Watson, A., and Scoy, K. V. (2001a). Chlorofluorocarbon-derived formation rates of the deep and bottom waters of the Weddell Sea. *J. Geophys. Res.* 106 (C2), 2899–2919. doi: 10.1029/2000JC900119

Merz, A. (1925). *Die Deutsche Atlantische Expedition auf dem Vermessungs- und Forschungsschiff "Meteor". 1. Bericht. Sitzungsberichte der Preussischen Akademie der Wissenschaften, Physikalische–Mathematische Klasse, Jahrgang*, Vol. 1925. 562–586.

Merz, A., and Wüst, G. (1922). Die atlantische vertikalzirkulation. *Z. Ges. Erdkunde Berlin*, 1–35.

Mizobata, K., Shimada, K., Aoki, S., and Kitade, Y. (2020). The cyclonic eddy train in the Indian Ocean sector of the Southern Ocean as revealed by satellite radar altimeters and in *situ* measurements. *J. Geophys. Res.: Oceans* 125, e2019JC015994. doi: 10.1029/2019JC015994

Moholdt, G., Padman, L., and Fricker, H. A. (2014). Basal mass budget of Ross and Filchner-Ronne ice shelves, Antarctica, derived from Lagrangian analysis of ICESat altimetry. *Journal of Geophysical Research: Earth Surface* 119, 2361–2380. doi: 10.1002/2014JF003171

Morlighem, M., Rignot, E., Binder, T., Blankenship, D., Drews, R., Eagles, G., et al. (2020). Deep glacial troughs and stabilizing ridges unveiled beneath the margins of the Antarctic ice sheet. *Nat. Geosci.* 13, 132–137. doi: 10.1038/s41561-019-0510-8

Morrison, A. K., Hogg, A. M., England, M. H., and Spence, P. (2020). Warm Circumpolar Deep Water transport toward Antarctica driven by local dense water export in canyons. *Sci. Adv.* 6, eaav2516. doi: 10.1126/sciadv.aav2516

Muench, R., Padman, L., Gordon, A., and Orsi, A. H. (2009). A dense water outflow from the Ross Sea, Antarctica: Mixing and the contribution of tides. *J. Mar. Syst.* 77 (4), 369–387. doi: 10.1016/j.jmarsys.2008.11.003

Müller, S. A., Joos, F., Edwards, N. R., and Stocker, T. F. (2006). Water mass distribution and ventilation time scales in a cost-efficient, three-dimensional ocean model. *J. Clim.* 19, 5479–5499. doi: 10.1175/JCLI3911.1

Murata, A., Kumamoto, Y.-i., and Sasaki, K.-i. (2019). Decadal-scale increases of anthropogenic CO_2 in Antarctic bottom water in the Indian and western Pacific sectors of the Southern Ocean. *Geophys. Res. Lett.* 46, 833–841. doi: 10.1029/2018GL080604

Nakata, K., Ohshima, K. I., and Nihashi, S. (2019). Estimation of thin ice thickness and discrimination of ice type from AMSR-E passive microwave data. *IEEE Transactions on Geoscience and Remote Sensing* 57, 1, 263–276. doi: 10.1109/TGRS.2018.2853590

Nakata, K., Ohshima, K. I., and Nihashi, S. (2021). Mapping of active frazil for Antarctic coastal polynyas, with an estimation of sea-ice production. *Geophys. Res. Lett.* 48 (6), e2020GL091353. doi: 10.1029/2020GL091353

Naveira Garabato, A. C., Frajka-Williams, E. E., Spingys, C. P., Legg, S., Polzin, K. L., Forryan, A., et al. (2019). Rapid mixing and exchange of deep-ocean waters in an abyssal boundary current. *Proc. Natl. Acad. Sci. U.S.A.* 116, 13233–13238. doi: 10.1073/pnas.1904087116

Naveira Garabato, A. C., McDonagh, E. L., Stevens, D. P., Heywood, K. J., and Sanders, R. J. (2002). On the export of antarctic bottom water from the Weddell sea. *Deep Sea Res. Part II* 49, 4715–4742. doi: 10.1016/S0967?0645(02)00156?X

Naveira Garabato, A. C., Williams, A. P., and Bacon, S. (2014). The three-dimensional overturning circulation of the Southern Ocean during the WOCE era. *Progr. Oceanogr.* 120, 41–78. doi: 10.1016/j.pocean.2013.07.018

Naveira Garabato, A. C., Zika, J. D., Jullion, L., Brown, P. J., Holland, P. R., Meredith, M. P., et al. (2016). The thermodynamic balance of the Weddell Gyre. *Geophys. Res. Lett.* 43, 317–325. doi: 10.1002/2015GL066658

Nelson, M., Queste, B., Smith, I., Leonard, G., Webber, B., and Hughes, K. (2017). Measurements of Ice Shelf Water beneath the front of the Ross Ice Shelf using gliders. *Ann. Glaci.* 58 (74), 41–50. doi: 10.1017/aog.2017.34

Newman, L., Heil, P., Trebilco, R., Katsumata, K., Constable, A. J., van Wijk, E., et al. (2019). Delivering sustained, coordinated and integrated observations of the Southern Ocean for global impact. *Front. Mar. Sci.* doi: 10.3389/fmars.2019.00433

Nicholls, K. W., Boehme, L., Biuw, M., and Fedak, M. A. (2008). Wintertime ocean conditions over the southern Weddell Sea continental shelf, Antarctica. *Geophys. Res. Lett.* 35, L21605. doi: 10.1029/2008GL035742

Nicholls, K. W., Corr, H. F. J., Stewart, C. L., Lok, L. B., Brennan, P. V., and Vaughan, D. G. (2015). A ground-based radar for measuring vertical strain rates and time-varying basal melt rates in ice sheets and shelves. *J. Glaciol.* 61, 1079–1087. doi: 10.3189/2015JoG15J073

Nicholls, K. W., Østerhus, S., Makinson, K., Gammelsrød, T., and Fahrbach, E. (2009). Ice-ocean processes over the continental shelf of the southern Weddell Sea, Antarctica. *A review. Rev. Geophys.* 47, 1–23. doi: 10.1029/2007RG000250

Nihashi, S., and Ohshima, K. I. (2015). Circumpolar mapping of Antarctic coastal polynyas and landfast sea ice: relationship and variability. *J. Clim.* 28, 3650–3670. doi: 10.1175/jcli-d-14-00369.1

Nunes Vaz, R. A., and Lennon, G. W. (1996). Physical oceanography of the Prydz Bay region of Antarctic waters. *Deep Sea Res. Part I: Oceanogr. Res. Papers* 43, 603–641. doi: 10.1016/0967-0637(96)00028-3

Ohashi, Y., Yamamoto-Kawai, M., Kusahara, K., Sasaki, K., and Ohshima, K. I. (2022). Age distribution of Antarctic Bottom Water off Cape Darnley, East Antarctica, estimated using chlorofluorocarbon and sulfur hexafluoride. *Sci. Rep.* 12, 8462. doi: 10.1038/s41598-022-12109-4

Ohshima, K. I., Fukamachi, Y., Ito, M., Nakata, K., Simizu, D., Ono, K., et al. (2022). Dominant frazil ice production in the Cape Darnley polynya leading to Antarctic Bottom Water formation. *Sci. Adv.* 8, eadc9174. doi: 10.1126/sciadv.adc9174

Ohshima, K. I., Fukamachi, Y., Williams, G. D., Nihashi, S., Roquet, F., Kitade, Y., et al. (2013). Antarctic Bottom Water production by intense sea-ice formation in the Cape Darnley polynya. *Nat. Geosci.* 6, 235–240. doi: 10.1038/ngeo1738

Oke, P. R., Rykova, T., Pilo, G. S., and Lovell, J. L. (2022). Estimating Argo float trajectories under ice. *Earth Space Sci.* 9, e2022EA002312. doi: 10.1029/2022EA002312

Olbers, D., Borowski, D., Völker, C., and Wölf, J.-O. (2004). The dynamical balance, transport and circulation of the Antarctic Circumpolar Current. *Antarct. Sci.* 16, 439–470. doi: 10.1017/S0954102004002251

Orsi, A. H., Jacobs, S. S., Gordon, A. L., and Visbeck, M. (2001). Cooling and ventilating the abyssal ocean. *Geophys. Res. Lett.* 28 (15), 2923–2926. doi: 10.1029/2001gl012830

Orsi, A. H., Johnson, G. C., and Bullister, J. L. (1999). Circulation, mixing and production of Antarctic Bottom Water. *Prog. Oceanogr.* 43, 55–109. doi: 10.1016/S0079-6611(99)00004-X

Orsi, A., Smethie, W., and Bullister, J. (2002). On the total input of Antarctic waters to the deep ocean: a preliminary estimate from chlorofluorocarbon measurements. *J. Geophys. Res.* 107, 3122. doi: 10.1029/2001JC000976

Orsi, A. H., and Whitworth, T. III (2005). *Hydrographic atlas of the World Ocean Circulation Experiment (WOCE)* Vol. 1. Eds. M. Sparrow, P. Chapman and J. Gould (Southern Ocean: International WOCE Project Office).

Orsi, A., and Wiederwohl, C. L. (2009). A recount of Ross Sea waters. *Deep. Res. Part II* 56, 778–795. doi: 10.1016/j.dsr2.2008.10.033

Osse, T. J., and Eriksen, C. C. (2007). The deepglider: a full ocean depth glider for oceanographic research. *OCEANS* (Vancouver, BC), 2007, 1–12.

Padman, L., Howard, S. L., Orsi, A. H., and Muench, R. D. (2009). Tides of the northwestern Ross Sea and their impact on dense outflows of Antarctic Bottom Water. *Deep-Sea Res. II* 56, 818–834. doi: 10.1016/j.dsr2.2008.10.026

Pillsbury, D. R., and Jacobs, S. S. (1985). Preliminary observations from long-term current meter moorings near the Ross ice shelf, Antarctica. *Oceanol. Antarctic Continental Shelf. Washington D.C.: Am. Geophys. Union.* 43, 87–107.

Portela, E., Rintoul, S. R., Bestley, S., Herraiz-Borreguero, L., van Wijk, E., McMahon, C. R., et al. (2021). Seasonal transformation and spatial variability of water masses within MacKenzie polynya, Prydz Bay. *J. Geophys. Res.: Oceans* 126, e2021JC017748. doi: 10.1029/2021JC017748

Porter, D. F., Springer, S. R., Padman, L., Fricker, H. A., Tinto, K. J., Riser, S. C., et al. (2019). Evolution of the seasonal surface mixed layer of the Ross Sea, Antarctica, observed with autonomous profiling floats. *J. Geophys. Res.: Oceans* 124, 4934–4953. doi: 10.1029/2018JC014683

Purkey, S. G., and Johnson, G. C. (2010). Warming of global abyssal and deep Southern Ocean waters between the 1990s and 2000s: contributions to global heat and sea level rise budgets. *J. Clim.* 23, 6336–6351. doi: 10.1175/2010jcli3682.1

Purkey, S. G., and Johnson, G. C. (2012). Global contraction of antarctic bottom water between the 1980s and 2000s. *J. Clim.* 25, 5830–5844. doi: 10.1175/JCLI-D-11-00612.1

Purkey, S. G., and Johnson, G. C. (2013). Antarctic Bottom Water warming and freshening: Contributions to sea level rise, ocean freshwater budgets, and global heat gain. *J. Clim.* 26, 6105–6122. doi: 10.1175/JCLI-D-12-00834.1

Purkey, S. G., Johnson, G. C., Talley, L. D., Sloyan, B. M., Wijffels, S. E., Smethie, W., et al. (2019). Continued bottom water warming and freshening in the South Pacific Ocean. *J. Geophys. Res.* 124, 1778–1794. doi: 10.1029/2018JC014775

Purkey, S. G., Smethie, W. M., Gebbie, G., Gordon, A. L., Sonnerup, R. E., Warner, M. J., et al. (2018). A synoptic view of the ventilation and circulation of Antarctic Bottom Water from chlorofluorocarbons and natural tracers. *Ann. Rev. Mar. Sci.* 10, 503–327. doi: 10.1146/annurev-marine-121916-063414

Rackow, T., Wesche, C., Timmermann, R., Hellmer, H. H., Juricke, S., and Jung, T. (2017). A simulation of small to giant Antarctic iceberg evolution: differential impact on climatology estimates: melt and drift of small to giant icebergs. *J. Geophys. Res.: Oceans* 122, 3170–3190. doi: 10.1002/2016JC012513

Rae, J. W. B., and Broecker, W. (2018). What fraction of the Pacific and Indian oceans' deep water is formed in the Southern Ocean? *Biogeosciences* 15, 3779–3794. doi: 10.5194/bg-15-3779-2018

Rafter, P. A., Gray, W. R., Hines, S. K. V., Burke, A., Costa, K. M., Gottschalk, J., et al. (2022). Global reorganization of deep-sea circulation and carbon storage after the last ice age. *Sci. Adv.* 8 (46). doi: 10.1126/sciadv.abq5434

Reid, J. L. (1989). On the total geostrophic circulation of the South Atlantic Ocean: Flow patterns, tracers and transports. *Progr. Oceanogr.* 23 (3), 149–244. doi: 10.1016/0079-6611(89)90001-3

Reid, J. L. (1994). On the total geostrophic circulation of the North Atlantic Ocean: Flow patterns, tracers, and transports. *Progr. Oceanogr.* 33 (1), 1–92. doi: 10.1016/0079-6611(94)90014-0

Reid, J. L. (1997). On the total geostrophic circulation of the Pacific Ocean: Flow patterns, tracers, and transports. *Progr. Oceanogr.* 39 (4), 263–352. doi: 10.1016/s0079-6611(97)00012-8

Renner, A. H. H., Heywood, K. J., and Thorpe, S. E. (2009). Validation of three global ocean models in the Weddell Sea. *Ocean Model.* 30 (1), 1–15. doi: 10.1016/j.ocemod.2009.05.007

Ribeiro, N., Herraiz-Borreguero, L., Rintoul, S. R., McMahon, C. R., Hindell, M., Harcourt, R., et al. (2021). Warm modified Circumpolar Deep Water intrusions drive ice shelf melt and inhibit Dense Shelf Water formation in Vincennes Bay, East Antarctica. *J. Geophys. Res.: Oceans* 126, e2020JC016998. doi: 10.1029/2020JC016998

Richardson, P. L. (2008). On the history of meridional overturning circulation schematic diagrams. *Prog. Oceanogr.* 76, 466–486. doi: 10.1016/j.pocean.2008.01.005

Rignot, E., Jacobs, S., Mouginot, J., and Scheuchl, B. (2013). Ice-shelf melting around Antarctica. *Science* 341, 266–270. doi: 10.1126/science.1235798

Rintoul, S. R. (1998). *On the origin and influence of Adélie land bottom water* (Washington, DC: American Geophysical Union). doi: 10.1029/AR075p0151

Rintoul, S. R. (2007). Rapid freshening of Antarctic Bottom Water formed in the Indian and Pacifc oceans. *Geophys. Res. Lett.* 34, 1–5. doi: 10.1029/2006GL028550

Ríos, A. F., Velo, A., Pardo, P. C., Hoppema, M., and Pérez, F. F. (2012). An update of anthropogenic CO_2 storage rates in the western South Atlantic basin and the role of Antarctic Bottom Water. *J. Mar. Syst.* 94, 197–203. doi: 10.1016/j.jmarsys.2011.11.023

Riser, S. C., Freeland, H. J., Roemmich, D., Wijffels, S., Troisi, A., Belbeoch, M., et al. (2016). Fifteen years of ocean observations with the global Argo array. *Nat. Clim. Change* 6, 145–153. doi: 10.1038/nclimate2872

Rivaro, P., Ianni, C., Magi, E., Massolo, S., Budillon, G., and Smethie., W. M. (2015). Distribution and ventilation of water masses in the western Ross Sea inferred from CFC measurements. *Deep-Sea Res. Part I*, 97. doi: 10.1016/j.dsr.2014.11.009

Robinson, N. J., Williams, M. J. M., Barrett, P. J., and Pyne, A. R. (2010). Observations of flow and ice-ocean interaction beneath the McMurdo Ice Shelf, Antarctica. *J. Geophys. Res.* 115, C03025. doi: 10.1029/2008JC005255

Robinson, N. J., Williams, M. J. M., Stevens, C. L., Langhorne, P. J., and Haskell, T. G. (2014). Evolution of a supercooled Ice Shelf Water plume with an actively growing subice platelet matrix. *J. Geophys. Res.: Oceans* 119, 3425–3446. doi: 10.1002/2013JC009399

Roper, D., Harris, C. A., Salavasidis, G., Pebody, M., Templeton, R., Prampart, T., et al. (2021). Autosub long range 6000: A multiple-month endurance AUV for deep-ocean monitoring and survey. *IEEE J. Ocean. Eng.* 46, 1179–1191. doi: 10.1109/JOE.2021.3058416

Roquet, F., Wunsch, C., Forget, G., Heimbach, P., Guinet, C., Reverdin, G., et al. (2013). Estimates of the Southern Ocean general circulation improved by animal-borne instruments. *Geophys. Res. Lett.* 40, 6176–6180. doi: 10.1002/2013GL058304

Rousselet, L., Cessi, P., and Forget, G. (2021). Coupling of the mid-depth and abyssal components of the global overturning circulation according to a state estimate. *Sci. Adv.* 7 (21), eabf5478. doi: 10.1126/sciadv.abf5478

Rusciano, E., Budillon, G., Fusco, G., and Spezie, G. (2013). Evidence of atmosphere–sea ice–ocean coupling in the Terra Nova Bay polynya (Ross Sea—Antarctica). *Cont. Shelf Res.* 61-62, 112–124. doi: 10.1016/j.csr.2013.04.002

Saha, S., Moorthi, S., Pan, H.-L., Wu, X., Wang, J., Nadiga, S., et al. (2010). The NCEP climate forecast system reanalysis. *Bull. Am. Meteorol. Soc* 91, 1015–1058. doi: 10.1175/2010BAMS3001.1

Sambrotto, R. N., Matsuda, A., Vaillancourt, R., Brown, M., Langdon, C., Jacobs, S. S., et al. (2003). Summer plankton production and nutrient consumption patterns in the mertz glacier region of East Antarctica. *Deep Sea Res. Part II: Topical Stud. Oceanogr.* 50, 1393–1414. doi: 10.1016/S0967-0645(03)00076-6

Sasai, Y., Ishida, A., Yamanaka, Y., and Sasaki, H. (2004). Chlorofluorocarbons in a global ocean eddy-resolving OGCM: Pathway and formation of Antarctic Bottom Water. *Geophys. Res. Lett.* 31 (12), L12305. doi: 10.1029/2004gl019895

Schlosser, P., Bayer, R., Foldvik, A., Gammelsrød, T., Rohardt, G., and Münnich, K. O. (1990). Oxygen 18 and helium as tracers of ice shelf water and water/ice interaction in the Weddell Sea. *J. Geophys. Res.* 95, 3253–3263. doi: 10.1029/JC095iC03p03253

Schlosser, P., Bullister, J. L., and Bayer, R. (1991). Studies of deep water formation and circulation in the Weddell Sea using natural and anthropogenic tracers. *Mar. Chem.* 35, 97–122. doi: 10.1016/S0304-4203(09)90011-1

Schmidtko, S., Heywood, K. J., Thompson, A. F., and Aoki, S. (2014). Multidecadal warming of Antarctic waters. *Science* 346, 1227–1231. doi: 10.1126/science.1256117

Selker, J. S., Thevenaz, L., Huwald, H., Mallet, A., Luxemburg, W., Van De Giesen, N., et al. (2006). Distributed fiber-optic temperature sensing for hydrologic systems. *Water Res. Res.* 42, W12202. doi: 10.1029/2006WR005326

Semper, S., and Darelius, E. (2017). Seasonal resonance of diurnal continental shelf waves in the southern Weddell Sea. *Ocean Sci.* 13, 77–93. doi: 10.5194/os-2016-36

Shadwick, E. H., Rintoul, S. R., Tilbrook, B., Williams, G. D., Young, N., Fraser, A. D., et al. (2013). Glacier tongue calving reduced dense water formation and enhanced carbon uptake. *Geophys. Res. Lett.* 40, 904–909. doi: 10.1002/grl.50178

Shimada, K., Aoki, S., Ohshima, K. I., and Rintoul, S. R. (2012). Influence of Ross Sea Bottom Water changes on the warming and freshening of the Antarctic Bottom Water in the Australian-Antarctic Basin. *Ocean Sci.* 8, 419–432. doi: 10.5194/os-8-419-2012

Shimada, K., Kitade, Y., Aoki, S., Mizoabata, K., Cheng, L., Takahashi, K. T., et al. (2022). Shoaling of abyssal ventilation in the Eastern Indian Sector of the Southern Ocean. *Commun. Earth Environ.* 3, 120. doi: 10.1038/s43247-022-00445-2

Sigman, D. M., and Boyle, E. A. (2000). Glacial/interglacial variations in atmospheric carbon dioxide. *Nature* 407 (6806), 859–869. doi: 10.1038/35038000

Silvano, A., Foppert, A., Rintoul, S. R., Holland, P. R., Tamura, T., Kimura, N., et al. (2020). Recent recovery of Antarctic Bottom Water formation in the Ross Sea driven by climate anomalies. *Nat. Geosci.* 13, 780–786. doi: 10.1038/s41561-020-00655-3

Silvano, A., Rintoul, S. R., Kusahara, K., Peña-Molino, B., van Wijk, E., Gwyther, D. E., et al. (2019). Seasonality of warm water intrusions onto the continental shelf near the Totten Glacier. *J. Geophys. Res.: Oceans* 124, 4272–4289. doi: 10.1029/2018JC014634

Silvano, A., Rintoul, S. R., Peña-Molino, B., Hobbs, W. R., van Wijk, E., Aoki, S., et al. (2018). Freshening by glacial meltwater enhances melting of ice shelves and reduces formation of Antarctic Bottom Water. *Sci. Adv.* 4, eaa9467. doi: 10.1126/sciadv.aap9467

Sloyan, B. M., and Rintoul, S. R. (2001). The Southern Ocean limb of the global deep overturning circulation. *J. Phys. Oceanogr.* 31, 143–173. doi: 10.1175/1520-0485(2001)031<0143:tsolot>2.0.co;2

Smethie, W. M., and Jacobs, S. S. (2005). Circulation and melting under the Ross ice shelf: Estimates from evolving CFC, salinity and temperature fields in the Ross Sea. *Deep Sea Res. Part I: Oceanographic Res. Pap.* 52, 959–978. doi: 10.1016/j.dsr.2004.11.016

Smith, N. R., Zhaoqian, D., Kerry, K. R., and Wright, S. (1984). Water masses and circulation in the region of Prydz Bay, Antarctica. *Deep Sea Res. Part A* 31 (9), 1121–1147. doi: 10.1016/0198-0149(84)90016-5

Snow, K., Rintoul, S. R., Sloyan, B. M., and Hogg, A. M. (2018). Change in Dense Shelf Water and Adélie Land Bottom Water precipitated by iceberg calving. *Geophys. Res. Lett.* 45, 2380–2387. doi: 10.1002/2017GL076195

Solodoch, A., Stewart, A. L., Hogg, A.M., and Manucharyan, G. (2023). Machine learning-derived inference of the meridional overturning circulation from satellite-observable variables in an ocean state estimate. *J. Adv. Model. Earth Sys.* 15, e2022MS003370. doi: 10.1029/2022MS003370

Solodoch, A., Stewart, A. L., Hogg, A. M., Morrison, A. K., Kiss, A. E., Thompson, A. F., et al. (2022). How does Antarctic Bottom Water cross the Southern Ocean? *Geophys. Res. Lett.* 49, e2021GL097211. doi: 10.1029/2021GL097211

Spingys, C. P., Naveira Garabato, A. C., Legg, S., Polzin, K. L., Povl Abrahamsen, E., Buckingham, C. E., et al. (2021). Mixing and transformation in a deep western boundary current: a case study. *J. Phys. Oceanogr.* 51, 1205–1222. doi: 10.1175/JPO-D-20-0132.1

Stevens, C., Hulbe, C., Brewer, M., Stewart, C., Robinson, N., Ohneiser, C., et al. (2020). Ocean mixing and heat transport processes observed under the Ross Ice Shelf control its basal melting. *Proc. Natl. Acad. Sci.* 117, 16799–16804. doi: 10.1073/pnas.1910760117

Stevens, C., Sang Lee, W. S., Fusco, G., Yun, S., Grant, B., Robinson, N., et al. (2017). The influence of the Drygalski Ice Tongue on the local ocean. *Ann. Glaciol.* 58, 51–59. doi: 10.1017/aog.2017.4

Stewart, A. L., Chi, X., Solodoch, A., and Hogg, A. M. (2021). High-frequency fluctuations in Antarctic Bottom Water transport driven by Southern Ocean winds. *Geophys. Res. Lett.* 48, e2021GL094569. doi: 10.1029/2021GL094569

Stewart, C. L., Christoffersen, P., Nicholls, K. W., Williams, M. J., and Dowdeswell, J. A. (2019). Basal melting of Ross Ice Shelf from solar heat absorption in an ice-front polynya. *Nat. Geosci.* 12 (6), 435. doi: 10.1038/s41561-019-0356-0

Stewart, A. L., and Hogg, A. M. (2017). Reshaping the antarctic circumpolar current via antarctic bottom water export. *J. Phys. Oceanogr.* 47 (10), 2577–2601. doi: 10.1175/JPO-D-17-0007.1

Stommel, H. (1958). The abyssal circulation. *Deep-Sea Res.* 5, 80–82. doi: 10.1016/S0146-6291(58)80014-4

Sverdrup, H. U., Johnson, M. W., and Fleming, R. H. (1942). *The oceans: their physics, chemistry and general biology* (New York, NY: Prentice Hall).

Swift, J. H., and Orsi, A. H. (2012). Sixty-four days of hydrography and storms: RVIB Nathaniel B. Palmer's 2011 S04P Cruise. *Oceanography* 25 (3), 54–55. doi: 10.5670/oceanog.2012.74

Talley, L. D. (2013). Closure of the global overturning circulation through the Indian, Pacific and Southern Oceans: schematics and transports. *Oceanography* 26, 80–97. doi: 10.5670/oceanog.2013.07

Talley, L. D., Pickard, G. L., Emery, W. J., and Swift, J. H. (2011). *Descriptive physical oceanography: An introduction. 6th ed* (Elsevier Ltd).

Tamura, T., Ohshima, K. I., Fraser, A. D., and Williams, G. D. (2016). Sea Ice production variability in Antarctic coastal polynyas. *J. Geophys. Res.: Oceans* 121, 2967–2979. doi: 10.1002/2015JC011537

Tamura, T., Ohshima, K. I., and Nihashi, S. (2008). Mapping of sea ice production for Antarctic coastal polynyas. *Geophys. Res. Lett.* 35, 1–5. doi: 10.1029/2007GL032903

Tandon, N. F., Saenko, O. A., Cane, M. A., and Kushner, P. J. (2020). Interannual variability of the global meridional overturning circulation dominated by Pacific variability. *J. Phys. Oceanogr.* 50 (3), 559–574. doi: 10.1175/JPO-D-19-0129.1

Tapley, B. D., Watkins, M. M., Flechtner, F., Reigber, C., Bettadpur, S., Rodell, M., et al. (2019). Contributions of GRACE to understanding climate change. *Nat. Clim. Change* 9, 358–369. doi: 10.1038/s41558-019-0456-2

Testor, P., de Young, B., Rudnick, D. L., Glenn, S., Hayes, D., Lee, C. M., et al. (2019). OceanGliders: A component of the integrated GOOS. *Front. Mar. Sci.* 6. doi: 10.3389/fmars.2019.00422

Thomas, G., Purkey, S. G., Roemmich, D., Foppert, A., and Rintoul, S. R. (2020). Spatial variability of Antarctic bottom water in the Australian Antarctic Basin from 2018–2020 captured by Deep Argo. *Geophys. Res. Lett.* 47, e2020GL089467. doi: 10.1029/2020GL089467

Thompson, C. W., and Murray, J. (1895) *Report on the scientific results of the voyage of H.M.S. Challenger during the years 1872-76. Summary of scientific results, first part*. Available at: https://www.biodiversitylibrary.org/bibliography/6513#/summary.

Thompson, L., Smith, M., Thomson, J., Stammerjohn, S., Ackley, S., and Loose, B. (2020). Frazil ice growth and production during katabatic wind events in the Ross Sea, Antarctica. *Cryosphere* 14 (10), 3329–3347. doi: 10.5194/tc-14-3329-2020

Tinto, K. J., Padman, L., Siddoway, C. S., Springer, S. R., Fricker, H. A., Das, I., et al. (2019). Ross Ice Shelf response to climate driven by the tectonic imprint on seafloor bathymetry. *Nat. Geosci.* 12 (6), 441–449. doi: 10.1038/s41561-019-0370-2

Toole, J. M., Krishfield, R. A., Timmermans, M.-L., and Proshutinsky, A. (2011). The ice-tethered profiler: Argo of the Arctic. *Oceanography* 24, 126–135. doi: 10.5670/oceanog.2011.64

Van Sebille, E., Spence, P., Mazloff, M. R., England, M. H., Rintoul, S. R., and Saenko, O. A. (2013). Abyssal connections of Antarctic bottom water in a Southern Ocean state estimate. *Geophys. Res. Lett.* 40 (10), 2177–2182. doi: 10.1002/grl.50483

van Wijk, E. M., and Rintoul, S. R. (2014). Freshening drives contraction of Antarctic Bottom Water in the Australian Antarctic Basin. *Geophys. Res. Lett.* 41, 1657–1664. doi: 10.1002/2013GL058921

van Wijk, E. M., Rintoul, S. R., Wallace, L. O., Ribeiro, N., and Herraiz-Borreguero, L. (2022). Vulnerability of Denman Glacier to ocean heat flux revealed by profiling float observations. *Geophys. Res. Lett.* 49, e2022GL100460. doi: 10.1029/2022GL100460

Wallace, L. O., van Wijk, E. M., Rintoul, S. R., and Hally, B. (2020). Bathymetry constrained navigation of Argo floats under sea ice on the Antarctic continental shelf. *Geophys. Res. Lett.* 47 (11), e2020GL087019. doi: 10.1029/2020GL087019

Ward, M. L., and Hogg, A. M. (2011). Establishment of momentum balance by form stress in a wind-driven channel. *Ocean Model.* 40(2), 133–146. doi: 10.1016/j.ocemod.2011.08.004

Warren, B. (1981). "Deep circulation of the world ocean," in *Evolution of physical oceanography*. Eds. B. A. Warren and C. Wunsch (MIT Press), 6–41.

Watts, J., Bell, T. G., Anderson, K., Butterworth, B. J., Miller, S., Else, B., et al. (2022). Impact of sea ice on air-sea CO2 exchange - a critical review of polar eddy covariance studies. *Prog. Oceanogr.* 201, 102741. doi: 10.1016/j.pocean.2022.102741

Weiss, R. F., Östlund, H. G., and Craig, H. (1979). Geochemical studies of the Weddell sea. *Deep Sea Res. Part A Oceanogr. Res. Papers* 26, 1093–1120. doi: 10.1016/0198-0149(79)90059-1

Wen, J., Wang, Y., Wang, W., Jezek, K. C., Liu, H., and Allison, I. (2010). Basal melting and freezing under the Amery Ice Shelf, East Antarctica. *J. Glaciol.* 56 (195), 81–90. doi: 10.3189/002214310791190820

Weppernig, R., Schlosser, P., Khatiwala, S., and Fairbanks, R. (1996). Isotope data from ice station Weddell: Implications for deep water formation in the Weddell Sea. *J. Geophys. Res.* 101 (C11), 25,723–25,739. doi: 10.1029/96JC01895

Whitworth, T. I. I. I., and Orsi, A. H. (2006). Antarctic Bottom Water production and export by tides in the Ross Sea. *Geophys. Res. Lett.* 33, 1–4. doi: 10.1029/2006GL026357

Williams, G. D., Aoki, S., Jacobs, S. S., Rintoul, S. R., Tamura, T., and Bindoff, N. L. (2010). Antarctic bottom water from the adélie and george V land coast, east Antarctica (140–149°E). *J. Geophys. Res.: Oceans* 115, C04027. doi: 10.1029/2009JC005812

Williams, G. D., and Bindoff, N. L. (2003). Wintertime oceanography of the adélie depression. *Deep-Sea Res. Part II: Topical Stud. Oceanogr.* 50 (8–9), 1373–1392. doi: 10.1016/S0967-0645(03)00074-2

Williams, G. D., Bindoff, N. L., Marsland, S. J., and Rintoul, S. R. (2008). Formation and export of dense shelf water from the Adélie Depression, East Antarctica. *J. Geophys. Res.: Oceans* 113, 1–12. doi: 10.1029/2007JC004346

Williams, G. D., Herraiz-Borreguero, L., Roquet, F., Tamura, T., Ohshima, K. I., Fukamachi, Y., et al. (2016). The suppression of Antarctic bottom water formation by melting ice shelves in Prydz Bay. *Nat. Commun.* 7, 12577. doi: 10.1038/ncomms12577

Williams, T. J., Hillenbrand, C. D., Piotrowski, A. M., Allen, C. S., Frederichs, T., Smith, J. A., et al. (2019). Paleocirculation and ventilation history of southern ocean sourced deep water masses during the last 800,000 years. *Paleoceanogr. Paleoclimatol.* 34, 833–852. doi: 10.1029/2018PA003472

Williams, E. F., Zhan, Z., Martins, H. F., Fernández-Ruiz, M. R., Martín-López, S., González-Herráez, M., et al. (2022). Surface gravity wave interferometry and ocean current monitoring with ocean-bottom DAS. *J. Geophys. Res.: Oceans* 127, e2021JC018375. doi: 10.1029/2021JC018375

Wunsch, C. (1996). *The ocean circulation inverse problem* (New York, NY: Cambridge University Press).

Wunsch, C., and Heimbach, P. (2007). Practical global oceanic state estimation. *Physica D* 230, 197–208. doi: 10.1016/j.physd.2006.09.040

Wüst, G. (1935). *Schichtung und Zirkulation des Atlantischen Ozeans. Die Stratophäre. In: Wissenschaftliche Ergebnisse der Deutschen Atlantischen Expedition auf dem Forschungs—und Vermessungsschiff "Meteor" 1925–1927* Vol. 6. Ed. W. J. Emery (Amerind, New Delhi: The Stratosphere of the Atlantic Ocean). 112 pp.

Wüst, G. (1949). Die Kreisläufe der atlantischen Wassermassen, ein neuer Versuch räumlicher Darstellung. *Forschungen und Fortschr.* 25 (1949), 285–289.

Wüst, G. (1964). The major deep-sea expeditions and Research Vessels 1873-1960: a contribution to the history of oceanography. *Prog. Oceanogr.* 2, 1–52. doi: 10.1016/0079-6611(64)90002-3

Wüst, G. (1968). *History of investigations of the longitudinal deep-sea circulation, (1800–1922)* (Bull. Inst oceanogr, Monaco, Congr int history oceanography), 109–120.

Yabuki, T., Suga, T., Hanawa, K., Matsuoka, K., Kiwada, H., and Watanabe, T. (2006). Possible source of the Antarctic bottom water in the Prydz Bay region. *J. Oceanogr.* 62 (5), 649–655. doi: 10.1007/s10872-006-0083-1

Yamazaki, K., Aoki, S., Katsumata, K., Hirano, D., and Nakayama, Y. (2021). Multidecadal poleward shift of the southern boundary of the Antarctic Circumpolar Current off East Antarctica. *Sci. Adv.* 7 (24), eabf8755. doi: 10.1126/sciadv.abf8755

Yamazaki, K., Aoki, S., Shimada, K., Kobayashi, T., and Kitade, Y. (2020). Structure of the subpolar gyre in the Australian-Antarctic Basin derived from Argo floats. *J. Geophys. Res.: Oceans* 125, e2019JC015406. doi: 10.1029/2019JC015406

Yang, H. W., Kim, T.-W., Dutrieux, P., Wåhlin, A., Jenkins, A., Ha, H. K., et al. (2022). Seasonal variability of ocean circulation near the Dotson ice shelf, Antarctica. *Nat. Commun.* 13 (1), 1138. doi: 10.1038/s41467-022-28751-5

Yoon, S.-T., Lee, W. S., Stevens, C., Jendersie, S., Nam, S., Yun, S., et al. (2020). Variability in high-salinity shelf water production in the Terra Nova Bay polynya, Antarctica. *Ocean Sci.* 16, 373–388. doi: 10.5194/os-16-373-2020

Zhou, S., Meijers, A. J. S., Meredith, M. P., Abrahamsen, E. P., Holland, P. R., Silvano, A., et al. (2023). Slowdown of Antarctic Bottom Water export driven by climatic wind and sea-ice changes. *Nat. Clim. Change* 13 (7), 701–709. doi: 10.1038/s41558-023-01695-4

Zilberman, N. V., Roemmich, D. H., and Gilson, J. (2020). Deep-ocean circulation in the Southwest Pacific Ocean interior: Estimates of the mean flow and variability using Deep Argo data. *Geophys. Res. Lett.* 47, e2020GL088342. doi: 10.1029/2020GL088342